THE ENERGY SPECTRA OF PROTONS EMITTED FROM NUCLEI BOMBARDED WITH FAST NEUTRONS.

by

W. JACK

DEPARTMENT OF NATURAL PHILOSOPHY

UNIVERSITY OF GLASGOW

PRESENTED AS A THESIS FOR THE DEGREE OF Ph.D.

IN THE UNIVERSITY OF GLASGOW

DECEMBER, 1959.

ProQuest LLC.
789 East Eisenhower Parkway
P.O. Box 1346
Ann Arbor, MI 48106 – 1346

The Energy Spectra of Protons Emitted by Nuclei Bombarded with Fast Neutrons.

Following an introductory chapter reviewing the interpretation of nuclear reactions induced by particles of medium energies a description is given of two scintillation counter experiments which were performed in order to determine the energy spectra of protons emitted from medium weight nuclei when bombarded with fast neutrons from the T-D reaction. In the first experiment a novel form of neutron shielding is used, and the energy spectrum of protons emitted into a large solid angle ($\sim$ 3.5 steradian) at 90^{o} is measured, using a CsI(Tl) proton spectrometer. The extreme forward and backward directions being excluded, it is hoped that the spectra obtained are not influenced greatly by protons resulting from processes of direct interaction and so may usefully be compared with the predictions of the statistical theory. Thin separated isotope targets of ^{27}Al, ^{54}Fe, ^{56}Fe, ^{58}Ni, ^{60}Ni, ^{59}Co, ^{63}Cu, ^{65}Cu and ^{64}Zn were bombarded with neutrons of energy 14.1 MeV in this experiment, and "nuclear temperatures" are derived from the spectra which are found to have a pure exponential form. These "nuclear temperatures" are used to derive values of "a" the parameter in the empirical level density formula $\omega(E) = C.\exp\left[2(aE)^{\frac{1}{2}}\right]$. "Nuclear temperatures" were also measured for the isotopes ^{54}Fe,

^{58}Ni and ^{64}Zn using incident neutrons of energies 12.9 and 15.7 MeV. It is found that the "nuclear temperature" increases with excitation energy in the manner expected from the Fermi gas model of the nucleus.

In the second experiment, a telescope consisting of two CsI(Tl) scintillation counters is used to measure the energy spectra of protons emitted into a small solid angle in the forward direction. This telescope is unusual in that the dE/dx counter is a thin crystal of CsI(Tl). The separated isotope targets used in the previous experiment and also an additional target of ^{19}F, in the form CF_2, were used in this experiment. The spectra measured have a large contribution from direct interaction processes and are also examined for evidence of "single particle" or anomalous effects. It is found that there is no evidence for an anomalous type of reaction similar to that found in the inelastic scattering of protons. It is shown that several peaks in the spectra at an excitation energy of the residual nucleus of approximately 7 MeV may be interpreted as being due to n,d pick-up reactions.

PREFACE.

The work described in this thesis was carried out during the period August, 1957 - August, 1959 in the Department of Natural Philosophy, The University of Glasgow. For part of this period, the author assisted in the day to day running of the high tension generators used in the experiments, and for more than a year he has been responsible for the maintenance of these machines.

The thesis presents the results and interpretation of two scintillation counter experiments to determine the energy spectra of protons emitted from medium weight nuclei bombarded with fast neutrons from the reaction $^{3}H(d,n)^{4}He$.

Following an introductory chapter reviewing the interpretation of intermediate energy reactions, Chapter II describes the techniques used by other workers to measure n,p proton energy spectra, and a summary of the results obtained is given.

Chapter III describes the development of a scintillation counter technique to measure the

energy spectra of n,p protons emitted into approximately 4π. This experiment, in which a novel form of neutron shielding is employed, was performed in collaboration with Dr. R.S. Storey and Dr. A. Ward.

The development of a scintillation counter telescope of unusual design is described in Chapter IV. This telescope was used to measure the energy spectra of n,p protons emitted into a small solid angle in the forward direction. The author was solely responsible for this project, but wishes to acknowledge the assistance of Dr. A. Ward during the development stage.

The interpretations of the two experiments are given in Chapters V and VI and are entirely due to the author.

I should like to thank Professor P.I. Dee for his sustained interest and encouragement and for many helpful discussions.

December, 1959. W. Jack.

Footnote:- In the course of this work, an

interesting effect concerning the fluorescence decay times of the light emitted from CsI(Tl) for particles of different ionisation densities was discovered. This work done in collaboration with Dr. R.S. Storey and Dr. A. Ward is published in Proc. Phys. Soc., 72, 1. The results of Chapter III have been accepted for publication in the Proceedings of the Physical Society, and the results presented in Chapter IV have also been submitted for publication in this journal.

CONTENTS.

Chapter 1.

The Interpretation of Nuclear Reactions Induced by Intermediate Energy Nucleons.

I.1 Introduction.

A study of the nuclear reactions induced by nucleons of intermediate energy (10-30 MeV) contributes to our knowledge of nuclear structure and the interactions between nucleons inside the nucleus. Before 1936, the interaction of an incident nucleon with the nucleus was represented by replacing the nucleon-nucleon interactions inside the nucleus by a real potential well of nuclear dimensions. This model, with its well known single particle "size" resonances, was unable to explain the predominance of absorption over scattering, and the narrow resonances observed in slow neutron experiments, and was replaced by the compound nucleus model of Bohr, 1936.

The compound nucleus is a strong coupling model where it is assumed that the energy of the incident particle is shared rapidly among the nuclear constituents due to the strong interactions which are present. It is further assumed that the compound nucleus is formed immediately the incident particle reaches the nuclear surface, and that the decay of the compound nucleus occurs when a statistical fluctuation places enough energy on a particle for it to escape. On this model, the narrow

resonances of the slow neutron experiments correspond to quantum states of a many body system, the width of the resonance, Γ , being related to the lifetime of the compound nucleus by $\tau_c \simeq \frac{\hbar}{\Gamma}$. The decay of a compound nucleus formed in a discrete state is independent of its mode of formation, since the quantum state is wholly defined by its energy, parity, and angular momentum. As the excitation energy of the compound nucleus is increased, the probability of decay increases, so a point is reached where the level widths Γ are greater than the level spacings D. This is the situation which occurs in nuclear reactions initiated by intermediate energy nucleons and which has lent so much interest to this field. Blatt & Weisskopf, 1952, have shown that the wave function representing the compound nucleus is periodic with period $t \simeq \frac{\hbar}{D}$ if all the decay channels are closed. This means that if $\Gamma > D$ the extent of formation of the compound nucleus is in some doubt. In addition, the decay will not necessarily be independent of the mode of formation since the phases of the levels of the compound state may depend upon the way the compound nucleus is created. At sufficiently high excitation, the "statistical" assumption is usually made that the phase relations are random, and positive and negative interference terms cancel out leading to a decay independent of the mode of formation. At very high

energies, > 100 MeV, $\Gamma \gg D$ and in this case the width Γ is so great that the compound nucleus can not be said to exist. Here the interaction between an incident nucleon and the nucleus is wholly of a direct character. The interest in intermediate energy reactions stems from the fact that their description lies between the extremes of a direct nucleon-nucleon interaction applicable at very high energies, and the compound nucleus description which has had so much success in low energy nuclear physics.

Until 1952, the compound nucleus model with its picture of strong nucleon-nucleon interactions inside the nucleus was applied with great success to many low energy reactions. However, the experiments of Barschall, 1952, on the total elastic cross sections for neutrons in the range 0.1 - 3.0 MeV indicated that a modification of the picture of a completely black nucleus was necessary. It was found that these cross sections showed broad resonances which varied systematically with energy and atomic mass number in a manner reminiscent of the early single particle model with its broad "size" resonances. This behaviour was explained by the "cloudy crystal-ball" model developed by Feshbach et al., 1954, in which the incident nucleon moves in a complex potential field. This model is more usually known as the "optical model"

after Fernbach et al., 1949, who used this method in the interpretation of very high energy nuclear reactions. The incident nucleon does not form a compound nucleus upon reaching the nuclear surface, but retains its identity for some time moving in a complex potential well $U = -(V + iW)$ where V is the potential of the early single particle model, and W is related to the probability of capture of the incident particle to form a compound nucleus. Among others, Woods and Saxon, 1954, have applied the optical model to the analysis of the angular distributions of elastically scattered 18 MeV protons, and the elastic scattering of 14 MeV neutrons has been treated similarly by Culler et al., 1956. Three points of interest raised in the application of the optical model at intermediate energies are, a) The fit to the data is much improved by rounding the edge of the potential well. This has the effect of reducing the amount of reflection at the nuclear surface with a corresponding increase in the absorption cross sections predicted. The rounding of the edge of the well is expected on the basis of the diffuse nuclear surface found by Hofstadter et al., 1953, in the elastic scattering of high energy electrons, but care must be exercised in a comparison of the radii of the potential

well and the nucleon (proton) distribution found by Hofstadter et al., since the former depends to some extent on the values of V and W. b) The variation of W with energy of incident particle can be compared with calculations of the mean free path of a nucleon inside the nucleus, Lane and Wandel, 1955. The mean free path λ is related to V and W by the expression $\frac{1}{\lambda^2} = 2\left[\left\{\left(\frac{W}{\epsilon+V}\right)^2+1\right\}^{\frac{1}{2}}-1\right]K^2$ where ϵ is the energy of the incident particle and K is the wave number of the particle inside the potential well. This formula yields a value of $\lambda = 3.6 \times 10^{-13}$cm. for 14 MeV neutrons. c) The variation of V with energy of incident particle is related to the concept of effective nucleon mass so successfully used in the theory of Brueckner, 1955, in which a description of the properties of nuclear matter is given starting from the basic nucleon-nucleon interactions. The "frivolous" model used by Lane and Wandel, 1955, (i.e. a non-interacting degenerate Fermi gas of nucleons in which the number of collisions is restricted by the Pauli principle) is made plausible on the basis of the Brueckner theory.

The optical model is also in accord with the shell model proposed by Mayer, 1949, and Haxel et al., 1949, to account for the discontinuities in nuclear properties

at "magic" numbers of neutrons and protons. This model also visualises individual nucleons moving in a potential well representing the effect of the interactions with other nucleons. The shell model potential contains a spin-orbit term, and Culler et al., 1956, have investigated the effect of this term in fitting the optical model to the 14 MeV neutron scattering data.

Summarising, one can say that there is ample evidence for an "intermediate" coupling model such as that formulated by Lane, Thomas and Wigner, 1955. In this model there is a compromise between the zero coupling of the individual particle states of the independent particle model, and the very strong coupling of the uniform model which represents compound nucleus behaviour. This compromise results in a superposition of single particle effects, such as size resonances, upon the compound nucleus effects.

I.2 The Compound Nucleus and the Statistical Theory.

Although we have seen that there is much evidence for a mean free path comparable to the nuclear radius for intermediate energy incident nucleons, this does not necessarily invalidate the compound nucleus conception for these reactions. When the effect of the reflection of nucleons at the nuclear surface is taken into account, it becomes probable that a large fraction of incident

14 MeV neutrons, say, may dissipate their energy in a cascade of low energy nucleons so forming a compound nucleus.

The problem of the decay of the compound nucleus was first treated quantitatively by Weisskopf, 1937, using the principle of detailed balancing. This theory, known as the statistical theory, is based on the assumption that the nuclear reaction is separable into two distinct stages, the formation and decay of a compound nucleus, the decay being independent of the mode of formation and being determined principally by the availability of levels in the residual nuclei. In a reaction of the type X(n,p)Y, the probability per unit time of the decay of the excited compound nucleus X^+ is given by

$$P(E_p)\,dE_p = \frac{2S+1}{\pi^2\hbar^3} \cdot M \cdot \sigma_c \cdot E_p \cdot \frac{\omega_r(E)}{\omega_c(E_c^+)}\,dE \quad \text{-----I.1.}$$

where the excitation energy of the compound nucleus $E_c^+ = E_p + E + B_p$ E_p being the kinetic energy of the emitted particle, E the energy of excitation of the residual nucleus, and B_p the binding energy of the emitted particle in the compound nucleus. M and S are the mass and spin of the emitted particle and σ_c is the cross section for the inverse reaction where the original emitted particle, energy E_p, is incident on the residual

nucleus with excitation energy E. $\omega_r(E)$ and $\omega_c(E_c^+)$ are the level densities in the excited residual and compound nuclei respectively.

When the compound nucleus is not in a discrete state, the independence of its disintegration requires the special assumption that the phases of the levels excited in the compound nucleus are random. This assumption implies an angular distribution of the emitted particles symmetrical about 90^o in the centre of mass system, and furthermore, we would not expect this angular distribution to vary rapidly with energy of bombarding particle. This last characteristic has been used to test the assumption in several cases, and in the case of the heaviest nucleus investigated, ^{41}K, Eisberg and Hintz, 1956, found some indication that the assumption was invalid. (Measuring the angular distribution of 10 MeV protons inelastically scattered to the first excited state at 1.47 MeV in ^{40}A is not particularly good as a test of the independence assumption, since the simple character of the first excited state in the residual nucleus may imply that the interaction of the incident particle with the target nucleus is dominated by single particle behaviour.)

The cross section σ_c in equation I.1 can not be measured experimentally, but it is usually assumed to be given by $\sigma_c = \sum_{\ell=0}^{R/\lambda\!\!\!^{-}} \pi \lambda\!\!\!^{-2}(2\ell+1)T_\ell$ where $\lambda\!\!\!^{-}$ is the wavelength

(divided by 2π) of the emitted particle, R is the nuclear radius, and T_ℓ is the transmission coefficient of the nuclear surface barrier when the angular momentum of the particle is $\ell\hbar$. T_ℓ is usually calculated for a real potential well, and includes the effect of the Coulomb barrier for charged particles. From the optical model, one might expect fluctuations in σ_c due to the effect of size resonances. Nemirovski, 1956, has examined this question in the case of neutrons of energy $2\frac{1}{2}$ - 4 MeV, but finds fluctuations small in comparison with the term $E_p \cdot \omega(E)$ in equation I.1. The effect will be further masked in the case of protons by the large variations in σ_c due to the Coulomb barrier.

Values of σ_c for protons have been tabulated by Blatt and Weisskopf, 1952, and Shapiro, 1953. It is found that a square well with a nuclear radius parameter r_o = 1.5×10^{-13}cm. gives a good fit to the p,n excitation function data of Blaser et al., 1951. This fit to data relating to protons of energy $<$ 6.5 MeV incident on ^{63}Cu, ^{65}Cu, ^{66}Zn, ^{67}Zn and ^{68}Zn is important when we consider the most suitable value of σ_c to use in the analysis of n,p evaporation spectra in the medium weight isotopes. Although the value of r_o used is greater than that found by Hofstadter et al., 1953, viz. r_o = 1.2×10^{-13}cm., the increased transmission for

the larger value of r_0 partially compensates for the increased penetrability caused by the diffuse nature of the surface of the proton distribution in the nucleus, - Scott, 1954, and Evans, 1959.

I.3. Evaporation Spectra.

a) Nuclear Temperature.

In nuclear reactions where the statistical theory is applicable, equation I.1. predicts that the energy spectrum of particles emitted will be given by $dn/dE_p \propto E_p \cdot \sigma_c \cdot \omega_r(E)$. Due to the rapidly increasing availability of levels in the residual nucleus with excitation energy, the spectra are approximately Maxwellian in form, and are usually referred to as "evaporation" spectra after Frenkel, 1936. It is customary to analyse these spectra in terms of a parameter T defined by $\frac{1}{T} = \frac{d}{dE} \log \omega_r(E) = \frac{d}{dE}\left\{\frac{dn/dE_p}{E_p \cdot \sigma_c}\right\}$. The parameter T is called the "nuclear temperature" following from the practice of writing $\log \omega(E) \simeq S(E)$ where S is entropy. We find, $dn/dE_p \propto E_p \cdot \sigma_c \cdot \exp[S_r(E)]$

But $$S_r(E) = S_r(E_c^+ - B_p - E_p)$$

$$= S_r(E_c^+ - B_p) - E_p\left(\frac{dS}{dE}\right)_{E_c^+ - B_p} \text{ provided } E_p \ll E_c^+ - B_p$$

letting $\frac{1}{T} = \left(\frac{dS}{dE}\right)_{E_c^+ - B_p}$ we find

$$\frac{dn}{dE_p} \propto E_p \cdot \sigma_c \cdot \exp[S_r(E_c^+ - B_p)] \cdot \exp\left[-\frac{E_p}{T}\right]$$

This equation reveals the Maxwellian form of the spectra, and shows that in the approximation T represents the nuclear temperature of the residual nucleus at its maximum excitation energy. T is related to the true nuclear temperature θ by the equation,

$$\frac{d}{dE}\log\omega(E) = \frac{1}{T} = \frac{1}{\theta} - \frac{1}{2}\frac{d}{dE}\log\left(\theta^2 \cdot \frac{dE}{d\theta}\right) \quad \text{----I.2.}$$

It can be shown, Bethe, 1937, that the nuclear equation of state is given by $E = aT^n$ where $n = 2$ for the Fermi gas model and $n = \frac{7}{3}$ for the liquid drop model. Taking $n = 2$, we find that $\theta = T - \frac{3T^2}{4E}$ which implies that for the reactions we will be concerned with $\theta \simeq T$ within 10%.

For the Fermi gas model, Bethe, 1937, finds $a = \frac{A}{f}$ where A is the nuclear mass number, and $f = 8.8$ MeV with $r_o = 1.51 \times 10^{-13}$ cm. Lang and Le Couteur, 1954, fitting the available experimental data, show $E = \frac{A}{f} T^2$ where $f = 10.5$ MeV. The calculation of f from the Fermi gas model is quite sensitive to the choice of radius parameter r_o and using the Saxon potential radius $r_o = 1.33 \times 10^{-13}$ cm. would give $f = 11.3$ MeV in close agreement with the value of Lang and Le Couteur, 1954.

The constancy of measured nuclear temperatures of approximately 1 MeV led to suggestions by Cohen, 1953; Beard, 1954; Livesey, 1955; and Trainor and Dixon, 1956, that below 10 MeV excitation the nuclear temperature

remained constant at 1 MeV. This was interpreted as being due to a phase change in the nuclear matter in which all nucleons were excited into a Fermi gas above 10 MeV excitation, but below this energy progressively fewer nucleons were excited. Some doubt is cast on this hypothesis by the low nuclear temperatures ($\sim$ 0.5 MeV) obtained from the photoneutron spectra from Bi, Au and Ta bombarded with $\sim$ 14 MeV photons, Sargent and Bertozzi, 1957.

b) Level Density Formulae.

The level density formula deduced by Bethe, 1937, for a Fermi gas model is $\omega(E,J) = \text{Const.}\ (2J + 1)\ E_f^{-1}.\ x^{-4}.\ e^{x}$ where E_f is the Fermi energy, J is the spin of the levels concerned, and $x = \pi(\frac{AE}{E_f})^{\frac{1}{2}}$. For application to evaporation spectra it is sufficiently accurate to use the empirical form of this expression, (Blatt and Weisskopf, 1952) $\omega(E) = C \exp.\ \left[2(aE)^{\frac{1}{2}}\right]$ where "a" is the same constant appearing in $E = aT^2$. Recent improvements of Bethe's formula include those of Bloch, 1954; Newton, 1956; Ross, 1957 and Cameron, 1958. Newton, 1956, takes account of the shell model and introduces the idea of writing $\omega(E + \delta)$ instead of $\omega(E)$, the energy gap δ being determined by pairing energies. Cameron, 1958, has improved this treatment, and obtains good agreement with the level densities

given by the slow neutron experiments. This agreement is taken as confirmation of the proportionality of level density to (2J + 1). Ross, 1957, has also used the shell model approach, but finds poorer agreement with experiment than that given by the formula of Blatt and Weisskopf, 1952.

The expressions obtained above may be compared with the spectra of particles emitted into the backward hemisphere from excited nuclei, since it is hoped (in the absence of the "spot heating" effect) that such spectra will not be influenced by direct interactions. It is usual to plot log. $\frac{dn/dE_p}{E_p.\sigma_c}$ = log. $\omega_r(E)$ as a function of E or E_p, and this type of plot is called a "relative level density" plot. Using $\omega(E) = C.\exp\left[2(aE)^{\frac{1}{2}}\right]$ we would expect such plots to be concave down towards the energy axis. In fact this is rarely obtained, and many authors have commented on the pure exponential nature of the plots from reactions such as p,n; p,p^1; n,n^1; n,α;. This apparent anomaly is not serious however, since an examination of the expected shape of the level density function of Blatt and Weisskopf, 1952, (see Evans, 1959) reveals very little curvature in the plot of log $\omega(E)$ against E above E = 2 MeV, and the plot of Newton's formula is even straighter. It should be mentioned, too, that the formula $\omega(E) = C.\exp\left[2(aE)^{\frac{1}{2}}\right]$ neglects the term

in E^{-2} present in the Fermi gas derivations, and inclusion of this term will tend to straighten the predicted plots. The analysis of the evaporation spectra is complicated by the presence of direct interactions at the higher particle energies, and multiple particle reactions of the type n,np, say, at the lower energies and both these effects produce plots concave upwards.

Two evaporation experiments where the proportionality of $\omega(E)$ to $\exp(E^{\frac{1}{2}})$ has been observed are the α,p experiment of Eisberg et al., 1955, and the heavy ion experiment of Zucker, 1958. The latter experiment finds fair agreement with the formula of Lang and Le Couteur, 1954, $a = \frac{A}{10.5}$, since a value of $a = 5$ Mev^{-1} is found for the nucleus ^{40}K. It should be noted however, that replotting the results in terms of E instead of $E^{\frac{1}{2}}$ (Storey et al., 1959) a straight line plot of log $\omega(E)$ is obtained within the experimental error. The experiment of Eisberg et al., 1955, is anomalous in that the values of "a" obtained for Cu, Ag and Au are ~~anomalously~~ exceptionally low ($a \sim 1.3$ MeV^{-1}) and show no variation with A. Values of "a" may also be deduced by applying equation I.1 to excitation function data :-Brolley et al., 1952, (α,2n); Bleuler et al., 1953, (α,2n); (α,n) . The values of "a" obtained

(~ 2 MeV^{-1}) are anomalously low compared to those found by Lang and Le Couteur, 1954, and show little variation with A, this has been discussed by Igo and Wegner, 1956. Colli et al., 1959, have suggested that a similar anomaly arising in the analysis of the ratio of cross sections of the type $\sigma(X,2n) \div \sigma(X,n)$, (Weisskopf and Ewing, 1940) is due to the neglect of the probability of proton emission, but Porges, 1956, has disproved this hypothesis in the case of Ag.

Several authors, (Colli et al., 1957b; Thomson, 1956; Gugelot, 1954) have commented on the similarity of relative level density plots from different nuclear reactions in the same medium weight target nucleus when these plots are compared in terms of the emitted particle energy rather than in terms of the excitation energy of the residual nucleus. They have suggested that this may be evidence for a selection rule which depends upon the energy of the emitted particle. Cohen, 1953, also came to this conclusion, but the extent of the direct interaction contribution in the data then available was not fully realised.

c) Angular Distributions.

Before leaving the statistical theory, we may remark on its predictions concerning the angular distribution of emitted particles. Hauser and Feshbach,

1952, have shown that isotopic angular distributions are expected in reactions where there is a transition from a "statistical" region of the compound nucleus to a "statistical" region of the residual nucleus provided the level density of levels of spin J is proportional to $(2J + 1)$. Using the more general spin dependence $\omega(E,J) \propto a^{al}\ (2J + 1)\ \exp.\left[\frac{-\hbar^2}{2gT} J(J+1)\right]$ where "g" is an effective moment of inertia of the nucleus, Ericson and Strutinski, 1958, have calculated the expected assymmetries. The asymmetries calculated increase with the mass of particle emitted, and decrease with its kinetic energy, but the 0^o to 90^o asymmetry for reactions of the type (n,p), (p,p^1) is small. Experimentally it is found that the angular distribution of inelastically scattered 14 MeV neutrons is isotropic at the low energies up to 4 MeV, Rosen and Stewart, 1955, however it should be noted in passing that these low energy neutrons result in the main from the n,2n reaction, so it does not follow that this is a proof of the applicability of the statistical theory to the interaction of 14 MeV neutrons with nuclei. The angular distributions of higher energy particles, where reactions of the type n,2n are forbidden on account of their Q value, are invariably peaked in the forward direction

even although the energy of the emitted particle is small compared to that usually associated with direct interactions.

Summarizing, one can say that the shapes of the spectra, the values of "a" deduced, and the angular distributions are all at variance to a greater or lesser degree with the predictions of statistical theory in relation to intermediate energy evaporation spectra.

I.4 Direct Interaction.

The existence of a direct interaction process was suggested by the discrepancies noted in I.3, the forward peaked angular distributions of the large number of higher energy particles emitted in intermediate energy reactions, and the failure of statistical theory to account for the cross sections of n,p reactions in heavy elements. This new process was easily visualised too, with the growth of evidence on the diffuse nature of the nuclear surface, the individual particle orbits of the shell model, and the finite mean free path of a nucleon in nuclear matter demonstrated by the success of the optical model. This last factor is important in determining whether the direct interaction occurs in the nuclear surface or throughout the nuclear volume. From the energy dependence of V and W found by Melkanoff

et al., 1956, we expect the mean free path λ for protons in nuclear matter to be given by $\lambda \geq R$ for $E < 10$ MeV, and $\lambda < R$ for $E > 10$ MeV where R is the radius of a typical nucleus, say $6 - 8 \times 10^{-13}$ cm., and E is the energy of the incident proton. The increase in λ at low energies is due to the Pauli exclusion principle, and at very high energies (> 100 MeV) λ is also large due to the reduced nucleon-nucleon interaction cross section. This minimum value of λ for intermediate energy particles suggests that the direct interaction is most likely to occur in the surface of the nucleus. Indeed, even if we allow the mean free path to increase sufficiently to enable us to think in terms of a volume direct interaction, taking account of the reflection of the emitted particles at the nuclear surface (which depends on the diffuse nature of the surface) leads to the conclusion that surface direct interaction will predominate.

a) Surface Direct Interaction.

Measurements of n,p cross sections at 14 MeV in a wide range of elements by Paul and Clarke, 1953, were in violent disagreement with the predictions of the statistical model, the ratio σ (experimental) $\div$ σ(theory) ranging from 1 to 1000 as A varied from 1 to 200. (Later measurements by Coleman et al., 1959, have

shown that many of the cross sections measured by Paul and Clarke, 1953, were too high by an order of magnitude, but qualitatively the original result still stands.) McManus and Sharp, 1952, were able to show that since the n,p cross sections for the heavier elements, A >80, were so small, a small probability (5 to 10%) for direct interaction could account for the observed cross sections. This theory was developed by Austern, Butler and McManus, 1953, and is a surface direct interaction theory. An incident neutron of large impact parameter interacts with a proton outside the main core of the nucleus in the exponential tail of the wavefunction, and the impulse approximation of Chew, 1950, is made that neither neutron nor proton interacts with the nucleus during their mutual interaction. The angular distributions of proton groups corresponding to discrete low lying states in the residual nucleus predicted by this theory are similar to those of stripping reactions, and may be used to deduce the spins and parities of levels in the residual nucleus. In the simpler cases, the angular distributions are characterised by the set of "l" values where $l_n + l_p \geq l \geq |l_n - l_p|$ ~~and~~ l_p & l_n being the orbital angular momentum of a proton in the state of least binding in the target nucleus, and the orbital

angular momentum of the captured neutron (in state of least binding). The theory favours transitions to the low lying states of the residual nucleus. Butler, 1957, suggests that this theory can be extended to include many different nuclear reactions, and predicts that this type of interaction should be as probable as the stripping and pick-up reactions. Recently Butler et al., 1958, have modified their theory by introducing a complex potential well to account for the effect of the nucleus on the incident and emitted particles. They discuss classically, the reflection and refraction of the particles by the potential well, and show that the maxima and minima in the angular distributions can be interpreted as interference between particles emitted from different regions of the nuclear surface. The Butler theory has been applied with moderate success to the interpretation of angular distributions obtained from intermediate energy reactions. Eubank et al., 1958/59, have analysed the ^{32}S $(n,p)^{32}P$ reaction in this way, but the wide application of the theory in the n,p reaction is limited by lack of proton energy resolution to pick out discrete levels in the residual nucleus.

b) Volume Direct Interaction.

Hayakawa et al., 1955, and Brown and Muirhead, 1957, have formulated volume direct interaction theories along semi-classical lines treating the target nucleus as a degenerate Fermi gas of nucleons. The energy distributions predicted by these theories are relatively flat compared to those of the statistical theory, and the angular distributions are peaked in the forward direction. The cross section for the direct interaction of Hayakawa is much smaller than that of Brown and Muirhead. Coleman et al., 1959, claim that the Brown and Muirhead theory gives a good fit to their 14 MeV n,p cross section data, and this theory ~~gives quite~~ also ~~good~~ fits ~~to~~ the angular distribution of inelastically scattered 14 MeV neutrons obtained by Rosen and Stewart, 1955.

Some doubt has been cast on the validity of the theories above by the work of Elton and Gomes, 1957. These authors have investigated the hypothesis of Eisberg and Igo, 1954, that the inelastic scattering of 31 MeV protons proceeds by a direct interaction in the diffuse rim of the nucleus, and have shown that a knock-on scattering occurring throughout the nuclear volume can not account for the observed results because of total internal reflection effects at the nuclear surface.

They have shown furthermore, that it is probable that the surface direct interaction takes place in the extreme edge of the diffuse nuclear surface in the classically forbidden region.

The most precise volume direct interaction theory to date is that of Levinson and Bannerjee, 1957/58, who use a combination of shell model and optical model ideas. The incident and emitted particles are refracted and partially absorbed by a complex potential well, and the discrete excited state of the residual nucleus is described by a shell model wavefunction. Applying the theory to the reaction $^{12}C(p,p^1)^{12}C^*$, Q = -4.4 MeV, the differential cross section was fitted for the range of proton energies E_p = 14 to 185 MeV if a complex potential 2/3 of that found from the elastic scattering experiments was used. Recently, Glendenning, 1959, has shown that the Levinson and Bannerjee theory may be simplified by restricting the interaction to the nuclear surface. The fit of this new theory to the experimental results is sufficiently good to justify the exclusion of the nuclear interior, and confirms the conclusion of Elton and Gomes, 1957.

I.5. Single Particle and Anomalous Effects.

Blok and Jonker, 1957 and Colli et al., 1957c, have compared n,p energy spectra obtained with 14 MeV neutrons with d,p spectra leading to the same residual nucleus. They find, that for a given residual nucleus, the spectra exhibit broad intensity modulations, which occur at the same excitation energy of the residual nucleus in both reactions. This similarity is explained by supposing that the neutron in the d,p and n,p reactions prefers to be captured into a neutron single particle level of the residual nucleus with the core of the residual nucleus left undisturbed. A controversial point here is that the width of the giant resonances found seems to be much smaller than the width 2W expected from the optical model potential.

In the study of the inelastic scattering of 23 MeV protons, Cohen, 1957, found a broad group at approximately 2.5 MeV excitation energy of the residual nucleus. The presence of this broad group of inelastically scattered protons was independent of the mass of nucleus studied over a wide range of A and was unaffected by the closing of nuclear shells. This behaviour was referred to as anomalous inelastic scattering, and has been the subject of intensive investigations by Cohen et al., 1957/58/59,

who concluded from their observations that the anomalous peak was caused by the excitation of levels of a collective nature by a direct interaction in the surface of the nucleus. The theory of an interaction like this has been studied by Brink, 1955, who concludes that the excitation of rotational levels by a direct interaction may be important in the region of strongly deformed nuclei, i.e. A $\simeq$ 150 and 240. Tomasini, 1957, and Tamura and Choudhury, 1959, have proposed alternative explanations of the anomalous inelastic scattering. Tomasini, 1957, suggests that a particle which enters the nucleus and leaves it without being captured produces a perturbation of the nuclear potential while it is inside the nucleus, and allows the nucleus to make a transition to an excited level. Tamura and Choudhury, 1959, have applied the simple plane wave approximation of Austern et al., 1953, to a direct interaction in the nuclear surface taking account of the structure of the levels of the residual nucleus. They obtain fair agreement with experiment in the case of lead.

Chapter II.

Experimental Methods Used in the Study of Proton Energy Spectra from the n,p Reaction.

II.1 General Considerations.

A study of the proton energy spectra from n,p reactions induced by fast neutrons from the reaction $^{3}H(d,n)^{4}He$ Q = 17.577 MeV is rendered difficult by a) the low flux of neutrons available and b) nuclear reactions produced in the proton detector and its immediate surroundings by the neutrons. The work described in this thesis was carried out using the standard thin tritium-titanium target supplied by A.E.R.E., Harwell. This consists of 1/3 c.c. of tritium absorbed in a layer of titanium approx. 200 μgms./cm^2 thick evaporated on to a copper backing. The thickness of this target to a deutron beam of 300 Kv. is approx. 70 Kv. resulting in an extremely mono-energetic neutron source. With this type of tritium target a flux of 5 x 10^9 neutrons per second into 4π (angular distribution approximately isotropic) can be maintained for 15 hours. When this flux is compared with the directed beam of 6 x 10^{12} singly charged particles per second obtainable with an accelerator with a beam current of 1 μamp. it is evident that counting efficiency will be a major

consideration in any experiment. The problem of counting efficiency is also related to the fairly low n,p cross section of most elements and to the need for a thin foil of the target element so that the energy resolution of the proton spectrometer is not seriously impaired by the varying energy loss of protons leaving the target foil. The medium weight elements have the highest n,p cross-sections ranging from 100-500 mb., Paul and Clarke, 1953, and are the most suitable for study. In the heavier elements, the Coulomb barrier has a dominating influence, and cross sections are of the order of 10 to 1 mb., Coleman et al., 1959.

The extreme penetrability of the fast neutrons is illustrated by the fact that about 20 cm. of copper or steel are necessary to attenuate the flux by a factor of 20. This means that the proton detector and its immediate surroundings are always irradiated to some extent with fast neutrons. It must be remembered too, that any attempt to shield the proton detector will probably result in a decrease in the counting efficiency, and the effect of the flux of scattered neutrons from the room relative to the direct flux from the tritium target must be considered. An alternative to shielding, which also has the advantage of high counting efficiency, is to arrange the relative

positions of neutron source, target foil, and proton detector so that the flux of neutrons at the target foil is greater than that at the proton detector by an appreciable factor. This method has been employed in both nuclear emulsion (Allan, 1957) and scintillation counter (Colli et al., 1956) techniques. The background in the proton detector due to n,p reactions in its immediate surroundings can be minimised by the use of very heavy elements such as Pb, Bi and Au in the construction of the apparatus. Carbon, with an extremely negative n,p Q value (-12.59 MeV) is also a good background material with the additional advantage over the heavier elements that not so many β and γ rays are produced when it is irradiated with fast neutrons. However, its mechanical properties, and the reaction $^{12}C(n,n^1)3^4He$, Q = -7.28 MeV limit its application. Although the background due to protons may be reduced considerably by the materials mentioned, a highly undesirable background from β and γ rays remains. This low energy background begins at approximately 4 MeV and increases exponentially with decreasing energy. The proton detector chosen must eliminate these background effects and have a minimum contribution from protons produced in the detector itself.

II.2 The Nuclear Photographic Emulsion Technique.

This was the first technique to be applied to the problem (Brown et al., 1957; Allan, 1957/58/59; March and Morton, 1958 a, b, c; Peck, 1957; Haling et al., 1957) and has much to commend it. In particular, the background from β and γ rays is readily discriminated against, and it is usually possible to measure the angular distribution of the reaction products simultaneously with the energy spectrum. Containing hydrogen, the photographic emulsion is at a disadvantage in fast neutron work due to the large number of recoil protons from the n,p scattering reaction in the emulsion. This difficulty can be overcome, however, by a suitable geometry, or a shielding technique, and application of the relationship governing the momenta of the particles in n,p scattering is helpful in most cases. A more serious disadvantage is the difficulty of obtaining good statistical errors with this technique, and is a result of the length of time required to scan the plates. In a typical experiment such as that of March & Morton, 1958, on ^{60}Ni, 2498 tracks were examined of which 792 were due to background protons. In such an experiment, it will be realised that there is quite a large statistical error on a spectrum corresponding to protons emitted into a small solid angle in the forward direction.

In this type of experiment, a thin target foil of the isotope being studied is exposed to the source of fast neutrons with a suitable arrangement of photographic plates round it to detect the protons emitted. The proton energies are estimated by measuring the length of track produced in the emulsion by the proton. Because of the finite grain density along the track, there exists a region at the surface of the emulsion several microns in depth where it is impossible to distinguish external proton tracks from tracks produced by recoil protons in this surface layer. If the position of the neutron source is known accurately, application of the momentum relationship for n,p scattering can eliminate the recoil proton tracks, or alternatively a background run with no target foil may be necessary if many inelastically scattered neutrons are present in the neighbourhood of the emulsion.

Being able to distinguish so readily between protons and electrons, the lower limit of the energy spectrum in an emulsion experiment is much lower ($\sim$1 MeV) than in the counter experiments (3-4 MeV).

[The lower limit in the counter experiments is determined by the number of electron pulses, and even where a coincidence technique is used, the random

coincidence rate is usually prohibitively high at 3 MeV for a normal fast neutron flux.]

The nuclear emulsion technique is suitable therefore for the study of the n,np reaction whose Q value is given by the binding energy (negative) of the last proton in the target nucleus. It should be noted, however, that at the lower proton energies, large corrections are necessary for the amount of energy lost by the proton in escaping from the target foil. In addition, the range of a low energy proton in the emulsion is very short and considering the error in estimating the track length a greater percentage error will be present at the lower energies.

Summarizing, one can say that this technique is well suited to the problem under consideration, since the intrinsic energy resolution is good, a good signal to background ratio is obtained, and small, thin (7-30 mg./cm^2) targets in separated isotope form can be used. However, the low efficiency of the technique impairs the resolution, gives large statistical errors especially when the background is subtracted, and limits its application to a large programme of elements.

II.3 Scintillation Counter Techniques.

The work of Colli et al., 1956, which was the stimulus for the present programme, was the first

attempt to improve on the statistics of the n,p energy spectra using a counter method. Protons produced by the n,p reaction in a target foil of the naturally occurring element pass through one or two proportional counters filled with low pressure (7 cm.Hg) CO_2 and are stopped in a CsI(Tl) scintillation counter. Pulses from the counters are fed via discriminators to a coincidence unit, and the discriminator levels on the proportional counters are adjusted so that a coincidence pulse is obtained when a proton, but not an electron, passes through the counters. This coincidence pulse is used to gate a pulse height analyser which is fed with the pulses produced in the scintillation counter. After correcting for the small energy loss of the protons in the target foil and proportional counters, the proton energy spectrum is obtained if the luminescent response of the scintillation counter for protons is known. Colli et al., have measured this response by replacing the target foil with a hydrogenous radiator and recording the pulse height spectrum of recoil protons produced by the fast neutrons.

The counters are constructed from materials with a low n,p cross section, and that part of the background spectrum due to protons produced in the CsI

travelling backwards through the telescope producing a spurious coincidence is reduced to a minimum by arranging that the neutron source is considerably nearer the target foil than the CsI crystal. The choice of CsI(Tl) as scintillator is determined by the low n,p cross sections of ^{133}Cs and ^{127}I. Some doubt regarding the suitability of CsI for this application had existed, since Paul and Clarke, 1953, measured an n,p cross section of $> 230 \pm 140$ millibarns for ^{127}I. Coleman et al., 1959, now find a value of 11.7 ± 1.6 millibarns which is in accord with the high Coulomb barrier ($\sim$ 11 MeV) of ^{127}I. CsI is further recommended by its excellent mechanical properties, good luminescent response ($\sim 3/4$ that of NaI), and its non-hygroscopic nature.

Colli et al. have produced a notable improvement in the statistical error on n,p spectra, and their technique can obtain spectra from the heaviest elements and angular distributions in the case of the high yield elements. The technique might be improved by a) the use of a smaller target foil so that separated isotopes could be used, b) a more convenient and precise energy calibration, c) a reduction in the random coincidence rate so that higher neutron fluxes might be employed, d) a smaller angle of acceptance for the

protons emitted from the target (0-40° in the latest experiments) e) a more stable neutron monitor than the plastic phosphor scintillation counter used. It may be noted in passing, that Colli et al., obtained 5% energy resolution for a collimated beam of recoil protons in the calibration of the energy scale. Since the CsI crystal was mounted without a light guide, and covered practically the whole area of the photocathode, there is some doubt - considering the usual non-uniformities in photocathodes - whether this high standard of resolution was obtained in the actual experiment.

Eubank et al., 1959 a,b, have used a technique similar to that of Colli et al., and have investigated several of the heavier elements. The signal to background ratio was never greater than 1:2 in this case, and rather large thick targets were used, however credit must be given to the low n,p cross section elements attempted. The energy resolution was 12% and the energy calibration was by recoil protons. These recoil protons from a hydrogenous radiator were also used to calibrate a long counter which was used as neutron monitor. A criticism of this type of monitor is its sensitivity to neutrons produced by the D-D reaction, since the production of D-D neutrons is not always constant, and depends upon

the drift of the deutron beam in the beam tube and the age of the bombarded tritium target.

In the experiment of Verbinski et al., 1958, the angular distribution of protons emitted from some medium weight elements was obtained simultaneously with the energy spectrum using six shielded CsI scintillation counters. Despite elegant electronics - the associated particle technique was used to produce a collimated neutron beam - the results obtained are poor. The target thickness ($2\frac{1}{2}$ MeV thick for a 6 MeV proton) precludes the observation of any fine structure, and the counting rate of less than one count per minute in each counter yields extremely poor statistics. The merit of this experiment lies in the measurement of the angular distribution, but it is doubtful if this is better than that which can be obtained with the nuclear emulsion technique.

II.4 Experimental Results of Other Investigators.

The spectra obtained are mainly exponential in form with an excess of higher energy protons; the low energy protons have an approximately isotropic angular distribution while the higher energy protons have angular distributions peaked in the forward hemisphere, the anisotropy increasing with proton energy. In the nuclear emulsion techniques of Allan, 1957, and March

& Morton 1958 a, b, the n,np reaction has been observed, a discontinuity in the relative level density log plot occurring at the maximum proton energy permissible from this reaction. The poor statistics however, render a quantitative assignment of this reaction uncertain, and this results in some inaccuracy in the "nuclear temperature" deduced for the n,p reaction residual nucleus. Direct measurement of the n,np cross section by an activation method is difficult since the residual nucleus is usually long lived if not in fact stable, however, Purser and Titterton, 1959, have measured a cross section of 160 ± 40 millibarns in the case $^{58}Ni(n,np)^{57}Co$. This is in reasonable agreement with the value 220 millibarns deduced by Allan, 1957, from the proton energy spectrum.

The "nuclear temperatures" deduced from the nuclear emulsion experiments are considerably lower than those predicted using a Fermi gas model for the level density calculation. This may be due in part to the fact that the best statistics are obtained at the lowest proton energies where the presence of the n,np reaction may depress the measured temperature. In none of the cases investigated does the relative level density log plot show a concavity down towards

the energy axis, but of course this could be explained by the presence of the n,np reaction at low proton energies and direct interaction at the higher energies.

In the nuclear emulsion experiments, estimates of the amount of direct interaction present have been made by subtracting a Maxwellian (compound nucleus) distribution which fits the backward hemisphere spectra from the spectra measured in the forward directions. This leads to an estimate that at least 20% of the n,p cross section for medium weight elements (e.g. Fe, Ni) is due to direct interactions. If a direct interaction process with an exponential energy distribution and isotropic angular distribution is present, this estimate will be too low. March and Morton, 1958, a,b, find that the energy spectrum of the direct interaction protons is in qualitative but not quantitative agreement with the theory of Brown and Muirhead, 1957. No conclusions regarding anomalous structure similar to that of Cohen, 1957, can be made due to the poor statistics at the higher proton energies.

The early results of Colli et al., which were available at the start of the present programme stressed the disagreement of the spectra with the predictions of the statistical theory and emphasised the possibility of "modulations" in the spectra due to "anomalous" effects.

Due to the poor energy resolution, the evidence for these "anomalous" effects was not very convincing, relying as it did on discontinuities in the spectra rather than discrete peaks.

II.5 The Present Programme.

The need for the present programme was dictated by the apparent anomalies in the application of statistical theory to evaporation spectra noted in Chapter I, and the possible existence of "single particle" and anomalous effects. Our previous experience with CsI(Tl) scintillation counter proton spectrometers suggested that an improvement in the statistics of the emulsion type of experiment was possible, and at the same time we hoped to improve on the experimental technique of Colli et al. The programme was designed with two aims 1) the determination of evaporation spectra suitable for comparison with the statistical theory and 2) the measurement of the spectra of protons emitted into a small solid angle in the forward direction where direct and anomalous effects are most likely to occur. In 2) we hoped to improve the technique of Colli et al. by a) using separated isotope targets b) improving the energy resolution, energy calibration and neutron monitoring, and c) employing a much smaller solid angle of accept-

ance in the telescope so that angular distributions might be attempted at a later date.

Chapter III.

The Measurement of n,p Proton Energy Spectra for Comparison with the Statistical Theory.

III.1 Development of the Apparatus.

The geometry of this experiment was chosen so that direct interactions did not have an undue influence on the final result. Ideally, since most direct interaction theories predict angular distributions peaked in the forward hemisphere due to the conservation of momentum in the nucleon-nucleon interaction, one would like to measure the energy spectrum of protons emitted into a small solid angle in the backward hemisphere. (One would not choose the extreme backward direction of course, since little is known of the existence of the spot heating effect). The low efficiency, and more important, the poor signal to background ratio expected on account of the unfavourable relative positions of neutron source - detector- and target foil make this geometry unsuitable in practice, and we decided to try a 2π geometry. In the geometry envisaged, the thin target foil would be placed in close contact with a CsI(Tl) scintillation counter which would detect the protons emitted from the foil. If the neutron source lies in the same plane as the target foil, the geometry is effectively 2π, and

the resulting spectra should not be greatly distorted by the familiar direct interactions since Allan, 1957, and Colli et al., have shown that even at forward angles by far the greatest part of the spectrum can be attributed to protons from the decay of compound nuclei. It will be seen, that in the final model of the apparatus, protons emitted into the extreme forward and backward angles were not detected, further reducing the effect of direct interactions.

The success of this geometry, in which no coincidence techniques would be employed, depended on the extent to which we could suppress the production of protons in the CsI and its surroundings by the fast neutrons. In this respect the anomalously high n,p cross section for ^{127}I (230 $\pm$ 140 millibarns) quoted by Paul and Clarke, 1953, was not encouraging, however, a preliminary experiment proved that this measurement was too high by an order of magnitude. A CsI(Tl) crystal 1.5" in diameter and 0.080" thick was mounted on a Du Mont 6292 photomultiplier using silicone grease. The crystal was covered with a thin (0.2 mg./cm^2) aluminium foil to act as a light reflector, and a cover plate of 0.020" lead was placed on top. This assembly was irradiated with the T-D neutrons in a head on position, and the voltage pulses from the

photomultiplier, after suitable amplification, were fed to a pulse height analyser of the Hutchinson Scarrott, 1951, type. The neutrons were monitored using a plastic phosphor scintillation counter biassed half way along the recoil proton spectrum. A piece of 0.010" thick plastic (formula $(CH)_n$) was inserted between the aluminium foil and the lead cover plate, and the assembly was irradiated under the same conditions as before for the same number of neutron monitor counts. The new spectrum showed an unmistakeable increase due to recoil protons, and a simple calculation showed that the observed signal to background implied a cross section $\leqslant 50$ millibarns for the $^{127}I(n,p)^{127}Te$ reaction.

The electronics employed in this experiment and subsequent developments are shown in Appendix I. The voltage pulse from the Du Mont 6292 was clipped to 2 μsec length in a head amplifier, and an I.D.L. type 652 was used for additional amplification.

Reducing the thickness of the CsI(Tl) crystal to 0.050" (i.e. the range of a 15 MeV proton) the experiment was repeated with a piece of aluminium foil (21 mg./cm^2) between the lead cover plate and the thin aluminium light reflector. The two irradiations - foil in, - foil out, are shown in figure III,i.

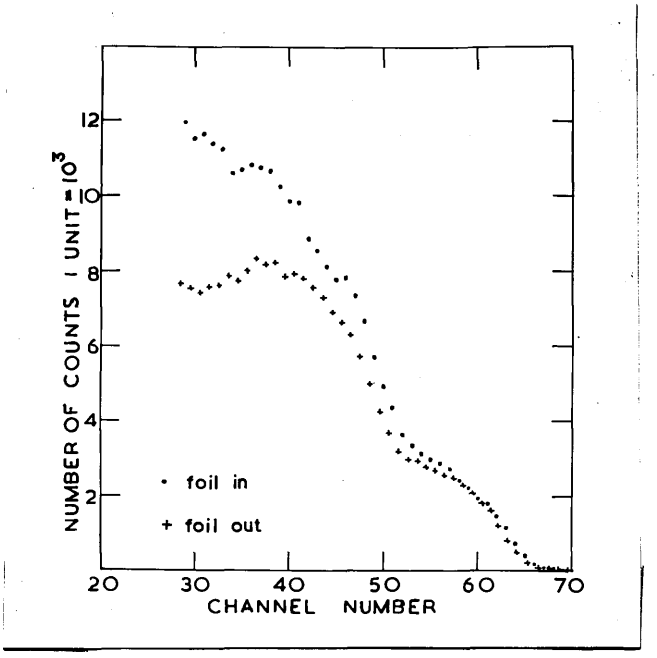

Figure III.i. Foil in, Foil out, pulse height spectra obtained for an aluminium foil 21 mg./cm^2.

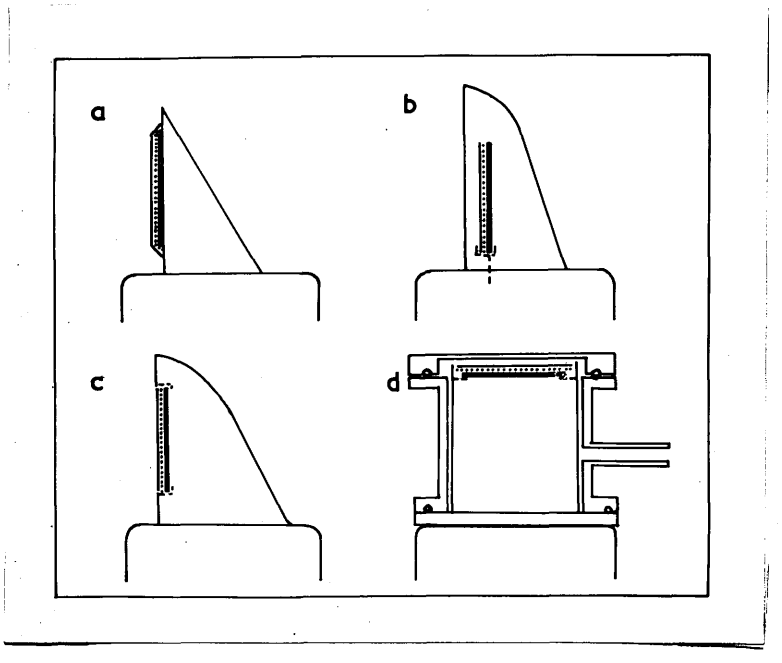

Figure III.ii. Stages in the development of the apparatus.
a) Glass Prism b) Reflector Mounting
c) Improved Reflector Mounting d) Vacuum Reflector Mounting.

Although the signal to background ratio is poor, this result is encouraging when the low ^{27}Al n,p cross section is considered (Paul and Clarke, 1953, σ = 52 $\pm$ 10 millibarns). The background spectrum in the CsI alone has steep edges in the neighbourhood of 14 and 11 MeV and a broad ~~bump~~ peak at 8 MeV. These edges are troublesome when the background is subtracted, since they lead to the introduction of spurious peaks in the subtracted spectrum if a slight gain shift occurs during one of the irradiations.

The pulse height response curve was obtained by irradiating the crystal with the proton groups from the reaction $^{10}B(d,p)^{11}B$, Q = 9.235, 7.097, 4.776, 4.201 MeV. Irradiating the whole crystal, the spectra obtained were poor; the resolution was 15% (full width at half maximum) and the peaks were assymmetrical. This assymmetry was removed and the resolution was improved to 7% if only the centre portion (1.5 cm. in diameter) of the crystal was used.

To improve the signal to background ratio, we decided to use a thinner CsI crystal. This new crystal was 1.1" in diameter and 0.032" thick and was mounted on a glass prism as shown in Figure III,ii,a. The reduced thickness, which corresponds to the range of an 11.5 MeV proton, has little effect on the spectra,

but this will be discussed in detail below. The author has found in a previous experiment that this type of light guide gives particularly good resolution, the light from any point in the scintillator being spread over a large area of the photocathode. It has the additional advantage that the scintillator can be irradiated at any angle between 0^{o} and 180^{o} without the photo-multiplier coming between the neutron source and the scintillator. The crystal was attached to the prism with a thin film of silicone grease as optical coupling, and was covered with a 0.2 mg./cm^{2} aluminium leaf and a 0.020" lead cover plate. The prism was wrapped in 0.002" aluminium foil which acted as a reflector. Irradiating the crystal with the $^{10}B(d,p)^{11}B$ proton groups to calibrate it, 6% energy resolution was obtained.

The new assembly was irradiated with T-D neutrons, the neutrons being incident from left to right in figure III, ii, a. Irradiations for equal numbers of neutron monitor counts were carried out a) with a foil of some element between the lead cover plate and the crystal assembly and b) with no foil present. The spectra obtained for 50 mg./cm^{2} foils of Au and Pt showed no significant increase over the foil out background spectrum. A 13 mg./cm^{2} foil of Al gave a

slightly better signal to background ratio than is shown in Figure III, i, where it will be remembered the Al foil was 21 mg./cm^2., and a 22 mg./cm^2 Ni foil, gave a signal to background ratio of unity.

The above spectra were due to protons emitted into the forward hemisphere. In an effort to measure the spectrum of protons emitted into the backward hemisphere, a Ni foil was irradiated with the neutrons incident from right to left in Figure III,ii,a. As was expected the spectrum obtained was dominated by recoil protons from the thin film of silicone grease. To overcome this difficulty, the assemblies shown in Figures III,ii,b and c were devised. In figure b, the crystal with its thin light reflector and lead cover plate were mounted with silver wire under a reflecting cavity made of 0.020" Pb lined with 0.2 mg./cm^2 aluminium leaf. Foil in, - foil out irradiations with a Ni foil and with the neutrons incident first from left to right, then from right to left gave an encouraging result, and led to the improved apparatus shown in Figure III,ii,c. Here, the crystal is mounted in a window of the lead reflector so that the foil can be changed easily and the apparatus calibrated. Instead of lining the lead with aluminium leaf, a reflecting cavity was formed by evaporating a thin layer of

aluminium on to the lead in a high vacuum. The spectra obtained for a 22 mg./cm^2 Ni foil for protons emitted into the forward and backward hemispheres with the appropriate background spectra are shown in Figure III,iii. An anisotropy of the order of 15% is present, and an interesting feature of the spectra is the presence of a slight peak at channel 23 in the "0°" spectrum. From the later experiments it will be seen that a plausible explanation of this discontinuity is that it is caused by an n,d transition.

Some of the 15% assymetry may be attributed to the characteristic angular distribution of the n,d pick-up reaction. A comparison of the relative isotopic abundances of ^{58}Ni and ^{60}Ni(68%, 26.2%) and their Q values for the n,p reaction (+ 0.6 and - 2.0 Mev) suggests that the spectra of Figure III,iii are mainly due to the ^{58}Ni(n,p)^{58}Co reaction. A similar experiment with a copper foil where the yield is down by a factor of 3 gave an assymmetry of the order of 50%. The ^{63}Cu(n,p)^{63}Ni reaction will dominate in this case; Allan, 1957 quotes a cross section $<$ 30 millibarns for the ^{65}Cu(n,p)^{65}Ni reaction, and relative isotopic abundances are ^{63}Cu - 69%; ^{65}Cu - 31%.

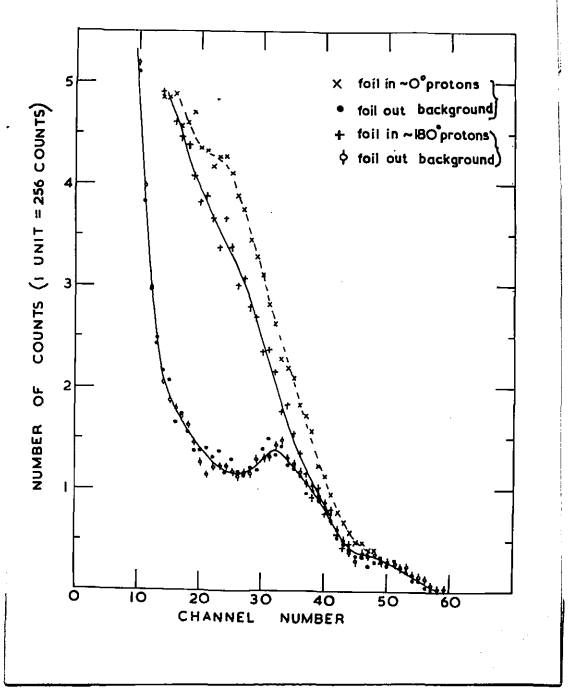

Figure III.iii. Foil in, Foil out, pulse ht. spectra for forward and backward hemispheres. Ni foil 22 mg./cm^2.

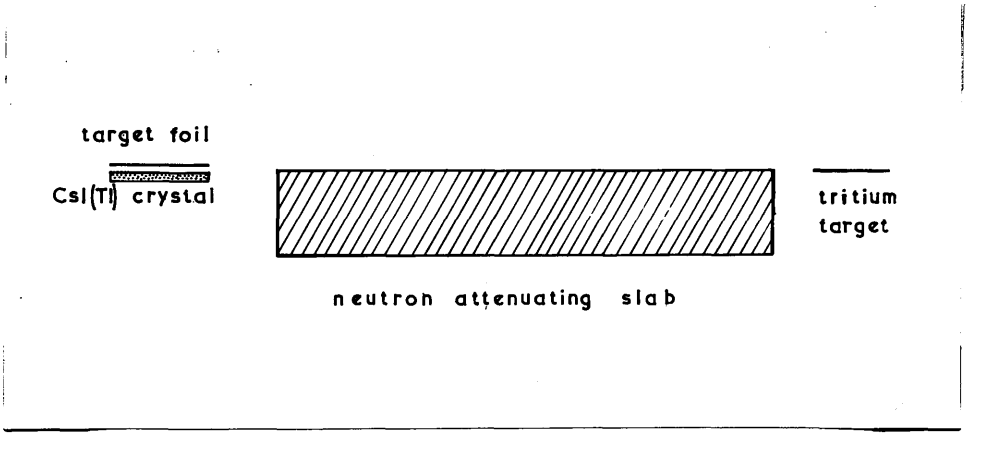

Figure III. 1V. Schematic diagram of the geometry of the apparatus.

Although the signal to background ratio was improved with this apparatus, it was found that the resolution was not good, (8%), the peaks having an assymmetrical shape, and the background subtraction was not particularly good either due to the broad peak in the background spectrum. To improve the resolution, and to investigate the possibility that the peak in the background spectrum might be partly due to air in the apparatus, the assembly shown in Figure III,ii,d was constructed. The crystal with its thin aluminium reflector and lead cover plate was mounted in the end of a reflecting cylinder formed from 0.020" lead covered with a thin layer of evaporated aluminium. This lead cylinder was enclosed in a brass cylinder which could be evacuated. The ends of this cylinder were removeable, the lower end being made of glass and was optically coupled to the photomultiplier using silicone grease. Upon irradiating the crystal when the apparatus was evacuated, the background spectrum obtained showed no significant difference from that obtained with air in the apparatus. This background spectrum is similar to that shown in figure III,iii, and it will be seen that the broad peak seems to contain some structure. The dual nature of the peak was confirmed in subsequent irradiations with the neutrons

incident at different angles. The n,d reaction Q values for ^{127}I and ^{133}Cs are both -4.1 MeV and it seems possible that the ground state pick-up reaction may be responsible for the discontinuity at 10 MeV since the bombarding neutron energy is 14.1 MeV. The major part of the peak between 7 and 11 MeV is due most probably to the straightforward n,p reaction in ^{133}Cs and ^{127}I, since the high Coulomb barrier ($\sim$11 MeV) will displace the maximum of the Maxwellian evaporation spectrum to higher energies.

To investigate the possibility that protons from the glass of the photomultiplier or the cylinder end were contributing appreciably to the spectra, the glass cylinder end was replaced by one made of "Perspex". Irradiating the apparatus in the head on position, no recoil protons from the perspex could reach the crystal, and the -12 MeV Q value of the $^{12}C(n,p)^{12}B$ reaction ensured that the carbon in the perspex did not contribute to the spectra. The background spectrum obtained was the same as that measured with a glass cylinder end.

Irradiating the apparatus with cover plates of lead, bismuth, gold, silver and graphite behind the crystal, the background spectra were recorded. There was very little variation in the spectra obtained, but bismuth seemed to give the lowest background at

the higher energies, while graphite gave the lowest background at the lower energies. These background reductions were inconsequential except in the case of silver where a background 50% higher than that of lead was obtained.

An examination of the pulse height spectra in the crystal at varying short times after irradiation showed that residual activities were not a serious problem, and would not contribute spurious pulses or affect the resolution to any extent.

Having reduced the background in the detector itself to a minimum, we were now in a position to consider the use of neutron collimation to reduce the signal to background ratio. The usual form of fast neutron collimator, consisting of a block of attenuating material with a hole through it, suffers from two disadvantages, a) an appreciable separation between the target foil and the detector is introduced leading to a large reduction in counting efficiency b) inelastic neutron scattering in the attenuating material produces a non-monoenergetic neutron beam. These difficulties are largely overcome in the form of shielding shown in Figure III,1V. The tritium-titanium neutron source lies in the same plane as the surface of a slab of the attenuating material, and the detecting CsI crystal,

with its plane parallel to this surface, is mounted just below the surface and in the geometrical shadow of the slab. The target foil, no longer in contact with the crystal, lies just above the surface and is exposed to the direct beam of neutrons. The small amount of attenuating material used reduces the amount of inelastic neutron scattering present, and the counting efficiency is reduced by only a factor of ~two compared to a 2π counting arrangement. Considering the extremely anisotropic angular distribution of elastically scattered fast neutrons, there may be an appreciable number of elastically scattered neutrons in the neighbourhood of the target foil. This will affect cross section measurements to some extent, but not the energy resolution since these neutrons scattered in the forward direction will have practically their original energy due to the small centre of mass effect involved.

This shielding arrangement proved successful in practice, but we will interrupt the development here to consider some features of the apparatus which have a bearing on the reliability of the final results.

III.2 Remarks.

a) Neutron Monitoring.

Our experience in reducing the background in CsI(Tl) scintillation counters irradiated with T-D neutrons led to the development by Dr. Storey of this group of a new type of neutron monitor. This monitor, a diagram of which is shown in Figure III,V, consists of a high efficiency proton recoil telescope where no coincidence arrangement is required to eliminate pulses due to electrons. The polythene radiator and CsI crystal are mounted in the ends of a lead cylinder of adjustable length, the light from the crystal being collected by an arrangement similar to that described above. The air in the apparatus was removed to avoid a small background caused by n,p and n,d reactions in nitrogen. The geometry of the telescope was chosen to correspond to the accurate computations of Bame et al., 1957, and the absolute efficiency is known to better than $\pm$ 3%. Figure III.V1, shows the pulse height distribution due to recoil protons when the monitor is irradiated with 14 MeV neutrons. The dashed curve shows the background spectrum when the polythene radiator is removed; the efficiency is corrected for this, the ratio of areas $\frac{A}{A+B} = 0.725$. This type of monitor is more stable than the more usual plastic

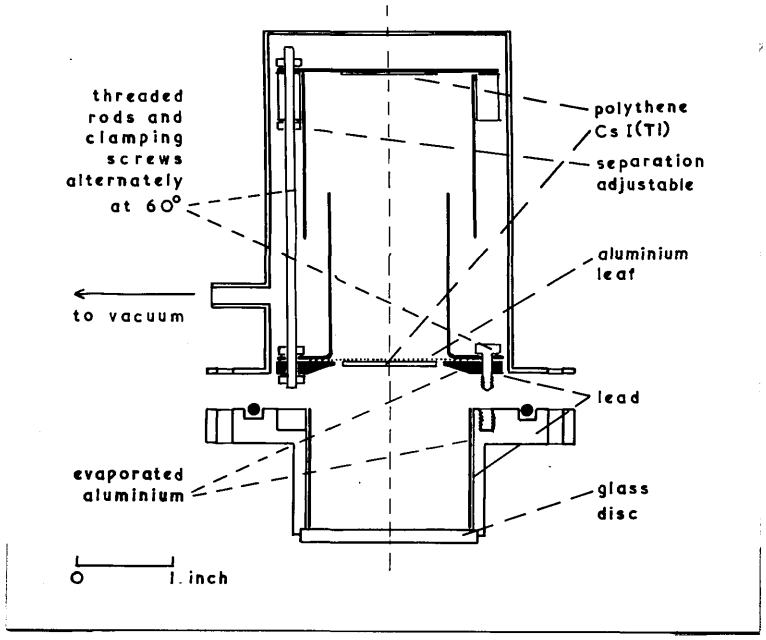

Figure III.V. High efficiency fast neutron monitor of the recoil proton type.

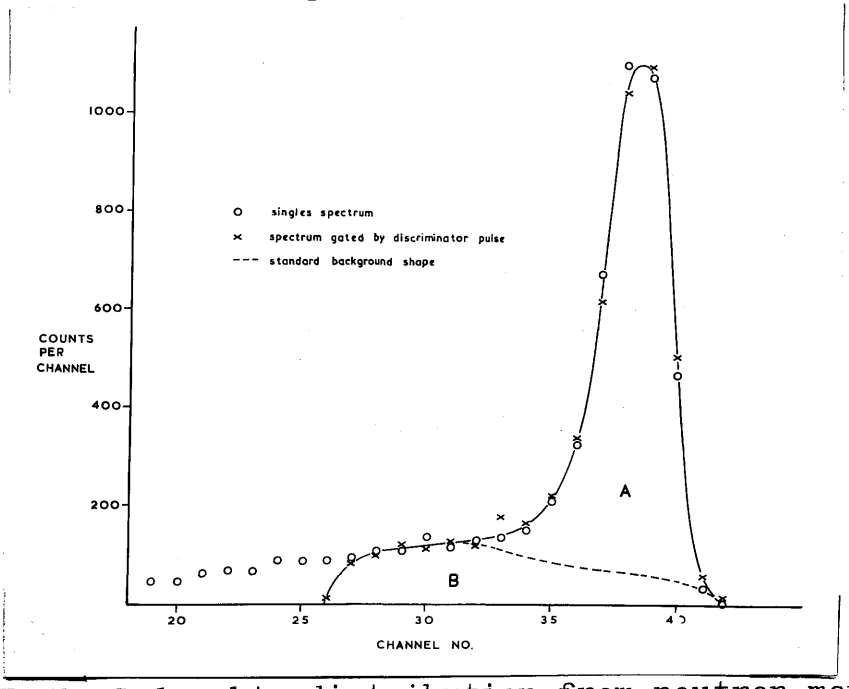

Figure III.VI. Pulse ht. distribution from neutron monitor irradiated with 14 MeV neutrons. O - single spectrum; x - spectrum gated by discriminator; ------background spectrum, polythene radiator removed.

phosphor scintillation counter, since, producing a peak, small changes in discriminator level and gain can be tolerated. In addition, it is directional in operation, and so the effects of inelastically scattered neutrons can be minimised. The monitor is surprisingly efficient - when the radiator is 8.5" from the neutron source the efficiency $\epsilon = 10^{-6}$ where ϵ is defined as the number of monitor counts ÷ number of neutrons/unit solid angle.

b) Validity of the Subtracted Spectrum.

It has been assumed up till now that the "foil in" - "foil out" spectrum represents the energy spectrum (taking the luminescent response of the CsI(Tl) into account) of protons from the n,pγ and n,pn reactions. This requires some justification. There is, of course, a contribution from the n,np reaction at the lower end of the spectrum, and in this region too the n,pp reaction is possible, but the latter reaction is rendered improbable when the effect of the Coulomb barrier is considered with competition from the n,pn reaction. When the compound nucleus formed by the incident fast neutron decays by emitting a proton, the excited residual nucleus left behind will decay by emitting a further particle or a cascade

of γ-rays. Upon reaching its ground state, the residual nucleus, which is invariably radioactive, will decay emitting β particles and γ-rays. Two cases arise; in case I the original proton is not detected but there is a possibility of detecting the subsequent radiation. In case II, which is the more serious one, part of the subsequent radiation may be detected simultaneously with the original proton.

Both cases depend upon the ability of the crystal to detect the subsequent radiation. Taking the case of neutrons first. These may be produced by the n,n^1; $n,2n$; n,np reactions in the target foil. Since the crystal used is of the order of 1 mm. thick, it will be a good approximation to say that the average thickness encountered by neutrons or γ-rays passing through the crystal is $\leq$ 2 mm. Taking the reaction cross section for fast neutrons in CsI at 2 barns, less than one neutron in a hundred will produce a nuclear reaction in passing through 2 mm. of CsI, and very few of these nuclear reactions would produce sufficient pulse height to affect the spectra, indeed using the n,p cross-section in Cs and I ($\sim$ 10 millibarns) we find that 4 in 10^5 neutrons will produce a proton. For γ-rays, the mass attenuation coeff. for the energy range 4 to 10 MeV (Evans, 1955, $\mu_0/\rho = 0.04$ cm^2/gm CsI.

μ_o/ρ=0.04 cm^2/gm. CsI) implies that 3.6% of these γ -rays interact with the crystal, and, due to the small size of the latter, hardly any of the γ -rays produce pulses equivalent to their full energy. In addition, there is a very small probability that the γ -ray cascade will contain γ -rays with energy greater than 4 MeV. We conclude that case I can be dismissed completely, neither neutrons nor γ-rays contributing appreciably to the final spectra.

In case II, we fear that the simultaneous detection of a γ-ray with the original proton will distort the spectra, because the output pulse from the scintillation counter will no longer be proportional to the original proton energy. Since the solid angle of acceptance of the CsI crystal for radiation from the target foil is approximately π, if we assume that the cascade γ -rays are distributed isotropically in space, only a quarter of the γ -rays associated with the proton will pass through the crystal. Using the data given in Evans, 1955, one finds that 9% of 0.5 MeV γ -rays will interact with a 2 mm. thickness of CsI, and again not all of these interactions will produce pulses large enough to affect the spectra. Combining the factors deduced, it seems unlikely that Case II is a serious source of error.

c) Energy Resolution and Counting Efficiency.

Since the protons are produced at different depths of the target foil, and emerge at quite oblique angles due to the "bad" geometry employed, a mono-energetic proton group will not produce a line spectrum even if the counter resolution is perfect. Assuming that to a first approximation the angular distribution of the protons is isotropic, Dr. R.S. Storey has calculated the efficiency and the expected distributions for 12, 8 and 4 MeV proton groups as a function of the geometry. The result is shown in Figure III,V11, where U is the separation of the target foil (15 mg./cm^2) from the crystal, the diameter of target foil and crystal being given by 2B. ϵ_p is the energy of the proton detected and $f(\epsilon_p)$ is the function relating the counting efficiencies of the different geometries to the 2π efficiency. The value U/2B = 0.133 was used in the actual experiment and this gave a solid angle of acceptance = $(0.56 \pm 0.02)2\pi$. The width of the top of the "peak" corresponds to the energy lost by a proton passing through the whole target thickness perpendicularly, and it is found that to a good approximation, the centroid of the peak (used in the correction of the energy scale of the spectra) lies at a distance 2/3 of this width from the energy of the

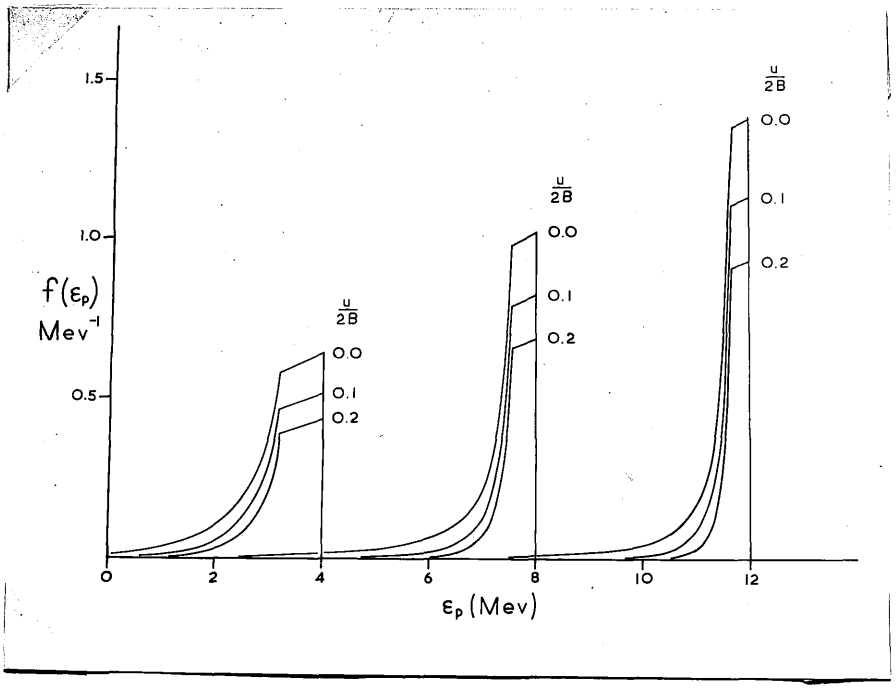

Figure III.V11. The calculated pulse ht. distributions for 12, 8 and 4 MeV protons emitted from a 15 mg./cm^2 medium weight target foil. The counting efficiencies relative to the "2π" efficiency are given as a function of the geometry. U = target foil, crystal separation; R = radius of crystal. Actual geometry used corresponds to U/2B = 0.133.

upper edge. This correction introduces a slight non-linearity into the energy scale with a resulting effect on the channel width. The final spectra are corrected for this slight effect.

d) Correction for Crystal Thickness.

We have seen how the crystal thickness chosen was slightly less than the range of the maximum energy protons expected in order to reduce the background from protons produced in the crystal itself and minimise the pulse height produced by γ-rays. It can be shown that the correction for this effect is negligible. In the experiment with 14 MeV neutrons the crystal chosen was 0.035" thick i.e. 400 mg./cm^2 or the range of a 12.3 MeV proton. We will assume as a first approximation that the angular distribution of the protons is isotropic, but in actual fact any peaking of this distribution in the forward direction will reduce the correction appreciably, since these protons traverse the crystal obliquely. Considering a 2π geometry for simplicity, those 14 MeV protons which traverse less than the range of a 14 MeV proton in CsI(490 mg./cm^2) will have reduced pulse heights. The 14 MeV protons emitted into a cone whose axis is perpendicular to the plane of the crystal and whose semi-angle α is given by cos α = 400/490 will be affected in this way, but the number of 14 MeV protons

involved is small ($< 1/5$ total) since the solid angle subtended by the cone is given by $2\pi(1 - \cos \alpha) = 2\pi(0.18)$. In most cases the reduction in pulse height will be small - the number emitted at angle α is proportional to sin α for an isotropic distribution. The correction also decreases rapidly as the initial proton energy approaches 12.3 MeV due to the non-linear character of the range energy relationship.

III,3 Final Form of the Apparatus.

The apparatus is shown in Figure III,VIII, the inset showing the crystal - target foil assembly on an enlarged scale. A general view of the apparatus is shown in Figure III,IX. Separated isotope targets of ^{54}Fe, ^{56}Fe, ^{58}Ni, ^{60}Ni, ^{65}Cu and ^{64}Zn were obtained from A.E.R.E., Harwell. These targets were in the form of a deposit 1.5 cm. in diameter and 15 mg./cm^2 thick on a platinum backing 0.005" thick and 1" square. They were mounted between an annulus and a disc of bismuth as shown, the complete target holder being secured to a bismuth ring which supported the crystal. The target foils could be interchanged without altering the target foil-crystal separation. Bismuth was chosen as the background material, since in addition to its high Z number it is also an odd-even element which inhibits

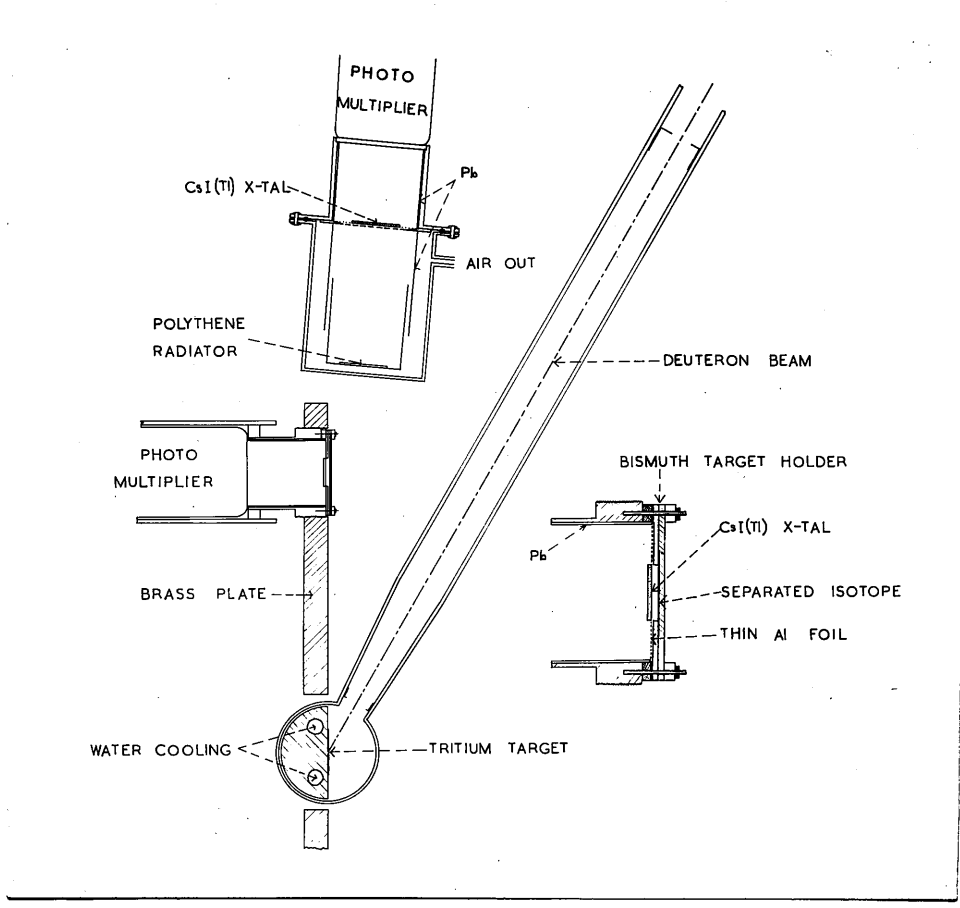

Figure III.V111. The Final Form of the Apparatus. The inset shows the crystal-target foil assembly on an enlarged scale.

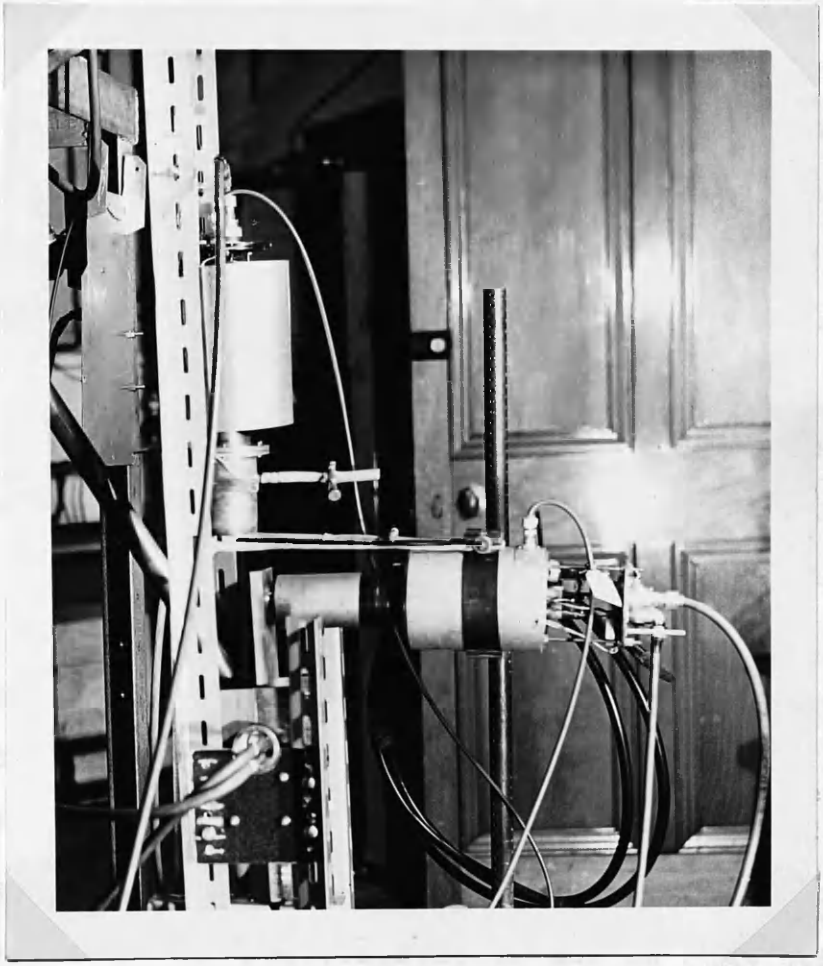

Figure III.1X. General View of the Final Apparatus.

the n,p reaction in competition with the n,n^1 reaction when the level densities in the residual nuclei are considered. Coleman et al., 1959, measure an n,p cross section of 1.3 ± 0.3 mb. for bismuth. Being rather brittle, bismuth resists mechanical deformation which helps us to maintain the target foil-crystal distance constant at 2 mm.

The crystal, 1.5 cm. in diameter, was mounted in the end of a reflecting cylinder; it was rigidly attached to its bismuth supporting ring by two 0.005" platinum wires with minute spot-welded platinum wire hooks. A leaf of 0.2 mg./cm^2 aluminium between the crystal and the target foil formed the reflecting end of the cylinder, the curved surface of which was constructed from 0.020" lead with a reflecting surface layer of evaporated aluminium. This lead cylinder was contained in an outer cylinder of brass, one end of which rested on the photocathode of the Du Mont 6292 photomultiplier, a light seal being formed with the mumetal shield. The other end of this cylinder was threaded and screwed into a hole in the attenuating slab, one revolution moving the crystal and target foil by 1 mm. relative to the surface of the attenuating slab.

The luminescent response of the CsI(Tl) crystal was measured using proton groups from the reactions

$^{3}He(d,p)^{4}He$ Q = 18.341 MeV, $^{10}B(d,p)^{11}B$ and $^{2}H(d,p)$ ^{3}H Q = 4.032 MeV. The response was found to be extremely linear with a slight positive intercept on the energy axis. This intercept was $\leq$ 0.1 MeV. Several photomultipliers were tested and the ^{10}B $(d,p)^{11}B$ spectrum from the photomultiplier selected gave 4% resolution for the 8.5 MeV proton group. This spectrum is shown in Figure III.x; the peaks labelled B are the proton groups from the $^{10}B(d,p)^{11}B$ reaction, the peaks labelled A are from the $^{10}B(d,\alpha)^{8}Be$, Q = 17.81, 15.08 MeV reactions. For convenience in checking the gain of the electronics, and to provide a calibration, the response of the crystal for electrons relative to that for protons was measured. The surprising result was obtained that the crystal was more efficient when excited by protons than by electrons. Furthermore, the relative efficiency was dependent on the clipping time employed. Table III.1 shows E_p* the energy of proton which gave the same pulse height as the total capture peak of the 0.662 MeV γ-ray from ^{137}Cs, the γ -ray pulse being amplified by a factor of ten relative to the proton pulse; E_p* is given as a fn. of τ the length of the clipped pulses. This variation of relative efficiency with length of clipping time suggested that a difference in the voltage pulse rise

TABLE III.1.

τ μsec.	0.5	1.0	2.0	4.0	∞
E_p^* MeV.	3.95 ±0.05	4.05 ±0.05	4.45 ±0.05	4.75 ±0.05	4.90 ±0.05
$\frac{6.62}{E_p^*}$	1.68	1.64	1.49	1.39	1.35

E_p^* is the energy of proton producing the same pulse height as a "6.62" MeV electron (i.e. the total capture peak of the 0.662 MeV γ-ray of ^{137}Cs amplified by a factor of ten). E_p^* and the relative efficiency $6.62/E_p^*$ are given as a function of τ the clipping time employed in the head amplifier.

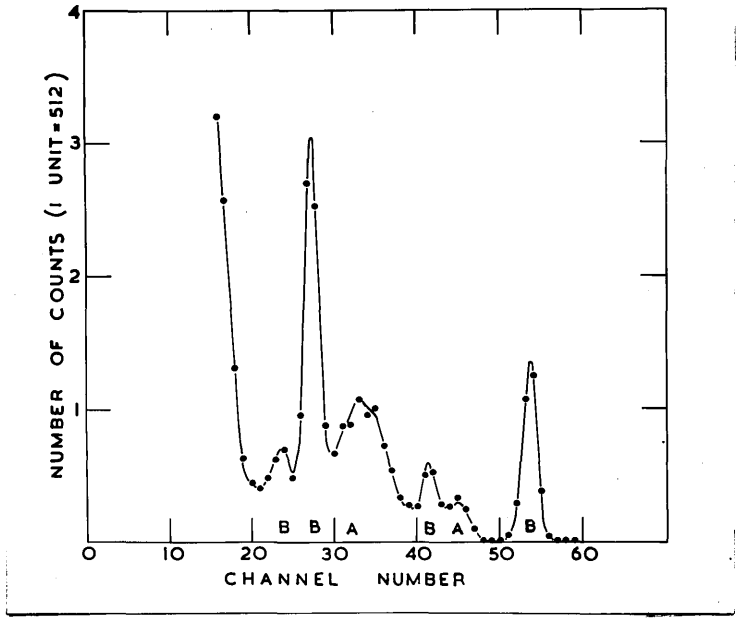

Figure III.X. Pulse ht. distribution from CsI(Tl) scintillation counter irradiated with protons and alpha particles from the reactions $^{10}B(d,p)^{11}B$ and $^{10}B(d,\alpha)^{8}Be$. The alpha particle and proton peaks are labelled A and B respectively.

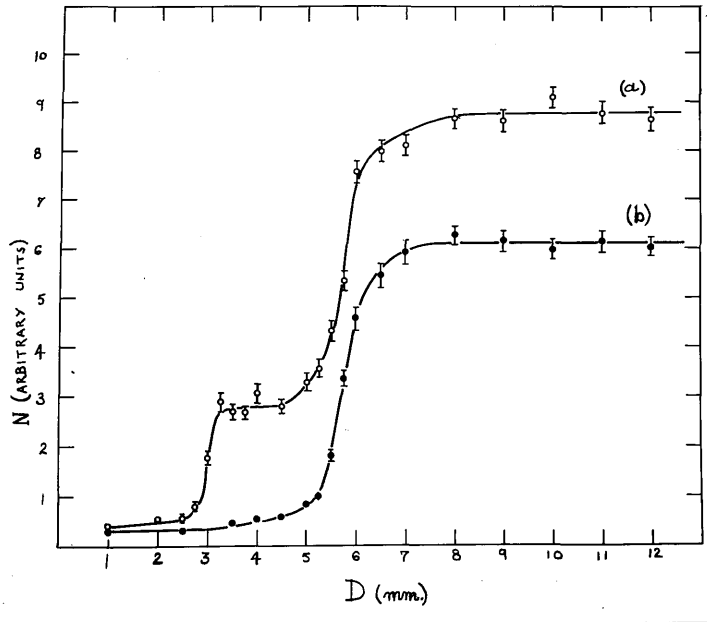

Figure III. XI. N, the number of counts corresponding to protons of energy > 8 MeV, for a fixed number of monitor counts, plotted as a function of the position of the crystal-target foil assembly relative to the brass plate. The zero of the abcissa scale is not significant. a) Ni foil 15 mg./cm^2 in. b) Foil out.

time existed for protons and electrons. This difference in the decay time of the luminescence excited by different types of particle was investigated in detail and the results are reported in Storey, Jack and Ward, 1958.

The apparatus of Figure III.V111, was designed so that, using the centre of mass motion of the deuteron, we could irradiate the target foil with different energies of neutron. With the target foil assembly mounted in the forward (not shown) and backward attenuating slabs, neutron energies of 15.7 and 13.0 MeV were obtained when the deuteron bombarding energy was 600 Kv. The spread in neutron energy was $\sim$ 0.1 MeV. The tritium-titanium target was attached to the cooling block with Wood's metal so that its surface lay in the machined surface of the attenuating slab, and the whole apparatus could rotate with respect to the deuteron beam so that a range of neutron energies could be obtained if desired. Measurements were also made with neutrons of energy 14.1 MeV. In this case the attenuating slab was twice as long (7.5") as that shown in Figure III.V111 and the deuteron beam was perpendicular to the attenuating slab. The energy of the bombarding deuterons was 160 Kv, and as at 600 Kv, beam currents were of the order of 100 μ amp. producing a neutron flux of about 5×10^9

neutrons/sec. into 4π.

The neutron monitor previously described was mounted near the target foil as shown so that variations in the neutron flux at the target foil due to the deuteron beam drifting from one side of the tritium target to the other were accounted for. The pulses from the neutron monitor were fed to a ratemeter as well as a scaler so that the neutron flux could be maintained constant.

Before carrying out measurements of n,p spectra, the best position of the crystal - target foil assembly relative to the brass plate was obtained by observing the number of pulses in the CsI(Tl) crystal for a fixed number of neutron monitor counts as the crystal - target assembly was rotated. The bias on the scaler recording the CsI(Tl) counts was set at approximately 8 MeV proton energy. It was found to be important to keep the photomultiplier firmly in contact with the end of the reflecting cylinder during this experiment so that no change in light collection efficiency occurred. A typical result is shown in Figure III.X1; the zero of the abcissa scale is not significant. The curve labelled b) was obtained with no target foil, and the curve a) for a 15 mg./cm^2 target of ^{58}Ni. No appreciable change was found in the positions of the edges when these runs were repeated, and a position about half-way

along the lower plateau in curve a) (D ~ 4 mm.) was chosen for the experiments. Figure III.X1. was obtained for the longer brass plate. Defining the attenuation as the ratio of the ordinates at D = 1 mm. and D = 8 mm. in curve b), the attenuation of the plate 7.5" long was 20:1 and of the brass plate 3.75" long about 4:1. The flat plateaus observed show that there is little evidence of appreciable scattering by the brass plate increasing the neutron flux above that measured on the monitor. Much of the width in the edge of curve b) is due to the finite thickness of the CsI(Tl) crystal.

Preliminary runs with platinum target foils showed that the background spectrum remained unchanged when the platinum foil was inserted into the target holder. Three runs were made at neutron energies 13 and 15.7 MeV for each of the isotopes ^{54}Fe, ^{58}Ni and ^{64}Zn, and three runs at 14.1 MeV were made for ^{27}Al, ^{54}Fe, ^{56}Fe, ^{58}Ni, ^{59}Co, ^{60}Ni, ^{63}Cu, ^{64}Zn and ^{65}Cu. For ^{27}Al and ^{63}Cu, natural foils of the element were used, a slight correction being necessary to the ^{63}Cu spectrum for the presence of ^{65}Cu (isotopic abundance 31%) which has a very low n,p cross section, Allan, 1957, $\sigma < 30$ millibarns. A target of ^{59}Co on a platinum

backing was prepared by Mr Lloyd of this department by electro-deposition. Each irradiation lasted half an hour, and between runs the gain of the photomultiplier was checked using a ^{137}Cs source of γ-rays. The position of the peak in the neutron monitor spectrum was also checked frequently. The results of each run were first plotted separately to check for consistency, then averaged. The background was measured six times at intervals between element irradiations using the same neutron flux, and each "foil out" background run was plotted separately before they were all averaged. As figure III.X1. implies, the signal to background ratio was good and the "foil in" "foil out" spectra for ^{58}Ni irradiated with 14.1 MeV neutrons are shown in Figure III.X11.

III.4 Experimental Results.

Each point of the subtracted spectra was corrected for small effects due to the finite thickness of the separated isotope target and was replotted on the proton energy scale. There was some evidence of structure in the spectra, but since this will be discussed in detail in the following chapters the data is presented in the form most suitable for comparison with the statistical theory. Figure III.X111. shows

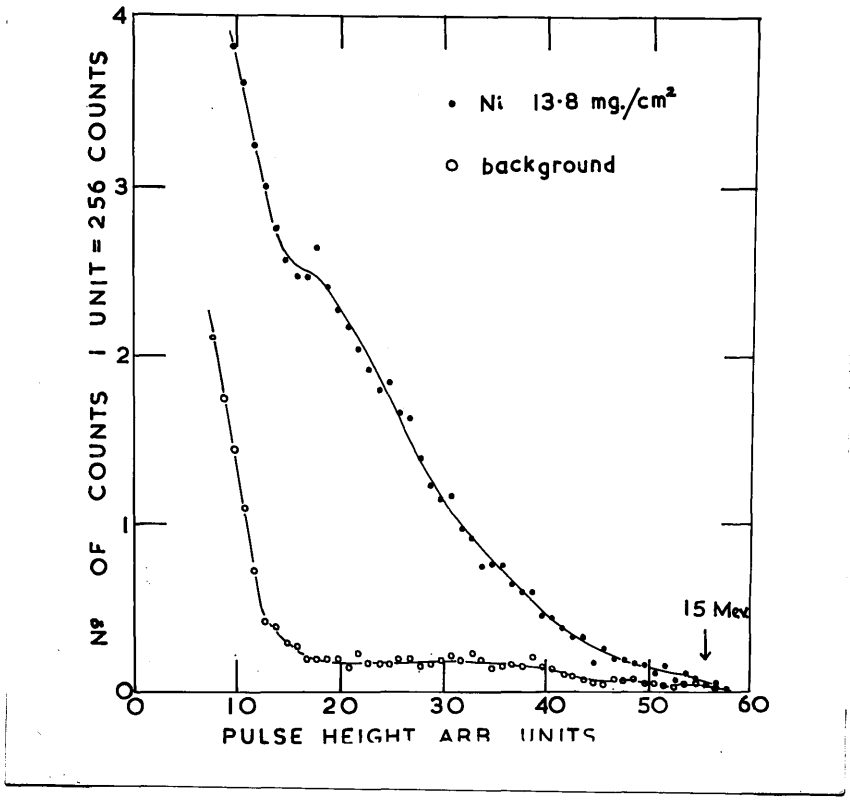

Figure III. X11. "Foil in","Foil out" spectra obtained with final apparatus for a 13.8 mg./cm^2 Ni foil.

the corrected data in the form $\log_{10}\left[\sigma(E_p) \div E_p\sigma_c\right]$ versus E_p where $\sigma(E_p)$ is the proton emission cross section per unit energy for protons of energy E_p, and σ_c is the cross section for formation of the compound nucleus by the inverse reaction where a proton of energy E_p is incident upon the excited residual nucleus of the present experiment. The values of σ_c were calculated from the tables of Blatt and Weisskopf (1952) using a value of $r_o = 1.5 \times 10^{-13}$cm. Figure III. XIII. shows the data obtained with a neutron bombarding energy of 14.1 MeV. For convenience the curves are displaced arbitrarily with respect to the ordinate scale. The energy spectra measured at 13.0 and 15.7 MeV are shown in Figure III.XIV and again the ordinates of the curves are displaced arbitrarily. The full lines in Figures III.XIII and III.XIV are the best straight lines which can be drawn through the points above about 6 MeV. The slopes of these lines represent what we will call a "nuclear temperature", denoted by T. The term "nuclear temperature" is used here for convenience, the relation between T and the true nuclear temperature θ has been discussed in Chapter I.

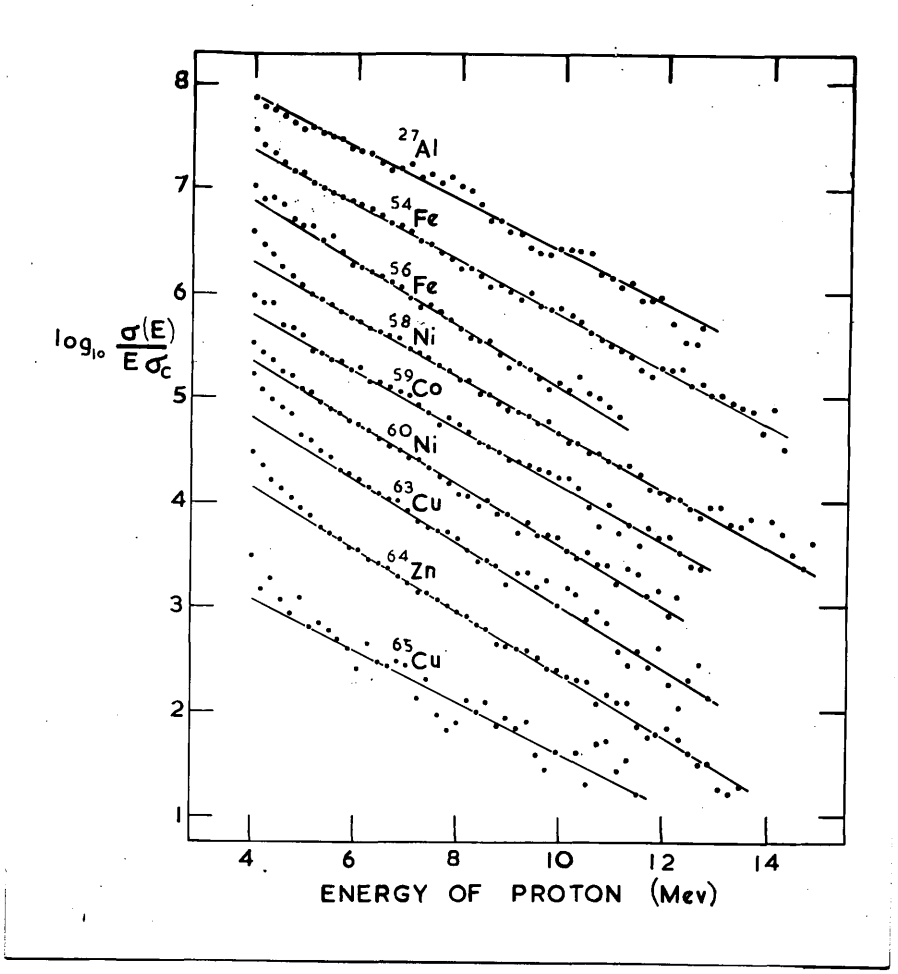

Fig. III.X111. Curves giving $dN/dEp \div Ep\sigma_c$ obtained from measurements of the energy spectra of protons from the n,p reaction in ^{27}Al, ^{54}Fe, ^{56}Fe, ^{58}Ni, ^{59}Co, ^{60}Ni, ^{63}Cu, ^{64}Zn and ^{65}Cu plotted as a function of the emitted proton energy E_p. The neutron bombarding energy was $^{p}14.1$ MeV. The curves are displaced arbitrarily with respect to the ordinate scale for convenience.

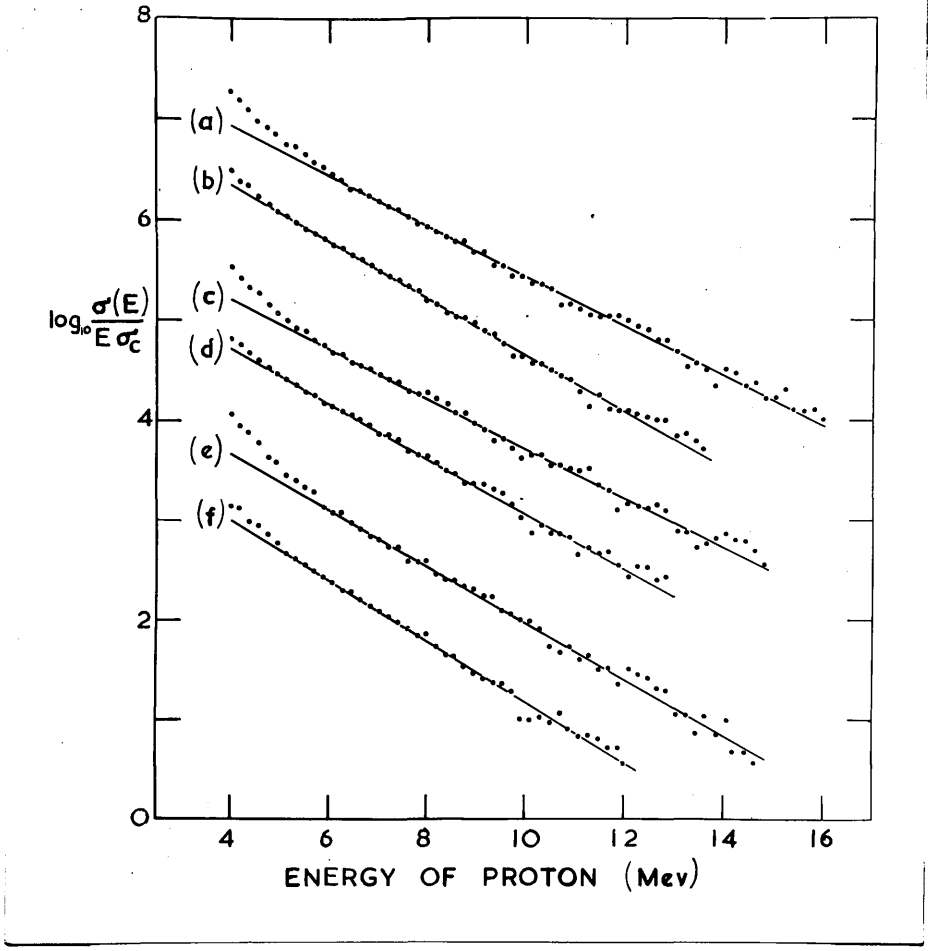

Figure III.XlV. Curves giving $dn/dEp \div Ep\sigma_c$ obtained from measurements of the energy spectra of protons from the n,p reaction in ^{58}Ni (a) and (b) ; ^{54}Fe (c) and (d) ; and ^{64}Zn (e) and (f), plotted as a function of E_p the energy of the emitted proton. The neutron bombarding energies were 15.7 and 12.9 MeV, the upper curve in each case corresponding to the higher bombarding energy. The curves are displaced arbitrarily with respect to the ordinate scale for convenience.

Extrapolating the lines in Figures III.X111 and III.X1V back to zero proton energy, and assuming that the angular distribution of the emitted protons is isotropic, the integrated cross section $\bar{\sigma}(n,p) = \sigma(n,p\gamma) + \sigma(n,pn)$ was calculated. The rise in the experimental points above the straight line below 6 MeV proton energy is attributed at least partly to the reaction n,np. Table III.2 shows the values of nuclear temperature T and $\bar{\sigma}(n,p)$ derived from this experiment. The points of Figures III.X111 and III. X1V were replotted using values of α_c corresponding to $r_o = 1.3 \times 10^{-13}$cm. and the new values of T were calculated. In Table III.2, T_1 is the nuclear temperature using $r_o = 1.5 \times 10^{-13}$cm. for α_c, and T_2 gives the corresponding temperature with $r_o = 1.3 \times 10^{-13}$cm. The unbracketted value is obtained using neutrons of energy 14.1 MeV, the bracketted values correspond to bombarding neutron energies 13.0 and 15.7 MeV the value at the lower energy being given first. The unbracketted value of $\bar{\sigma}(n,p)$ is the value at 14.1 MeV, the bracketted value corresponds to a neutron energy of 15.7 MeV. The fit of the line to the points above 6 MeV gives an error of $< 3\%$ in the derived value of T. The relative errors in the values of $\sigma(n,p)$ at the same neutron energy are about $\pm$ 5% but the absolute value

Table III.2.

Target Isotope	^{27}Al	^{54}Fe	^{56}Fe	^{58}Ni
n,p Q value MeV	-1.85	0.34	-2.93	0.62
T_1 MeV.	1.75	1.65(1.58;1.76)	1.45	1.575(1.54;1.74)
T_2 MeV.	1.69	1.58(1.52;1.69)	1.38	1.505(1.51;1.69)
$\bar{\sigma}$ (n,p)mb.	90	333(561)	90	534(754)

Target Isotope	^{59}Co	^{60}Ni	^{63}Cu	^{64}Zn	^{65}Cu
n,p Q value MeV.	-0.72	-2.03	+0.78	0.20	-1.02
T_1 MeV.	1.59	1.48	1.44	1.45(1.42;1.54)	1.76
T_2 MeV.	1.48	1.43	1.39	1.42(1.35;1.51)	1.58
$\bar{\sigma}$ (n,p)mb.	75	158	149	257(344)	30

T_1 and T_2 are the "nuclear temperatures" derived from the data using values of σ_c corresponding to $r_o = 1.5 \times 10^{-13}$ and $r_o = 1.3 \times 10^{-13}$ respectively. The unbracketted values refer to the experiment with neutrons of 14.1 MeV; the values in brackets correspond to neutrons of 13 and 15.7 MeV the value for 13 MeV being given first. $\bar{\sigma}$ (n,p) is the cross section for the emission of a proton. The unbracketted values correspond to a neutron bombarding energy of 14.1 MeV, the bracketted values refer to neutrons of 15.7 MeV. The error in the temperatures is ± 3% and the relative error in the cross sections is ± 5%. The absolute values of the cross sections may be in error by as much as ± 20%.

may be in error by as much as $\pm$ 20% due mainly to uncertainty in the absolute efficiency of counting protons from the targets.

Chapter IV.

The Energy Spectra of Protons Emitted in the Forward Direction.

The emphasis here is on the contribution of direct interactions, and possibly anomalous reactions, to the spectra. A comparison of the spectra obtained here with those of the last chapter where the compound nucleus was presumed to be the main reaction mechanism should prove helpful. For convenience, the spectra of the last chapter will be referred to as the "4π spectra".

IV.1 Development of a Counter Telescope.

The need for a counter telescope is dictated by the fact that, in detecting protons emitted in the forward direction, we are unable to shield the proton spectrometer which we will take to be a CsI(Tl) scintillation counter. Furthermore, in order to obtain angular resolution, the target foil must be separated from the CsI crystal by a distance of the order of several diameters, and the resulting reduced counting efficiency means that some way of eliminating pulses produced in the crystal itself must be found. We have described in Chapter II how this was achieved by Colli et al., 1956, using a counter telescope consisting of one or two proportional counters in coincidence with a CsI scintillation counter. The scintillation counter telescope described here replaces the dE/dx proportional

counters of Colli et al., by a scintillation counter consisting of a thin CsI(Tl) crystal mounted in a reflecting cavity. This has several advantages, a) unlike the proportional counter which may leak or "poison" over extended periods of time, the scintillation counter is very stable in operation, b) the use of separated isotopes requires small target foils with a correspondingly small dE/dx counter - the small active volume of the scintillation counter is particularly useful in this respect and may result in a lower random coincidence rate, c) although small proportional counters can be built to give pulses rising in 1 μsec., the decay time of the luminescence in CsI(Tl) for protons is 0.5 μsec (Storey et al., 1958) so that it is probable that a shorter coincidence resolving time can be used with a correspondingly reduced random coincidence rate.

A block diagram of the electronics used with all models of the telescope is shown in Figure IV.i. Pulses from the Du Mont 6292 photomultipliers were clipped to 2 μsec. length in the head amplifier unit (Appendix I) and were amplified by I.D.L. type 652 amplifiers. The outputs of the discriminators of these amplifiers were fed to a coincidence circuit of resolving time 2τ = 4μsec. (Appendix I). The output of the

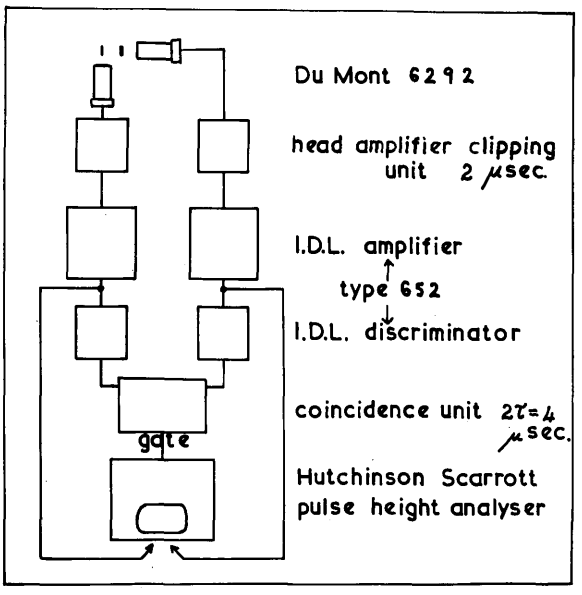

Figure IV.i. Block diagram of the electronics used with all models of scintillation counter telescope.

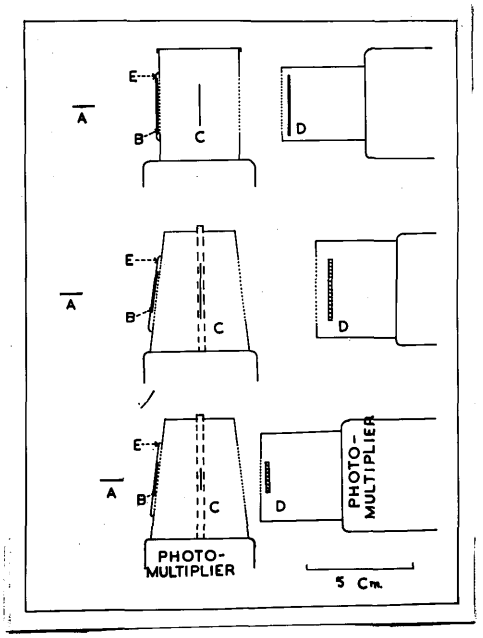

Figure IV.ii. The development of the telescope. MKS.I to III are shown from top to bottom. A-neutron source, B-target foil, C-thin crystal, D-thick crystal, E-target foil mount and background plate.

coincidence unit is used to gate pulses from either crystal before they are recorded on a hundred channel pulse height analyser (Hutchinson and Scarrott, 1951). Considering the decay time of the CsI(Tl) (0.5 μsec.), the resolving time of the coincidence unit is rather longer than is strictly necessary, however, this leads to very stable and efficient operation.

Part of the development of the telescope, MKs. I-III, is shown in Figure IV.ii. In each case A represents the neutron source which is shown in detail in Figure IV.1V. The advantages of this type of source are a) its accessibility, b) its small dimensions and c) the very small correction for absorption and scattering of the neutrons. The tritium-titanium target is attached with Wood's metal to a thin copper plate supported and cooled by two small water pipes. The beam tube is of glass with a ground glass cone joint as shown, and the lower section has a thin (1.8 mg./cm^2) window of "mylar". A hinged ^{10}B target on an iron backing is also mounted and can be manipulated with an external magnet. With this ^{10}B flap down, and a deuteron bombarding energy of $\sim$ 450 Kv., the apparatus can be calibrated with the $^{10}B(d,p)^{11}B$ proton groups. Under the latter conditions, some of the deuteron beam irradiates the tritium target, and the ^3He (formed by

the decay of the tritium) trapped in the 70 Kv. thick layer of titanium forms a prolific source of extremely monoenergetic 14.5 MeV protons from the reaction $^{3}He(d,p)^{4}He$, Q = 18.341 MeV. This reaction was used as the calibration point in the later models of the telescope, and although the reaction has a broad resonance in the neighbourhood of 400-430 Kv. a deuteron bombarding energy of 200-300 Kv. gives quite a high yield of protons from the usual tritium-titanium target. The ^{10}B flap is raised and a deuteron bombarding energy of 200-300 Kv. is used for the production of 14.1 MeV neutrons. Returning to Figure IV.ii, B represents the target foil and E its combined lead holder and background plate. C and D represent the thin and thick crystals respectively. These are mounted using 0.005" platinum wire in cylindrical reflecting cavities constructed from 0.020" lead with a thin layer of evaporated aluminium as reflector. The dotted lines represent 0.2 mg./cm^2 windows of aluminium leaf, and the dashed lines represent an inverted U shaped bismuth frame which held the thin crystal in MKs.II and III. The cavity in this case was not quite cylindrical being more like a truncated cone to improve the light collection efficiency. Mounting the crystals in this way reduced the

individual counting rate in each counter due to n,p reactions in the surroundings, and so minimised the random coincidence rate. As in Chapter III, this type of mount also improved the resolution obtained from crystal D.

MK.1 was a preliminary experiment to determine the signal to background ratio we might expect. The thin crystal was 0.007" thick and the crystal D was 0.032" thick. Details of the preparation of thin CsI crystals will be found in Appendix II. With the target holder E removed, the telescope was irradiated with the $^{10}B(d,p)^{11}B$ proton groups, and, examining the pulse height spectrum in each counter gated by the coincidence unit, the gain of both counters was adjusted. More will be said of this procedure later. The target holder E was replaced (with a target foil of Ni, 1" in diameter and 27 mg./cm^2 thick) in position, and the telescope was irradiated with 14.1 MeV neutrons. The "foil in", "foil out" spectra obtained for equal numbers of neutron monitor counts are shown in Figure IV.iii. where the upper and lower limits of the spectra correspond to proton energies of approximately 14 and 6 MeV respectively. Considering the large Ni target used, the signal to background ratio was not particularly good, and the broad peak in the background spectrum was unsatisfactory.

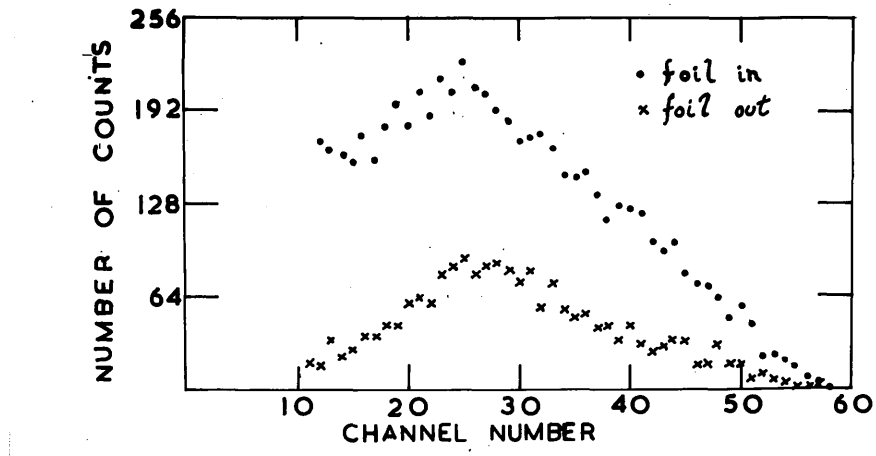

Figure IV.iii. "Foil in", "foil out" spectra obtained with a 27 mg./cm^2 Ni foil in MK.I. telescope.

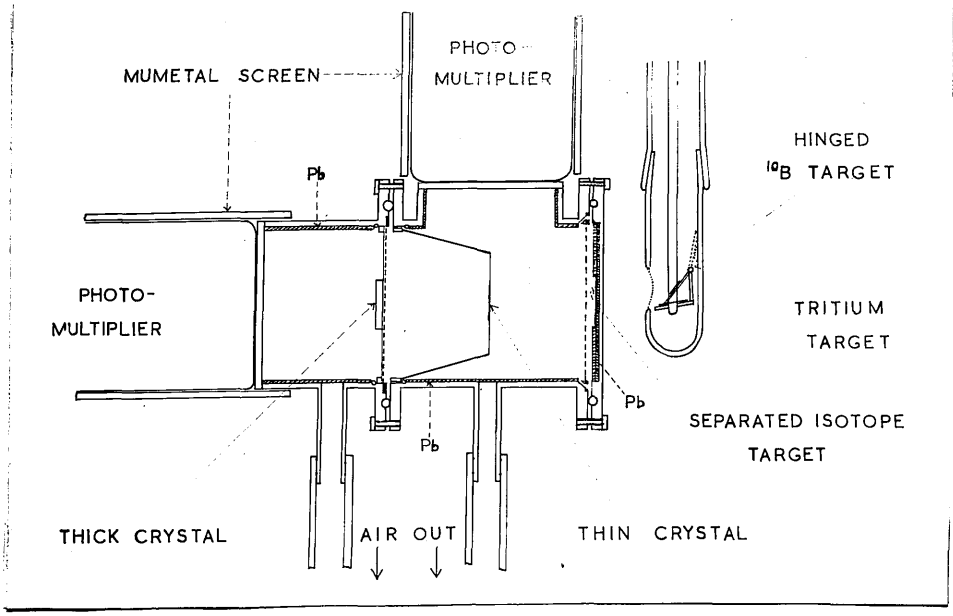

Figure IV.1V. MK.IV. The evacuated model of the telescope. The water cooled neutron source is also shown.

In MK.II, the target foil was reduced in size and thickness; the diameter was now 2 cm. and the thickness 13.5 mg./cm^2. To compensate for the smaller target, a larger thin crystal was used, and to keep the signal to background ratio reasonable, the thickness was reduced to 0.003". The crystal D used was 0.080" thick. This arrangement proved unsatisfactory in practice, the signal to background ratio with a Ni target being considerably poorer than that shown in Figure IV,iii. Much of this was due to the small amount of target material used, but we were convinced that some of the increased background was produced by protons ejected from the periphery of the thin crystal which was not so fully utilised by protons from the target foil as its centre.

In MK.III therefore, we decided to return to the same geometry used in MK.I, but we would compensate for the smaller amount of target material by using a thin crystal 1 cm. in diameter and 0.0025" thick. The target foil and thick crystal were reduced in diameter to 1.5 cm. and the thickness of the former was 13.5 mg./cm^2. The "foil in" "foil out" spectra with a Ni target were practically the same as these of Figure IV,iii with the important difference that the signal to background ratio was slightly improved especially at the higher

energies, and the width of the broad peak in the background was considerably decreased. Although the signal to background ratio was generally good and of the order of 5:1 for Ni, this very prominent peak in the background which will be seen in several of the following figures rendered the background subtraction uncertain in the region 8-9 MeV. Suspecting that this peak might be due to n,p reactions in the air in front of the thin crystal, the front half of this crystal's reflector was replaced by a flat reflecting lead plate. The background spectrum obtained showed a considerable reduction in the peak at $8\frac{1}{2}$ MeV, so we decided that the telescope must be evacuated.

This development, MK IV, is shown in Figure IV, 1V. The thin crystal is supported with its plane perpendicular to the axis of a cylinder lined with "aluminised" 0.020" Pb, and the ends of this cylindrical cavity are closed with aluminium foils, the front one being 0.2 mg./cm^2 thick. The thin crystal is supported by two 0.005" platinum wires attached to a semi-circular hoop of stiff molybdenum wire. Although the light collection from the thin crystal was far from ideal, the results are surprisingly good. The thick crystal was 0.063" thick and 1.5 cm. in diameter. The target foil holder was incorporated in the brass end plate of the telescope which

was removeable to allow calibration with the $^{10}B(d,p)^{11}B$ and $^{3}He(d,p)^{4}He$ proton groups.

Irradiating the evacuated telescope with 14.1 MeV neutrons with the empty target holder in position, the background spectrum shown in the lower half of Figure IV.V was obtained. When the telescope was irradiated with air in it for the same number of neutron monitor counts we obtained the spectrum due to the air alone shown in the upper half of Figure IV.V. This spectrum must be due to the nitrogen in the air since the Q values of the reactions $^{16}O(n,p)^{16}N$ and $^{16}O(n,d)^{15}N$ are -9.62 and -9.88 MeV respectively. To confirm this result, the telescope was irradiated for the same number of neutron monitor counts filled with, first, one atmosphere of oxygen, and then with one atmosphere of nitrogen. The result is shown in Figure IV.V1. In Figures IV.V and IV.V1 the full line arrows represent the positions of the groups of calibration protons. The dashed line arrows indicate the positions of the proton groups expected from the reaction $^{14}N(n,p)^{14}C$, Q= 0.627 MeV. ^{14}C has excited states at 6.09, 6.72 and 6.89 MeV (Ajzenberg and Lauritsen, 1955) and the n,p transitions to the 6.09 and 6.89 MeV states are indicated by the dashed arrows. At first sight the spectra would seem to indicate that the ground state

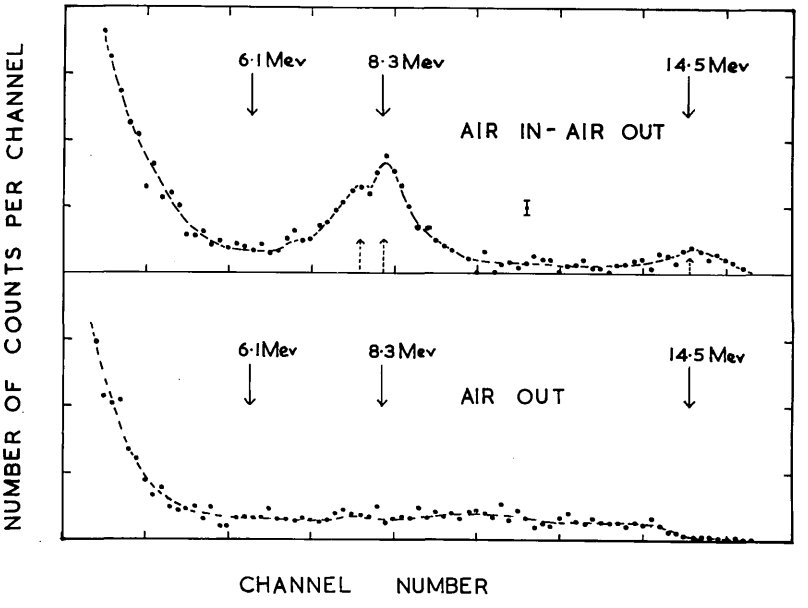

Figure IV.V. Spectra showing the effect of air in the MK.IV telescope. Top - spectrum due to air alone. Bottom - Background spectrum for same number of neutron monitor counts.

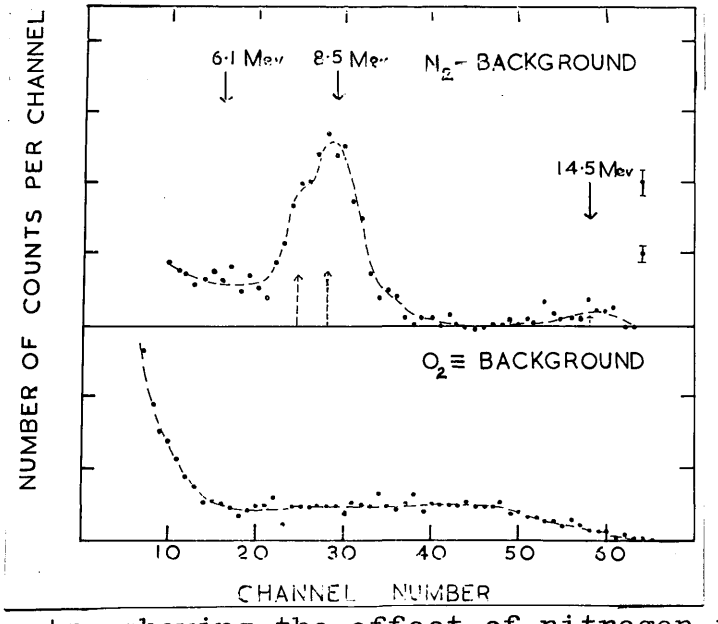

Figure IV.V1. Spectra showing the effect of nitrogen in the MK.IV telescope. Top - Spectrum due to nitrogen alone. Bottom - Oxygen spectrum ($\equiv$ Background) for same number of neutron monitor counts.

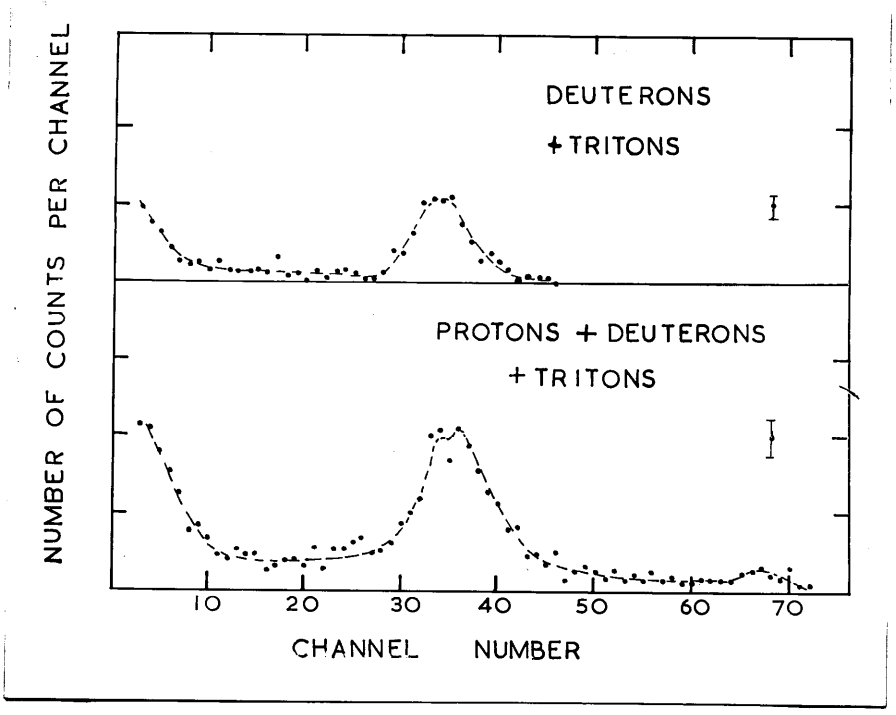

Figure IV.V11. Top - Spectrum due to air in MK.IV telescope with a high discriminator bias on the dE/dx counter so that protons are not detected. Bottom - spectrum for the same number of neutron monitor counts with a low discriminator bias.

$^{14}N(n,p)^{14}C$ reaction is weakly excited with very strong transitions to the excited states in ^{14}C, the structure in the spectrum being evident. However, considering the reactions $^{14}N(n,d)^{13}C$, Q = -5.316 MeV and $^{14}N(n,t)^{12}C$, Q = -4.007 MeV. the ground state transitions of these reactions would produce peaks in the spectrum at 8.2 and 9.0 MeV proton energy respectively if the additional energy loss in the thin crystal of deuterons and tritons relative to protons is taken into account. This calculation assumes that the luminescent response of CsI(Tl) for deuterons and tritons is the same as that for protons. It will be shown later that the response for deuterons is $\geqslant$ 97% that for protons, but in general one expects the luminescent response to fall off with increasing particle ionisation density, so that the triton peak could be as much as 0.5 MeV below 9 MeV. Figure IV.V11. shows the result of an attempt to determine the contribution of the deuteron and triton reactions to the peak at 8.5 MeV. The top half of this figure shows the spectrum which is obtained when the telescope, with air in it, is irradiated with the discriminator bias on the thin crystal chosen so that very few protons and almost all deuterons above 6 MeV are recorded. The lower spectrum was taken with the discriminator bias set low so that all protons and deuterons

were recorded. Both spectra were taken for the same number of neutron monitor counts, and it is apparent that ~ 50% of the 8.5 MeV peak is due to deuterons or tritons. The observation of the deuteron reaction is in accord with the results of Carlson, 1957, but it is surprising that this author does not mention the presence of the $^{14}N(n,p)^{14}C$ reaction. Fireman, 1953, has measured a cross section of 11 ± 2 millibarns for the $^{14}N(n,t)^{12}C$ reaction with fission neutrons.

Some preliminary measurements of the proton energy spectra from 15 mg./cm^2 targets of natural Ni, ^{58}Ni, ^{60}Ni, ^{54}Fe, ^{63}Cu and ^{64}Zn were made with the evacuated MK.IV telescope. The signal to background ratio was satisfactory, but two disturbing features were present. Firstly, the end points of the spectra for ^{60}Ni and ^{56}Fe were inconsistent with the Q values of the reactions $^{60}Ni(n,p)^{60}Co$, Q = -2.03 MeV, and $^{56}Fe(n,p)^{56}Mn$, Q = -2.93 MeV, and secondly, a prominent discontinuity in the natural Ni, and ^{58}Ni spectra at proton energy 7.3 MeV was evident. The apparent violation of the Q values will be discussed later. The "peak" at 7.3 MeV was interesting since it might be caused by an anomalous type of reaction, but we did not discount the possibility that it might be due to a contamination of the Ni foils. This contamination is extremely unlikely in the case of

Ni, but to ensure that the peak was not due to a gas such as nitrogen absorbed in the surface of the foil, the natural Ni foil was heated to red heat in a high vacuum. Irradiating this foil in the telescope, the spectrum obtained still showed the discontinuity at 7.3 MeV.

IV.2 The Final Model of the Telescope.

a) Geometry.

Although the performance of the MK.1V telescope was satisfactory, the method of changing target foils and obtaining energy calibrations and background runs was cumbersome. The MK.V. telescope shown in Figure IV.Viii was designed to overcome this difficulty. A general view of the apparatus is shown in Figure IV. 1X. The body of the MK 1V telescope is attached to a cylindrical chamber which houses the neutron source and the target changing device, and the telescope is permanently evacuated being connected to the vacuum system of the high tension generator. The separated isotope targets mentioned in the last chapter, together with thin (< 15 mg./cm^2) targets of natural copper, aluminium and CF_2 were mounted in lead holders on the rotating target mount shown. The twelve target holders were spaced equally on the mount, and by bringing the axis of target holder number six, say, on to the

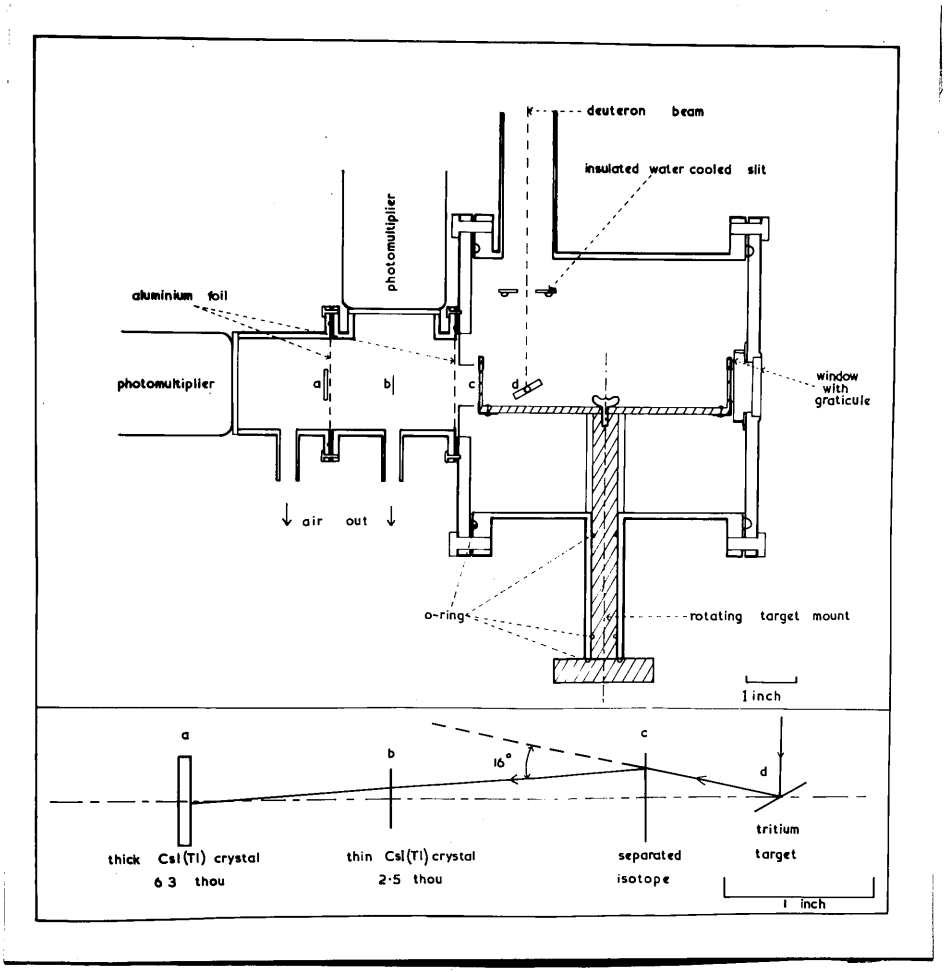

Figure IV. V111. MK.V. The final model of the scintillation counter telescope. The lower portion of the figure shows the geometry of the telescope on an enlarged scale.

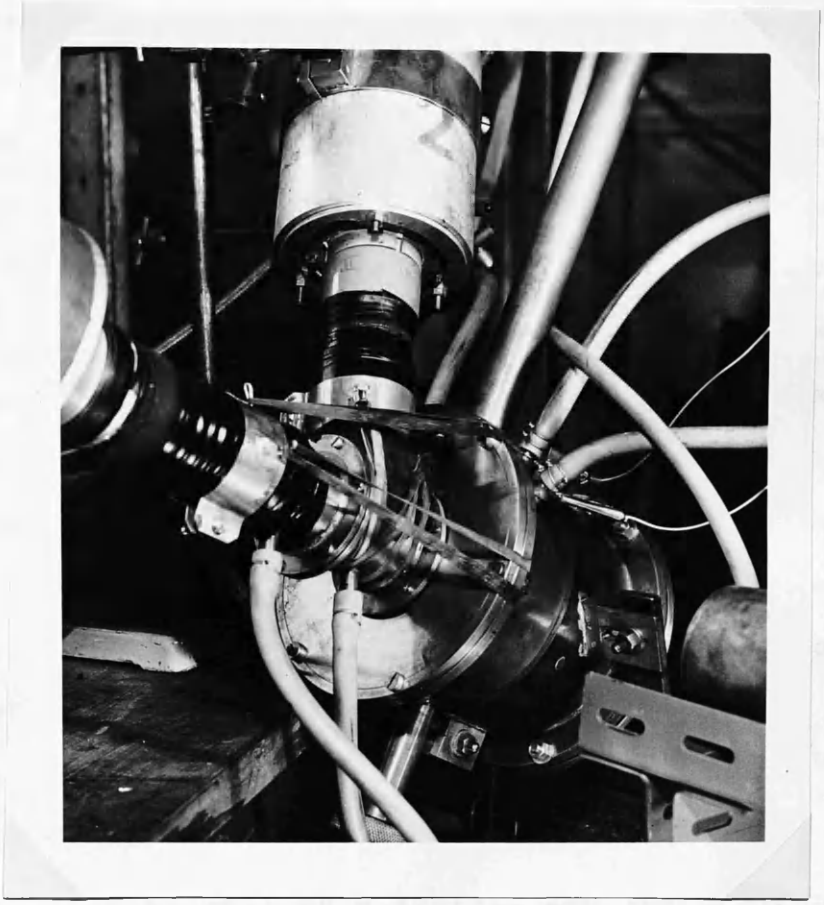

Figure IV.1X. A general view of the MK.V. telescope.

graticule shown, number twelve was accurately on the axis of the telescope. Background runs were obtained using an empty target holder, a preliminary experiment having shown no appreciable contribution from platinum.

The beam currents to the water cooled tritium target and insulated slits were measured, and enabled us to maintain a diffuse deuteron beam over the whole target area (9 mm. x 9 mm.). A beam current of 6 μamp. was sufficient to produce the flux of neutrons required (2×10^8 neutrons/sec. into 4π), and as the experiment progressed, the deuteron bombarding energy was raised from 200 to 300 Kv. to penetrate the thin layer of carbon deposited on the tritium target surface. This did not affect the neutron energy appreciably since we are observing neutrons emitted at 90° to the deuteron beam. The neutron monitor which was of the recoil proton type mentioned previously was mounted at 90° to the deuteron beam. The output of this monitor was fed to a ratemeter as well as a scaler, and the neutron flux was maintained constant to $\pm$ 10% to avoid fluctuations in the random coincidence rate.

The lower portion of Figure IV.Viii shows the main components of the telescope on an enlarged scale, the full line representing the path through the apparatus of the average deuteron, neutron and proton. It is seen

that the average angle of acceptance for protons was 16^{o}. The mean solid angle of acceptance for all points in the separated isotope target was 0.0245 steradian. This figure can be calculated quite accurately, the main source of error ($\pm$5%) being the uncertainty in the area of the thin crystal.

b) Calibration.

Due to the finite thickness of the thin crystal, and the variation with energy of energy lost by protons in the thin crystal, the pulse height response of the thick crystal against initial proton energy is not linear. This effect is useful, however, since at the lower proton energies where the resolution would be impaired by non uniformities in the thin crystal, the energy width of each channel is reduced somewhat. All the spectra obtained were corrected for the slight non-linearity of the energy scale and for the change in channel width with energy, account being taken of separated isotope target thickness as well as the thin crystal thickness. The lower limit of the spectrum was not determined by the background, but by the channel width correction; at this point the correction was 20% of the channel width at 14 MeV. This correction is greatest for the first few channels, and is down to 10% at 6.5 MeV. To estimate the average thickness of crystal

to use in these corrections, the thin crystal was used as an absorber in front of a CsI(Tl) scintillation counter proton spectrometer. The shift of the $^{10}B(d,p)^{11}B$ proton groups caused by the introduction of the crystal measured its average thickness.

The full line in Figure IV.X. shows the coincidence pulse height spectrum from the thick crystal when the telescope is exposed to the proton groups from the reactions $^{3}He(d,p)^{4}He$ and $^{10}B(d,p)^{11}B$. The energy resolution of the three peaks at 14.5, 8.3 and 6.1 MeV is 4.8, 6.3 and 7% respectively. By recording the peaks separately on an expanded scale, we were able to calculate the effect on the resolution of the finite separated isotope target thickness. This is shown as the dashed line in Figure IV.X., the energy resolution of the three peaks being 6.2, 8 and 14%.

In the experiment proper, the telescope was calibrated and the gain of the thick crystal pulse amplification system was checked using the reaction $^{3}He(d,p)^{4}He$. One of the empty target holders on the rotating mount had a small hole at its centre covered with 41 mg./cm^2 of aluminium, and by running the deuteron beam under exactly the same conditions as prevailed in an actual separated isotope irradiation an ample supply of 13.8 MeV protons was obtained to calibrate the energy

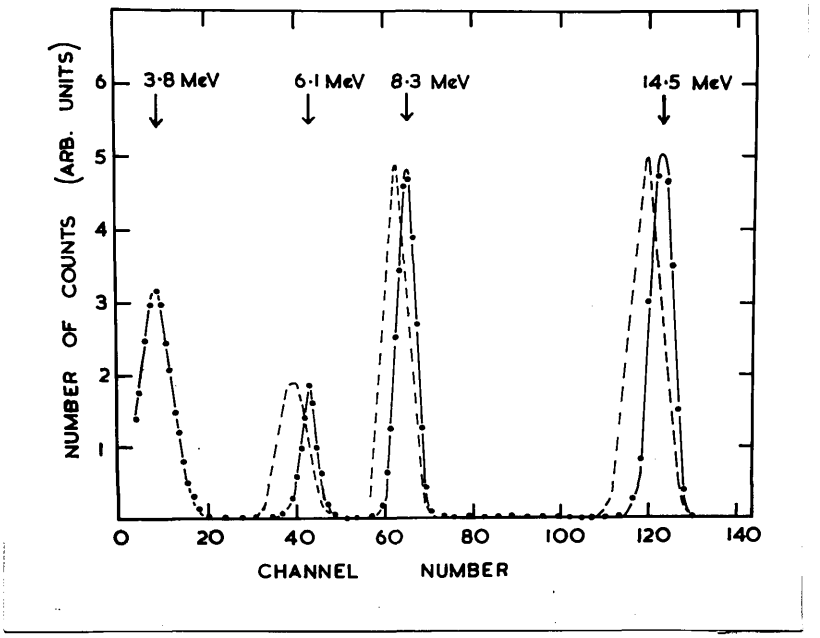

Figure IV.X. The coincidence spectrum in the thick crystal corresponding to proton groups from the reactions $^{3}He(d,p)^{4}He$ and $^{10}B(d,p)^{11}B$.

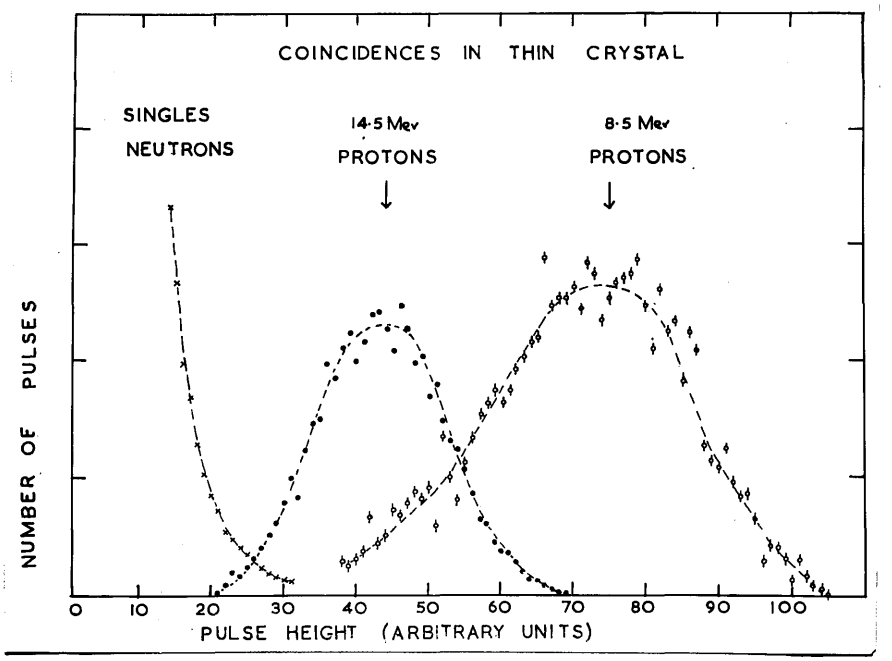

Figure IV.X1. The coincidence spectrum in the thin crystal corresponding to the dE/dx of protons of 14.5 and 8.5 MeV.

scale. Having the same flux of neutrons passing through both scintillation counters during irradiation and calibration avoided errors which might have arisen due to the dependence of photomultiplier gain on counting rate.

The 13.8 MeV protons were also used to determine the correct setting of the bias level of the thin crystal discriminator so that pulses due to protons were recorded while those due to electrons were rejected. This was accomplished by feeding the thin crystal pulses to the pulse height analyser which was gated by the coincidence unit. Figure IV.X1 shows spectra of this type obtained with the MK IV telescope. This figure which shows the coincidence spectra corresponding to the energy loss of 14.5 and 8.5 MeV protons in the thin crystal also shows the singles spectrum (mainly electrons) when the thin crystal is irradiated with 14.1 MeV neutrons. The discriminator level on the thin crystal is adjusted so that the "cut off" in the coincidence spectrum falls at channel 25 of Figure IV. X1. In this condition, the telescope will operate at maximum efficiency for all protons, since the energy loss of the protons in the thin crystal increases with decreasing proton energy. Deuterons and tritons will also be recorded by the telescope, but the thickness of the thin crystal precludes any possibility of alpha

particles being detected.

c) Experimental Method.

Each element was irradiated ten or more times, each irradiation lasting approximately 50 minutes, and background runs were interspersed with target runs. The gain of the thick crystal pulse height amplification system was checked at the end of each run with the 13.8 MeV protons; the drift was of the order of 1%. With the neutron flux of 2×10^8 neutrons/second into 4π, the random coincidence spectrum was 10% of the background spectrum which is shown in Figure IV.X11. Since this spectrum has a broad peak at 11 MeV and a sharp edge at 14 MeV, a bad background subtraction will introduce spurious peaks in the final spectrum. (It will be recalled that the background spectra shown in Figures IV. V, V1, were rather flatter than that of Figure IV.Xii. This was caused by the higher random coincidence rate in the preliminary experiments where a higher neutron flux was used to obtain good statistics quickly). To ensure a good background subtraction, the deuteron beam was de-focussed so that the neutron source did not change its position due to beam drift, the neutron flux was maintained constant within 10% minimising fluctuations in the random coincidence rate, and values of the ratio of counts in each target spectrum to counts in the nearest background spectrum were obtained for each irradiation.

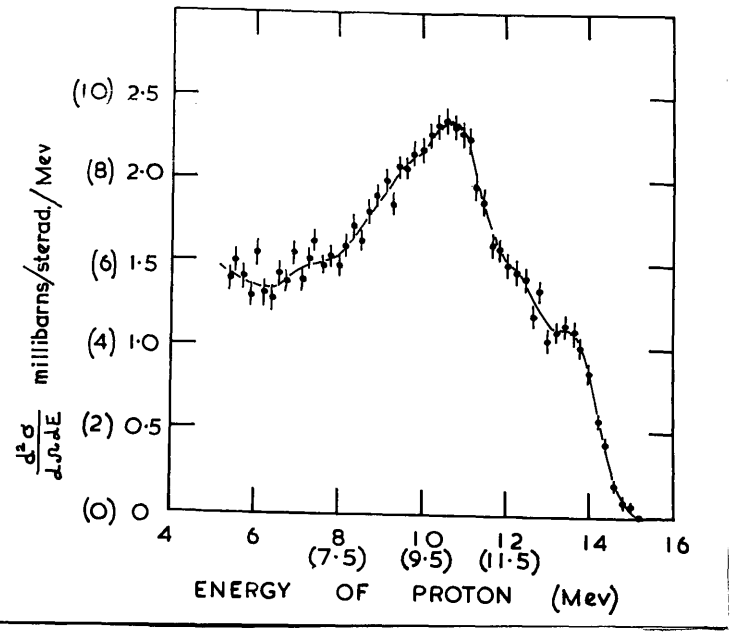

Figure IV.X11. The Background Spectrum. The unbracketted scales are given for comparison with the target spectra. The bracketted scales refer to the energy of protons emitted and cross section of n,p reactions in the thin crystal.

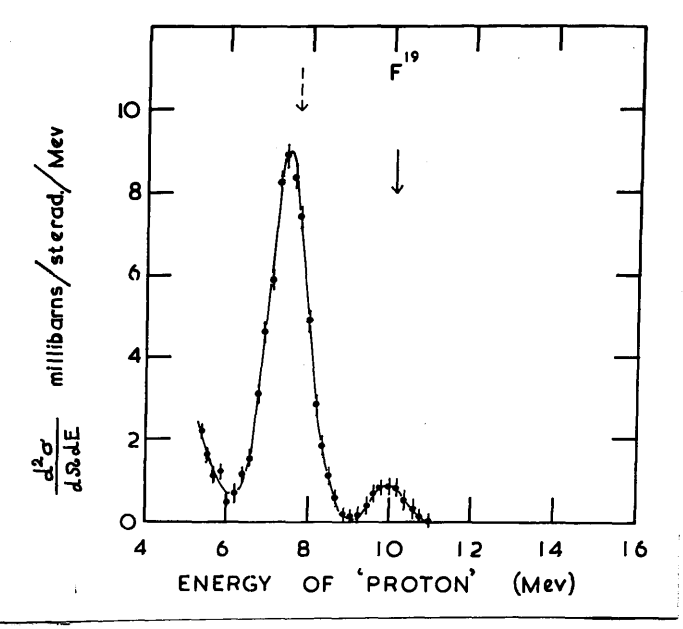

Figure IV.X111. The energy spectrum of protons and deutrons from ^{19}F. The full line arrow denotes the ground state n,p transition, while the broken line arrow denotes the ground state n,d transition.

The spread in the values of this ratio for most targets was $\pm 3\%$. The unbracketted scales in Figure IV.Xii are given for comparison with the final spectra.

IV.3 The Final Spectra.

Results.

The spectra obtained from the ten targets studied are shown in Figures IV.Xiii - xxiii. Except in Figure IV.xiii in which only one curve is shown, the present results are given by the large points with error attached, and the smaller points and dashed curve show the energy spectrum of protons emitted into approximately 4π obtained previously. The error shown takes into account the background subtraction. The full line and broken line arrows denote the expected positions of the n,p and n,d ground state transitions respectively, allowance being made in the latter case for the different energy loss of protons and deuterons in the separated isotope target and thin crystal.

The spectra are mainly exponential in form with an excess of higher energy protons and show evidence of structure in several cases at the high energy end of the spectra. In the case of the spectra for ^{54}Fe, ^{58}Ni, ^{65}Cu and ^{64}Zn there is also evidence for structure at a proton energy of approximately 7 to 8 MeV. This latter low energy ($\sim$ 7.5 MeV) structure has sometimes been

interpreted as being due to giant resonance or anomalous effects, but the present experiment will show that these groups may be attributed to the n,d pick-up reaction.

^{19}F, Figure IV.XIII - A CF_2 target 10.3 mg./cm^2 thick was used; there is no contribution to the spectrum from carbon which has large negative Q values for the n,p and n,d reactions. The spectrum is in good agreement with that obtained by Ribe, 1957, the peaks at 7.5 and 10 MeV being attributed to the ground state, n,d and n,p reactions respectively. Neglecting the correction to the efficiency of the telescope caused by its finite solid angle of acceptance and the anistropic angular distribution of the reaction products, we find cross-sections of 10.8 and 0.7 millibarns/steradian for the two peaks. At the average angle of acceptance of the telescope for isotropic reactions, namely 16°, Ribe finds a cross-section of 8 millibarns/steradian for the n,d reaction, which is in agreement with our value when the anisotropy of the reaction is considered. Remembering the fluorine has a single proton outside a closed shell of 8 protons it is understandable that the n,d reaction should be favoured. Ribe does not find the n,p ground state transition at 0°, but finds a cross-section of 0.7 millibarns/steradian at 30° for this peak. It is thought that the peak at 7.5 MeV is

due to deuterons entirely, since it is very symmetrical, and its width at half height (1.1 MeV) is fairly close to that calculated (0.9 MeV) for a transition to a single level. The proximity of the deuteron peak to its predicted position on the proton energy scale shows that the luminescent response of CsI(Tl) for deuterons is practically equal to that for protons.

Kondaiah et al., 1958, who measured the ratio of the n, α and n,p cross-sections in ^{19}F for 14.5 MeV neutrons using an activation technique found a value (1.2) which differed from that calculated on the basis of the statistical theory (3.5). In the derivation of the latter value, however, the assumption was made that both reactions proceed mainly to the ground state or to levels close to the ground state. The present results together with the cross-section of 135 millibarns for the $^{19}F(n,p)^{19}O$ reaction obtained by Paul and Clarke, 1953, show that this assumption is not valid in the case of the n,p reaction. In a further experiment, Kondaiah et al., 1959, irradiating a CaF_2 crystal with 15.1 MeV neutrons obtained a peak in the pulse height spectrum which they attributed to 10.6 MeV alpha particles from the ground state $^{19}F(n,\alpha)^{16}N$ reaction. Taking into account the relative luminescent response of the crystal for alpha particles and deuterons, it seems more probable that the peak obtained is due to 9.4 MeV deuterons from

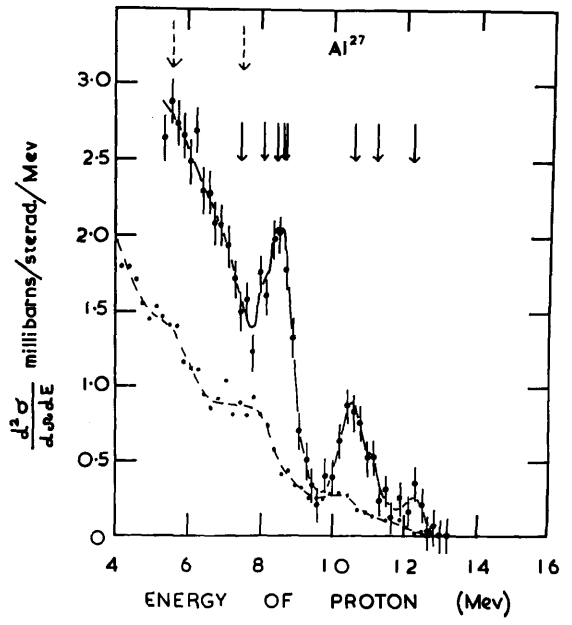

Figure IV.X1V. The energy spectrum of protons from $^{27}Al(n,p)^{27}Mg$. The full line arrows denote the ground and excited states of ^{27}Mg; the broken line arrows denote the ground and first excited state n,d transitions. The "4π" spectrum is shown by the smaller points and dashed curve.

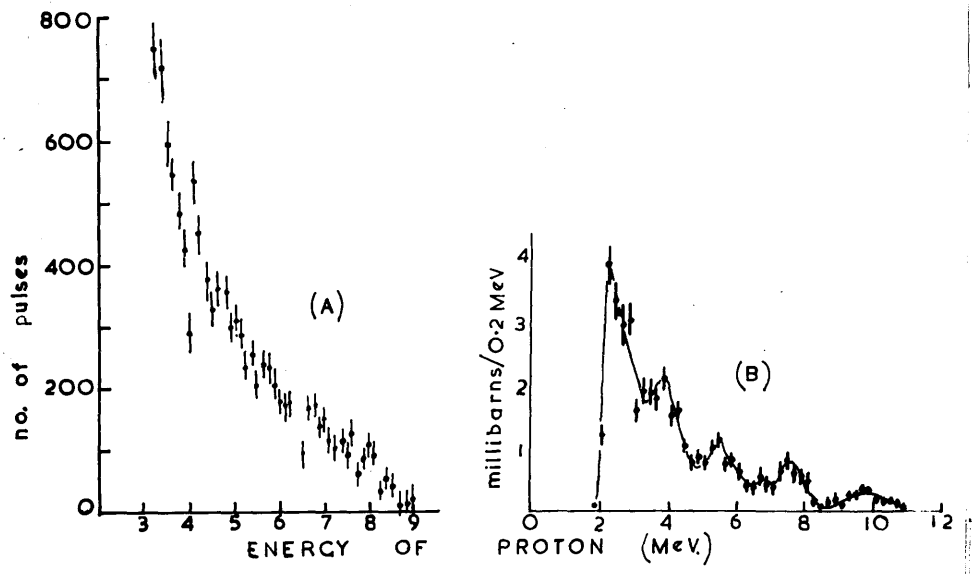

Figure IV.XV. The $^{27}Al(n,p)^{27}Mg$ spectra of A) Colli et al. 1957a and B) March and Morton, 1958c are given for comparison with figure IV.X1V.

the $^{19}F(n,d)^{18}O$, Q = -5.73 MeV ground state transition.

^{27}Al, Figure IV.XIV - The improved statistics and energy resolution of the present experiment are shown to advantage in this spectrum. The full line arrows represent $^{27}Al(n,p)^{27}Mg$ transitions to the ground, 0.99, 1.66, 3.5, 3.56, 3.76, 4.13 and 4.75 MeV levels in ^{27}Mg as given by Endt et al., 1952; Holt and Marsham, 1953; and Hinds et al., 1958, while the broken line arrows represent $^{27}Al(n,d)^{26}Mg$ transitions to the ground and 1.83 MeV levels in ^{26}Mg quoted by Endt and Kluyver, 1954. It is seen in agreement with Haling et al., 1957 and March and Morton, 1958c, that the ground state n,p transition is only weakly excited if at all, and the level at 1.66 MeV is not only confirmed but seems to be more strongly excited than the 0.99 MeV level. The peak between 8 and 9 MeV is in good agreement with the positions of the levels, and below 8 MeV the spectrum may be attributed to the increasing density of available levels. There is no indication of a large yield from the ground state $^{27}Al(n,d)^{26}Mg$ transition, but the tendency to peak at 6 MeV may be due in part to the n,d transition to the first excited state in ^{26}Mg at 1.83 MeV. Figure IV.XV shows the $^{27}Al(n,p)^{27}Mg$ of A) Colli et al. 1957a, and B) March and Morton, 1958c for comparison with the present result.

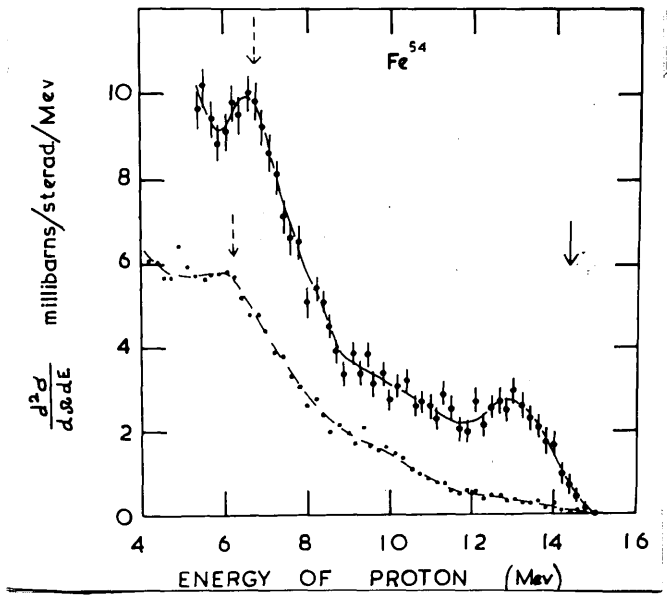

Figure IV.XVl. The energy spectrum of protons from ^{54}Fe (n,p)^{54}Mn. The full line arrow denotes the ground state n,p transition while the broken line arrow denotes the ground state n,d transition. The "4π" spectrum is shown by the smaller points and dashed curve. This convention is followed throughout.

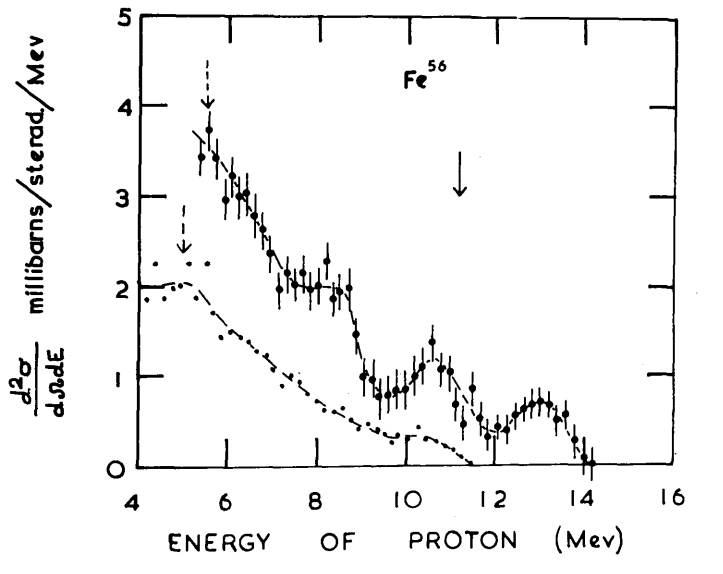

Figure IV.XVll. The energy spectrum of protons from the reaction $^{56}Fe(n,p)\ ^{56}Mn$.

^{54}Fe, Figure IV.XVI. The mainly exponential form of the ^{54}Fe(n,p)^{54}Mn spectrum with an excess of higher energy protons is consistent with the n,p Q value, (Q = 0.3 MeV) and shows peaks at 6.7 and 13.0 MeV, although the latter peak may contain a contribution from recoil protons if the ^{54}Fe is contaminated with hydrogen. When one considers that the level density in the odd-odd residual nucleus ^{54}Mn at an excitation energy of 7.7 MeV is likely to be of the order of several tens of levels per MeV, it seems likely that the 6.7 MeV peak is due to the ground state ^{54}Fe (n,d)^{53}Mn, Q =-6.58 MeV transition shown by the broken line arrow rather than the n,p reaction. Correcting for the greater effective target thickness in the 4π spectra, the lower curve in Figure IV.xvi also seems to show the deuteron transition.

^{56}Fe, Figure IV.XVII - Broad peaks are superimposed on this spectrum at 13, 10.6 and 8.6 MeV. The peak at 13 MeV which is inconsistent with the n,p Q value (Q = -2.93 MeV) will be discussed below. The spectrum obtained by Allan, 1957, for this reaction also violates the Q value; it is not exponential in form and shows peaks at 11.2, 8.6, 6.3 and 4.4 MeV. March and Morton 1958a and Colli et al. 1957a, find an exponential form for the spectrum and Colli et al., observe discontinuities

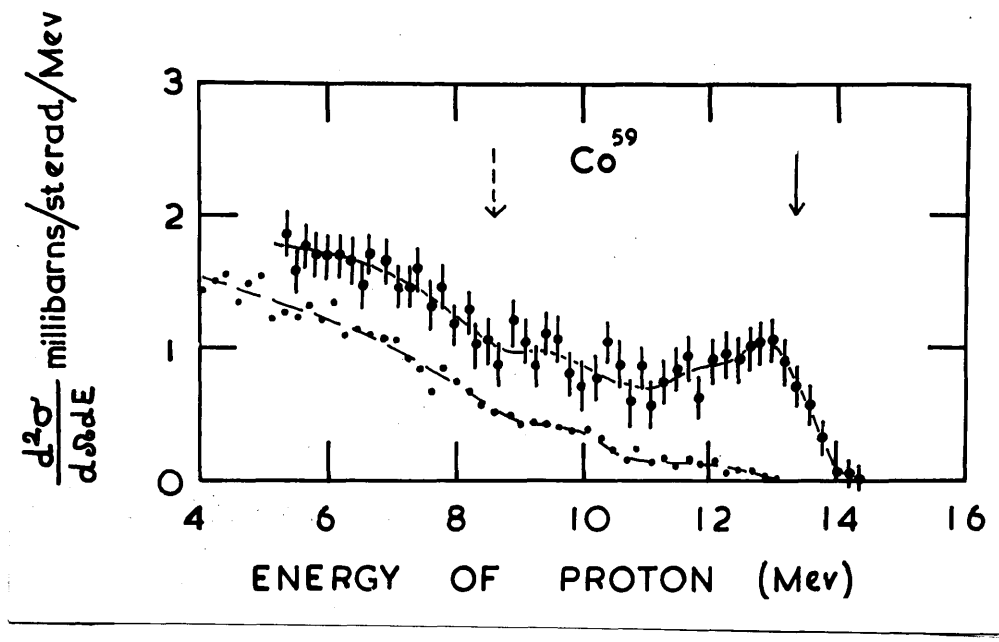

Figure IV.XVlll. The energy spectrum of protons from the reaction $^{59}Co(n,p)^{59}Fe$.

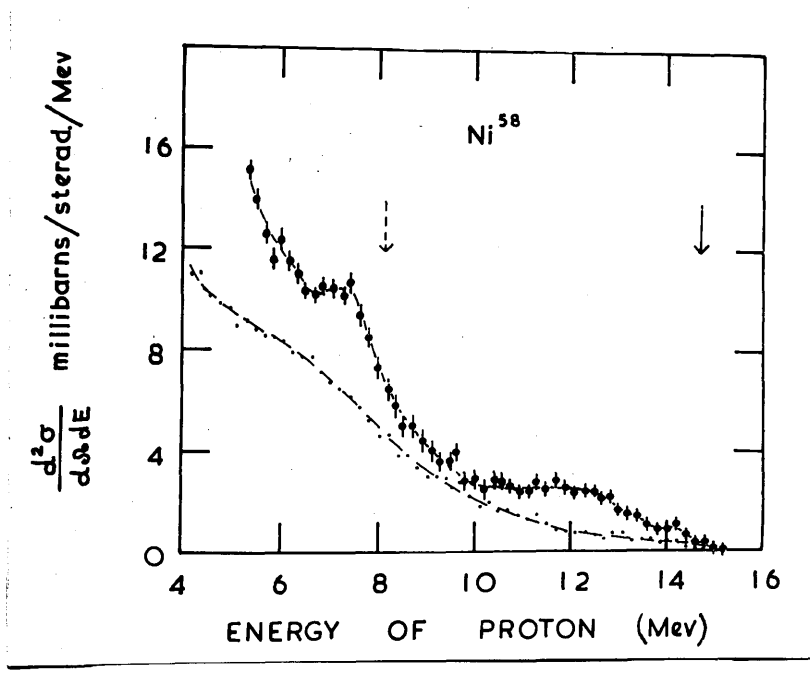

Figure IV.X1X. The energy spectrum of protons from the reaction $^{58}Ni(n,p)^{58}Co$.

at 10.3 and 8.3 MeV which seem to agree with those found here. Since the $^{56}Fe(n,d)^{55}Mn$ Q = -7.92 MeV ground state transition would appear at the lower limit of the spectrum, we can not say whether it contributes or not, however, the discontinuity in the lower curve at 5.1 MeV is close to the broken line arrow denoting the ground state n,d transition.

^{59}Co, Figure IV.XVIII - This spectrum is consistent with the Q value for the $^{59}Co(n,p)^{59}Fe$ Q = -0.72 MeV reaction, has a prominent peak at 13 MeV, and very slight discontinuities at 11.7 and 9.5 MeV. There is a marked excess of high energy protons in the present spectrum compared to the "4π" spectrum.

^{58}Ni, Figure IV.XIX - This is the highest yield isotope studied. The spectrum is exponential in form with a plateau of high energy protons, which is consistent with the n,p Q value. A prominent discontinuity in the spectrum at 7.3 MeV does not coincide with the $^{58}Ni(n,d)^{57}Co$ Q = -5.45 MeV ground state transition. This is not surprising on consideration of the spins of the ground state target and residual nuclei which are 0(+) and $\frac{7}{2}$ (-) respectively, since the large value of "ℓ" involved in the pick-up reaction will inhibit the ground state pick-up reaction and preclude its observation in the forward direction. The first excited

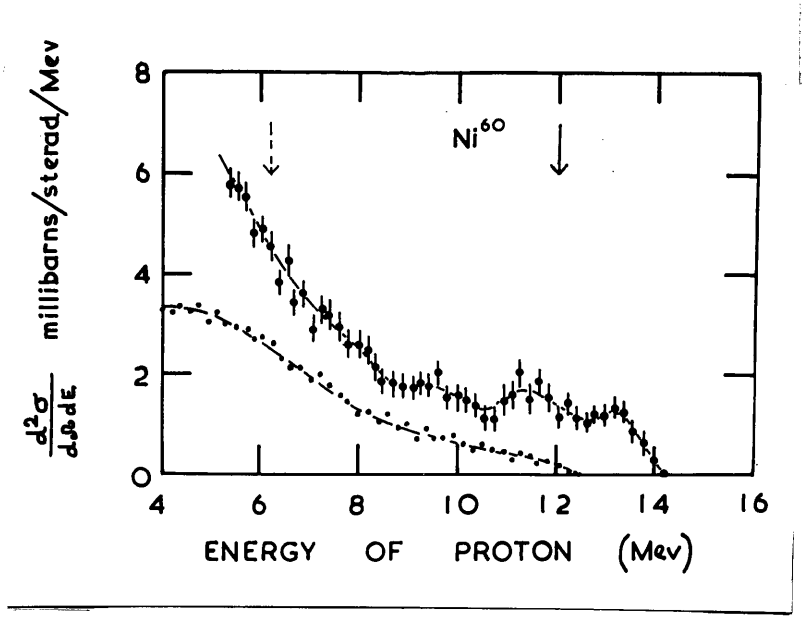

Figure IV.XX. The energy spectrum of protons from the reaction $^{60}Ni(n,p)^{60}Co$.

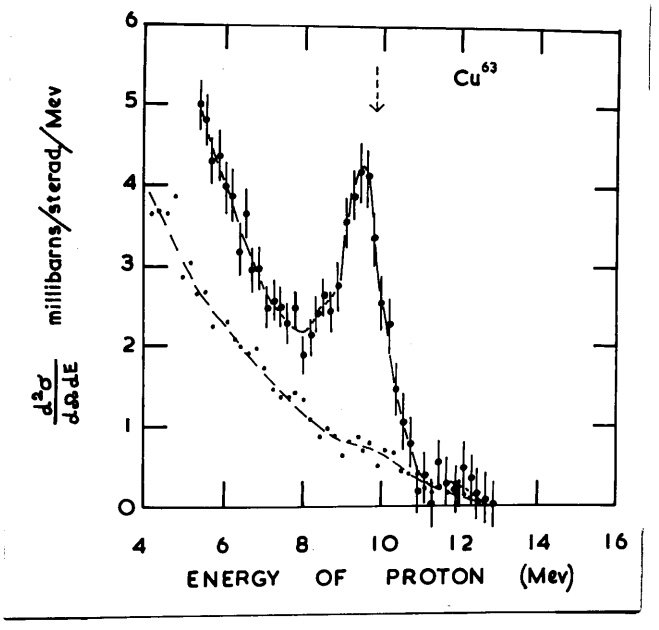

Figure IV.XX1. The energy spectrum of protons from the reaction $^{63}Cu(n,p)^{63}Ni$. The reaction $^{63}Cu(n,d)^{62}Ni$ is also present.

state in ^{57}Co given by Konijn et al., 1956, occurs at 1.36 MeV whereas the present result suggests an excited state at 0.9 MeV. Allan, 1957, finds no discontinuities between 7 and 10 MeV for ^{58}Ni, but there is a prominent edge in his spectrum at 6 MeV. This confirms the deuteron assignment in the present experiment, since being unable to distinguish between deuterons and protons in the nuclear emulsion, a 7.7 MeV. deuteron will look like a 5.8 MeV proton in Allan's experiment. Correcting for the different energy loss of protons and deuterons in the target and proportional counters, the edge found by Colli et al., 1957a; 1958b, at 7.3 MeV. proton energy probably corresponds to the deuteron found here.

^{60}Ni, Figure IV.XX - This spectrum is inconsistent with the n,p Q value (Q = -2.03 MeV) having a peak at 13.2 MeV, otherwise the spectrum is in broad agreement with those of March and Morton, 1958b, and Allan 1957, a slight discontinuity at 11.4 MeV in the present spectrum being confirmed by Allan. Another slight discontinuity at 9.6 MeV is evident, but there is no indication of a large contribution from the n,d ground state transition.

^{63}Cu, Figure IV.XX1 - Despite a Q value of +0.7 MeV for the ^{63}Cu(n,p)^{63}Ni reaction no yield is observed above 11 MeV in this spectrum. A prominent peak at

9.5 MeV is very near the predicted position of the $^{63}Cu(n,d)^{62}Ni$, Q = -3.7 MeV ground state transition. Allan, 1958, quoting peaks at 10.2 and 7.5 MeV for ^{63}Cu, ascribes those to n,p reactions comparable to the anomalous inelastic scattering of 23 MeV protons found by Cohen 1957, but remembering that the emulsion technique can not distinguish protons from deuterons, it is more probable that the peak found at 7.5 MeV is caused by 10.2 MeV deuterons rather than 7.5 MeV protons. If a correction for the different energy loss of a deuteron in Allan's target foil is made, (0.15 MeV) a very good fit is obtained to the Q value of the ground state n,d reaction. In Figure IV.XX1, then, it would appear that the main peak at 9.5 MeV is due to deuterons, while the slight edge at 10.2 MeV represents an n,p transition to a level or group of levels with excitation energy 4.5 MeV in ^{63}Ni. The edge at 8.5 MeV may be either an n,p transition or the n,d transition to the first excited state at 1.172 MeV, spin 2(+) in ^{62}Ni. Being obtained from a natural copper foil (69%^{63}Cu, 31%^{65}Cu), the ^{63}Cu spectrum contains a correction for the effect of ^{65}Cu in the original spectrum. The ^{65}Cu spectrum is of exceptionally low yield except for a peak at 8.3 MeV, but the edge obtained at 8.5 MeV in the ^{63}Cu spectrum is not a consequence of the subtraction of the ^{65}Cu 8.3 MeV peak.

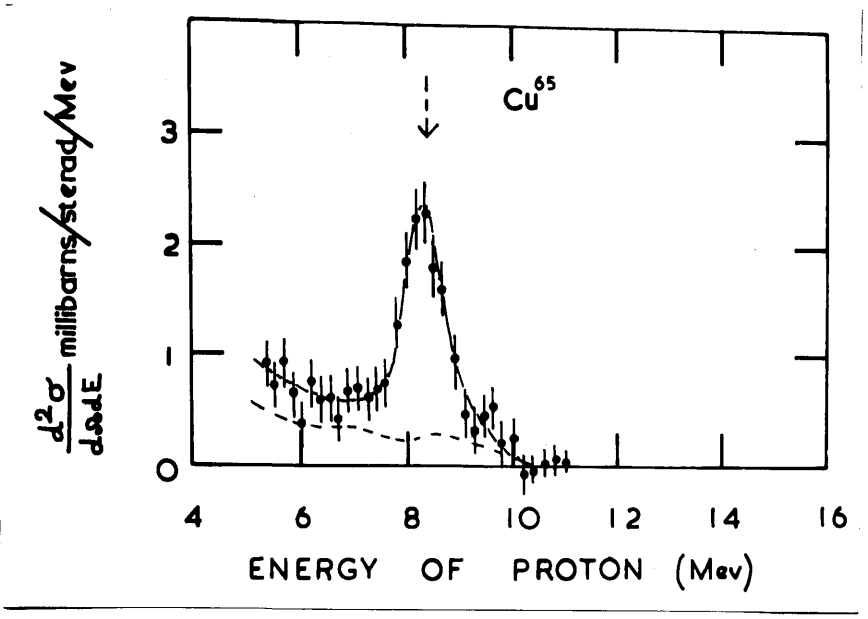

Figure IV.XX11. The energy spectrum of protons from the reaction $^{65}Cu(n,p)^{65}Ni$. The reaction $^{65}Cu(n,d)^{64}Ni$ is also present.

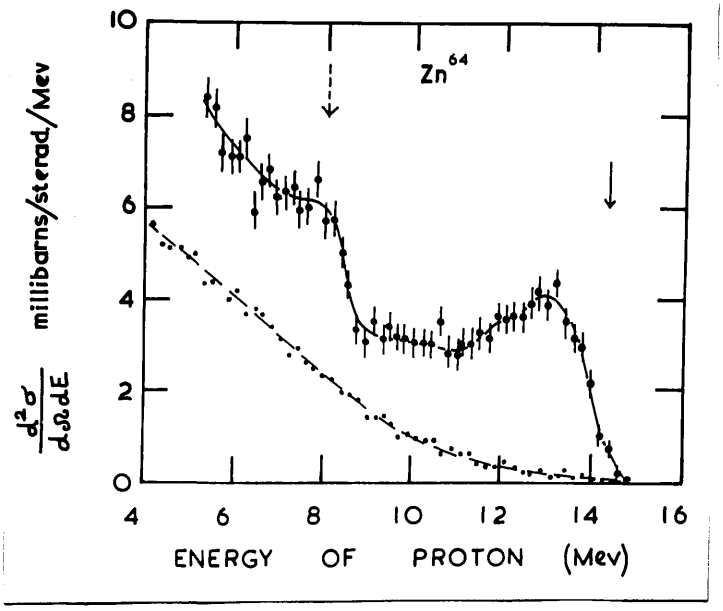

Figure IV.XX111. The energy spectrum of protons from the reaction $^{64}Zn(n,p)^{64}Cu$.

^{65}Cu, Figure LV.XX11 - This was the lowest yield element studied, no protons being observed beyond 10 MeV although the Q value is -1.02 MeV for the $^{65}Cu(n,p)^{65}Ni$ reaction. The prominent peak obtained at 8.3 MeV is only 0.1 MeV lower than the predicted position of the n,d ground state transition $^{65}Cu(n,d)^{64}Ni$, Q = -5.10 MeV. Making allowance for a background of n,p reactions, the cross-section for this peak is 1.6 millibarns/steradian. Allan, 1957, did not observe anything significantly above background for ^{65}Cu, It is not surprising that the n,d pick-up reaction is obtained for the copper isotopes, since the number of protons (Z = 29) is one more than the magic number 28, and the residual nuclei both have spin 0(+).

^{64}Zn, Figure IV.XX111 - This spectrum is consistent with the Q value of the reaction $^{64}Zn(n,p)^{64}Cu$ Q = +0.2 MeV and a sharp rise in the spectrum at the position of the $^{64}Zn(n,d)^{63}Cu$ Q = -5.45 MeV ground state transition is evident. There is an extreme contrast between the present result and the "4π" spectrum ~~of Storey et al~~ in the number of high energy protons present.

In Figure IV, XX1V, the data is presented in the form of the conventional "relative level density" log plot of $^{dn}/_{dE_p} \div E_p \sigma_c$ against E_p, where E_p is the energy of the proton emitted, and σ_c is the cross-

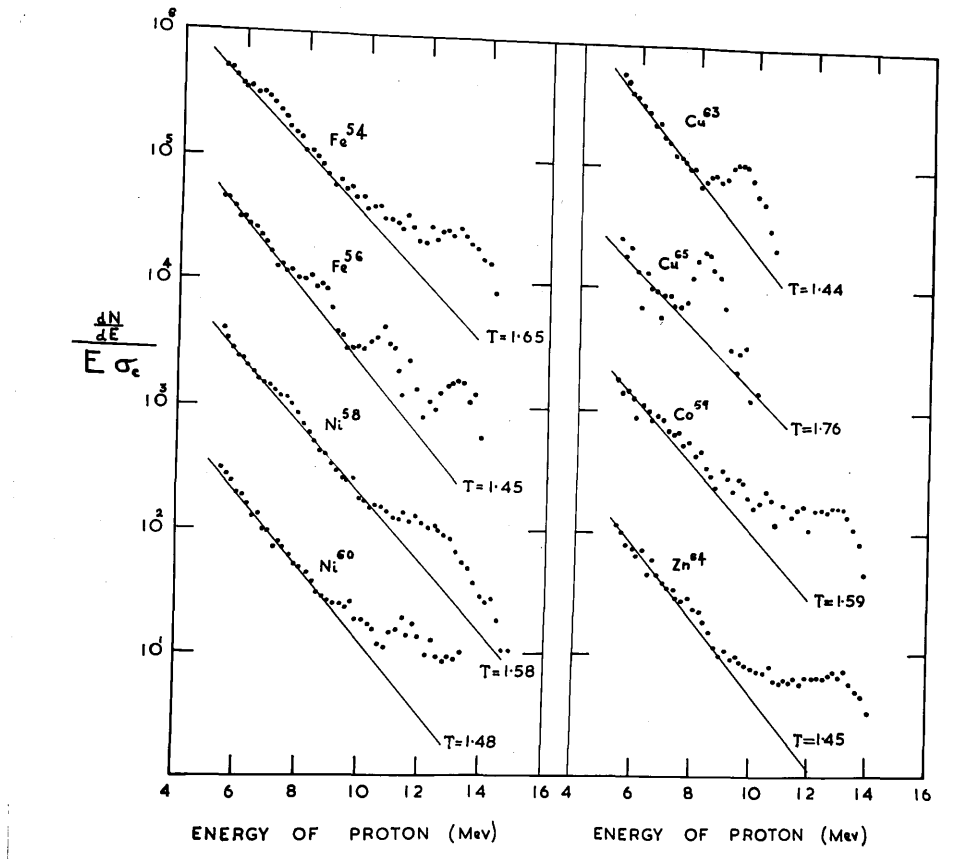

Figure IV.XXIV. Curves giving $dN/dE_p \div E_p\sigma_c$ versus E_p obtained from telescope measurements of the energy spectra of protons from n,p reactions in ^{54}Fe, ^{56}Fe, ^{58}Ni, ^{60}Ni, ^{63}Cu, ^{65}Cu, ^{59}Co and ^{64}Zn. E_p is the energy of the proton, and σ_c is the cross section for the inverse reaction corresponding to $r_o = 1.5 \times 10^{-13}$cm. The full line represents the "4π" nuclear temperature T. The curves are displaced arbitrarily with respect to the ordinate scale for convenience.

section for the inverse reaction where a proton of energy E_p interacts with the excited residual nucleus of the present experiment. Values of σ_c corresponding to $r_o = 1.5 \times 10^{-13}$cm. were taken from the tables of Blatt and Weisskopf, 1952. For convenience the curves are displaced arbitrarily with respect to the ordinate scale. The full line on each curve is not the best fit line for the present results, but represents the "nuclear temperature" measured from the 4π spectrum for the same reaction. A good fit is obtained between 6 and 9 MeV for all elements except ^{65}Cu and ^{59}Co; above 9 MeV there is an appreciable contribution from direct interaction processes. Aluminium is not included in Figure IV.XXIV, since being a light element, there are probably insufficient levels in ^{27}Mg between 4 and 7 MeV excitation energy to merit a statistical approach, however, the present result is a good fit to the 4π "nuclear temperature" of 1.75 MeV. ^{65}Cu is included for completeness, but the poor signal to background ratio for this element means that little significance can be attached to the present result. Nevertheless, it is interesting that the present result indicates a lower "temperature" (T = 1.5 MeV) than that measured from the 4π spectrum, (1.76 MeV), since the latter "temperature" is anomalously high when

compared with the Fermi gas model prediction. Having a low yield, it is possible that in the case of ^{59}Co many of the protons originate in direct interactions. Most theories of direct interaction result in a spectrum with a relatively greater number of higher energy protons than the spectrum determined by the level density of the residual nucleus, consequently higher "nuclear temperatures" are expected for spectra where direct interaction is present.

IV.4 Remarks.

a) The Apparent Violation of the n,p Q Value.

It has been noted that the spectra obtained from the ^{56}Fe and ^{60}Ni targets show an apparent violation of the n,p Q value. This is thought to be caused by the absorption of small quantities of hydrogen in the separated isotope targets during their preparation by electrodeposition. From the average angle of acceptance of the telescope, 16^{o}, we would expect a thin hydrogen target to produce a broad peak at 13 MeV, and this is in fact the result obtained. It will be noted, too, that the natural targets of fluorine and aluminium which also have negative n,p Q values do not show this effect.

~~Before discussing the results, some remarks concerning the~~

b) The Background Spectrum.

Apart from the 10% of this spectrum due to random

coincidences, most of the background must arise from reactions in the crystals themselves. The thick crystal contribution would not be expected to show structure since protons and other particles will be produced at all depths of it, and will lose varying amounts of energy getting out of the crystal to produce a coincidence pulse in the thin crystal. On this basis, the broad peak between 8 and 12 MeV is attributed to n,p n,d or n,α reactions in the thin crystal. The Q values of the reactions $^{127}I(n,\alpha)^{124}Sb$ and $^{133}Cs(n,\alpha)^{130}I$ are 4.4 and 4.0 MeV respectively, but assuming that the n,α reaction will be similar to the p,α reaction studied by Fulmer and Cohen, 1958, with 23 MeV protons, and taking into account the fluorescent response of alpha particles relative to protons in CsI(Tl), and the thickness of the thin crystal, an upper limit of 8 MeV is found for the peak of the evaporation spectrum of alpha particles. Considering the n,d reactions in ^{127}I and ^{133}Cs, (both Q values = -4.1 MeV) the ground state pick-up reactions would produce deuterons of energy 10 MeV, and taking their origin in the thin crystal into account these deuterons would be expected to appear at 10.3 MeV on the unbracketted energy scale of Figure IV.xii. We are led to the conclusion that the n,p

reaction is mainly responsible for the peak in the background, but a contribution from the n,d reaction cannot be ruled out. Calculating the ratio of the neutron fluxes at the two crystals, their efficiency for recording protons produced in each other, and the depth of thick crystal effective in this energy range, it may be deduced from the prominence of the peak that the angular distribution of the reaction producing it is strongly peaked in the forward direction. The bracketted scales refer to the cross-section and energy of protons emitted from the thin crystal.

CHAPTER V.

The Interpretation of the "4π" Spectra.

V.1 Statistical Theory and the Empirical Level Density Formula.

Examining the relative level density log plots of Figures III.X111 and III.X1V it is evident that the spectra are a good fit to a pure exponential distribution at proton energies greater than 6 MeV, and are not concave down towards the energy axis. Below 6 MeV, there is a tendency for the experimental points to lie above the pure exponential distribution. This may be attributed to protons from the n,np reaction together with some error associated with the values of σ_c used - increasing the radius parameter "r_o" used in the evaluation of σ_c decreases the amount of curvature present. Assuming the statistical theory applicable to the spectra, we are led to the conclusion that either a) the concavity of the spectra predicted by the empirical level density formula $\omega(E) = C \exp. \left[2(aE)^{\frac{1}{2}}\right]$ of Blatt and Weisskopf, 1952, is obscured by increasing contributions from direct interactions at the higher proton energies, or b) the level density function is a pure exponential. Alternatively, the statistical theory may not be relevant in this case, and the spectra do not represent relative level densities. This will be discussed later.

Using the spectra to estimate the parameter "a" in $\omega(E) = C \exp. \left[2 (aE)^{\frac{1}{2}}\right]$, two approximations can be made. In the first, we assume that we can extrapolate the "nuclear temperature" T back to zero proton energy. This is equivalent to the expansion used in Chapter I to derive the nuclear temperature T. The expansion is not very good in our case, since the lowest proton energy where T is determined, say 6 MeV, is not very small compared to the maximum excitation energy of the residual nucleus, $E^* \sim 14$ MeV. Using this approximation, viz. that the temperature T corresponds to the maximum excitation energy of the residual nucleus, we find the values of "a" shown in Table V.1 a) using the Fermi gas equation of state $E^* = aT^2$. In view of the crude approximation used, there is an extraordinary agreement between the values of "a" found and those derived by Lang and Le Couteur, 1954, and expected from the simple degenerate Fermi gas model of the nucleus, namely $a = \frac{A}{10.5}$ MeV^{-1}. Despite the small range of A considered, there seems to be evidence for the proportionality of "a" to A.

Analysing Figure III.XIV in the same way, we obtain values of "a" from the "nuclear temperatures" corresponding to the different maximum excitation energies of the residual nuclei formed when the targets

TABLE V.1.

	Target Nucleus	^{27}Al	^{54}Fe	^{56}Fe	^{58}Ni	^{60}Ni	^{63}Cu	^{64}Zn
a)	$a = E^*/T^2$, MeV^{-1}	4.0	5.3	5.3	6.0	5.5	7.2	6.8
b)	$a = E/T^2$, MeV^{-1}	1.8-1.3	3.3-2.0	2.6-1.0	2.6-1.8	2.7-1.4	4.6-3.4	4.3-2.6

a) Values of "a" derived from $a = E^*/T^2$ where E^* is the maximum energy of excitation possible in the residual nucleus, and T is the nuclear temperature measured from the "4π" spectra corresponding to a neutron bombarding energy of 14.1 MeV.

b) Limits on the value of "a" determined by the formula $a = E/T^2$ where E is the excitation energy of the residual nucleus at the point where the slope $\frac{1}{T}$ is determined.

^{54}Fe, ^{58}Ni and ^{64}Zn are bombarded with neutrons of 12.9, 14.1 and 15.7 MeV. These values of "a", shown in Table V.2., are approximately constant for each nucleus, confirming the Fermi gas equation of state $E^* = aT^2$. An unsatisfactory feature of this result is the fact that the truth of this law implies that the relative level density log plots should be concave down to the energy axis, since we expect to see a change of slope, representing nuclear temperature, with excitation energy. This difficulty is not so serious as it seems whenwe examine Figure III.XlV carefully. If we find a slope $\frac{1}{T}$ at proton energy 6 MeV in b) we would expect to find the same slope at proton energy 6 + 2.8 MeV in curve a). However, the difference in slope involved is very small, and remembering that the best statistics are obtained at the lower proton energies and that direct interaction is by no means unlikely for protons of 9 MeV, it is quite possible that it is the slope of the log plot at the lowest proton energies only which is related to the relative level density.

In the second method of approximation, we substitute the empirical level density formula $\omega(E) = C. \exp. \left[2 (aE)^{\frac{1}{2}}\right]$ in the basic evaporation energy spectrum $\frac{dn}{dE_p} = K.E_p.\sigma_c\,\omega(E)$ derived from the statistical theory.

TABLE V.2.

	Target Nucleus	^{54}Fe	^{58}Ni	^{64}Zn
a)	$a = E^*/T^2, MeV^{-1}$ $E_N = 12.9$ MeV	5.3	5.7	6.6
b)	$a = E^*/T^2, MeV^{-1}$ $E_N = 14.1$ MeV	5.3	5.9	6.8
c)	$a = E^*/T^2, MeV^{-1}$ $E_N = 15.7$ MeV	5.2	5.4	6.7

Values of "a" derived from $a = E^*/T^2$ where E^* is the maximum energy of excitation possible in the residual nucleus and T is the nuclear temperature measured from the "4π" spectra corresponding to neutron bombarding energies E_N = 12.9, 14.1 and 15.7 MeV. The proportionality of "a" to A ~~and B~~ is evident.

Remembering our definition of T, $\frac{1}{T} = \frac{d}{dE_p}\left\{\log \frac{dn/dE_p}{E_p \cdot \sigma_c}\right\}$ and performing the appropriate differentiation, we find $\frac{1}{T} = \left(\frac{a}{E}\right)^{\frac{1}{2}}$, i.e. $a = \frac{E}{T^2}$. Now examining the relative level density log plots obtained using the telescope, Figure IV.XX1V., it is seen that agreement with the "4π" nuclear temperatures is found in the range E_p = 6 to 9 MeV. If we assume that the straight line representing the nuclear temperature is the tangent to the level density curve in the range 6 to 9 MeV proton energy, we obtain limits on the value of "a" by inserting the corresponding values of E in $a = \frac{E}{T^2}$. The values of "a" obtained in this way are shown in Table V.1.b). Perhaps most weight should be attached to the value of "a" corresponding to the higher excitation energy, since it will be less affected by direct interactions. It is seen that, in general, the new values of "a" are approximately half those predicted by the simple Fermi gas model of the nucleus, $a \simeq \frac{A}{10.5}$ MeV.

Brueckner, 1955, has shown that many of the properties of the nucleus can be calculated by assuming that nuclear matter consists of a Fermi gas with the effect of the strong nucleon-nucleon interactions taken into account by replacing the real mass of the nucleon in the nucleus by an effective mass approximately half

the real one. Clementel and Villi, 1958, have applied this concept to the statistical theory, and have shown that the predicted value of "a" is reduced in the ratio (effective mass) ÷ (real mass). This is easily derived, since we have seen how the level density calculation of Bethe, 1937, leads to $\omega(E) \propto^{al} \exp. \left[\pi\left(\frac{AE}{E_F}\right)^{\frac{1}{2}}\right]$ ~~$\pi\left(\frac{AE}{E_F}\right)^{\frac{1}{2}}$~~ where E_F is the Fermi energy i.e. "a" $\propto^{al} \frac{1}{E_F}$. But $E_F = \frac{h^2}{2M}\left\{\frac{3N}{4\pi V}\right\}^{2/3}$ where M is the mass of a Fermion (nucleon), and N is the number of Fermions confined in a volume V. It follows then that "a" $\propto^{al}$ M.

Analysing the spectra by the second method of approximation leads to values of "a" which confirm the concept of an effective nucleon mass in nuclear matter $\simeq \frac{1}{2}$ real nucleon mass. It will be noted too, that the lower values of "a" derived by the second analysis are in closer agreement with those derived from excitation function data (a $\sim$ 2 MeV^{-1} for medium weight nuclei).

V.2 <u>The Pure Exponential Level Density Formula</u>.

As mentioned previously, many experiments have produced relative level density log plots which show a pure exponential distribution. One of the latest of these, Fulbright et al., 1959, is particularly convincing since it is obtained for inelastic alpha particle scattering where, at first sight anyway, one would expect a minimum contribution from direct interactions.

Some other results showing this same effect are shown in Figures V.i,ii,iii. In Figure V.i., the 150^{o} spectra of Gugelot, 1954, for the inelastic scattering of 18 MeV protons are re-analysed, and it is seen that for the medium weight elements Fe, Ni and Cu the middle region of the spectra (which is unaffected by multiple reactions and direct interactions) shows a pure exponential behaviour. Figure V.ii. compares the $Cu(p,p^{1})Cu^{*}$ spectrum of Gugelot, 1954, with the energy spectrum of neutrons from the $^{63}Cu(p,n)^{63}Zn$ reaction studied by Thomson, 1956. Again the middle region of the spectra shows a pure exponential distribution. The energy spectra at 90^{o} of protons and alpha particles emitted from the excited nucleus (39.3 MeV)^{41}Ca formed in the heavy ion experiment of Zucker, 1958, (^{27}Al + ^{14}N) are shown in Figure V.iii. Zucker, 1958, finds a straight line distribution plotting $\log\left\{\frac{dn/dE_p}{E_p\sigma_c}\right\}$ versus $E_p^{\frac{1}{2}}$, but it is seen that plotting the results in terms of E_p gives a tolerably good fit to a pure exponential distribution.

Neglecting, for the moment, the differences in measured "nuclear temperatures", and assuming the statistical theory applicable, it appears that there is considerable evidence to support the view that the level density distribution is a pure exponential.

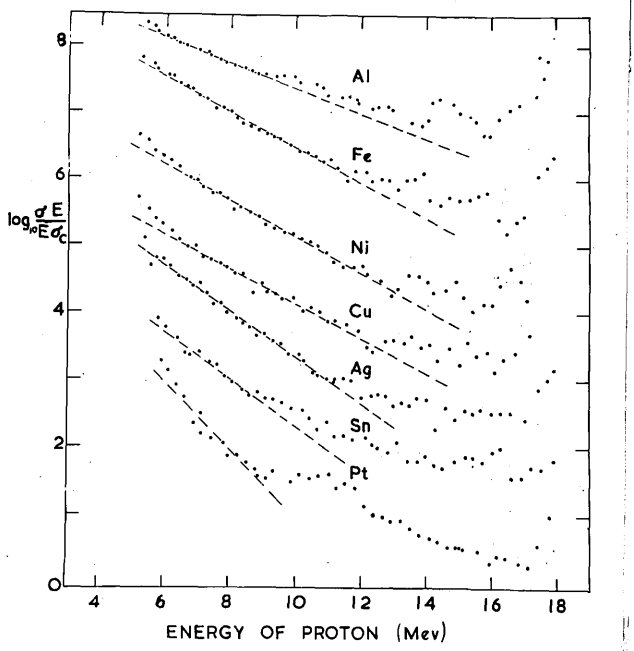

Figure V.i. The energy spectra of inelastically scattered protons of 18 MeV, Gugelot, 1954. The spectra are measured at 150°. The curves are displaced arbitrarily with respect to the ordinate scale.

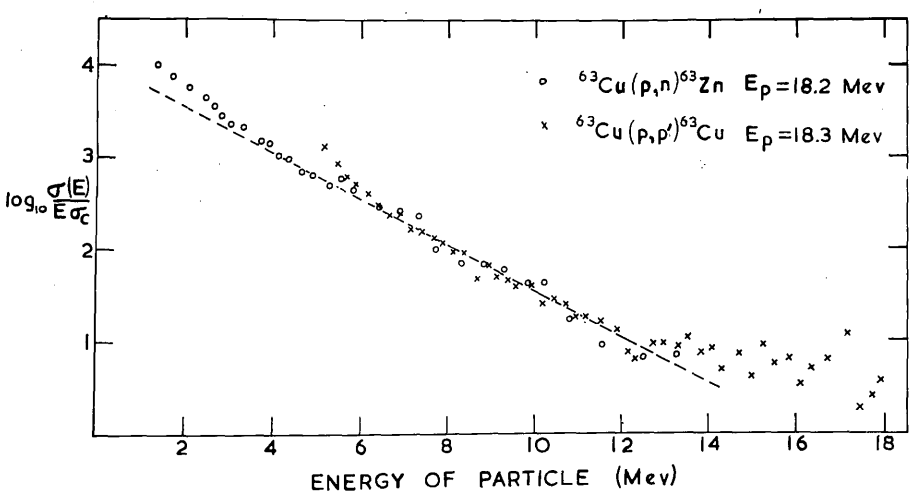

Figure V.ii. The neutron (Thomson, 1956) and proton (Gugelot 1954) energy spectra for ^{63}Cu bombarded with 18.2 MeV protons. The curves are displaced arbitrarily with respect to the ordinate scale.

Indeed, the analysis of the present results suggests that such a distribution extrapolates at high excitation energies ($\sim$ 14 MeV) to that expected from the simple degenerate Fermi gas model of the nucleus, and at lower excitation energies ($\sim$ 7MeV) to that predicted by the modified (Brueckner effective mass concept) Fermi gas model. This picture is not unreasonable, since Ericson, 1958, has derived a level density formula from a degenerate Fermi gas model which takes into account the nucleon-nucleon interactions associated with pairing effects, and finds that the predicted "nuclear temperature" at low excitation energies varies more slowly with energy than than predicted on the simple independent particle Fermi gas model.

V.3 Cross Sections and Statistical Theory.

According to the statistical theory, the probability of emission of a proton of energy E_p in the range dE_p is given by

$$F_p(E_p)dE_p = K.E_p.\sigma_p\omega_p(E)dE_p$$ where K is a constant depending on the compound nucleus, σ_p is the cross section for the inverse reaction where a proton of energy E_p is incident on the excited residual nucleus energy E to form a compound nucleus of energy E_c^*, and $\omega_p(E)$ is the level density at excitation energy E in the residual nucleus.

Similarly for neutrons $F_N(E_N)dE_N = K.E_N.\sigma_N \Omega_N(E)dE_N$.

We will use the conventional approximation

$\log \Omega(E) \simeq S(E)$.

$S_p(E) = S_p(E_c^* - E_p - B_p)$ where B_p is the binding energy of the proton in the compound nucleus.

$= S_p(E_c^* - E_p - B_N - \Delta)$ where $\Delta = B_p - B_N$ is the difference in the proton and neutron binding energies.

Expanding $= S_p(E_c^* - E_p - B_N) - \Delta\left(\frac{ds}{dE}\right)_{E_c^* - E_p - B_N}$

Now, $\left(\frac{ds}{dE}\right)_{E_c^* - E_p - B_N}$ represents the reciprocal of a nuclear temperature T evaluated at excitation energy $E_c^* - E_p - B_N$. But this is precisely the energy region where we determine the nuclear temperature from the evaporation spectra, so the two temperatures are identical. We may note, too, that the expansion used is valid since the maximum value of Δ is 3 MeV, and taking a nuclear temperature of 1.5 MeV, the average value of $E_{P,N}$ is $\sim$ 3 MeV so that $E_c^* - E_{p,N} - B_N \sim$ 11 MeV on the average.

It follows that the ratio

$$\frac{F_P(E_P)}{F_N(E_N)} = \frac{K.E_P.\sigma_P.\exp.[S_P(E_c^* - E_P - B_N)].\exp.[-\Delta/T]}{K.E_N.\sigma_N.\exp.[S_N(E_c^* - E_N - B_N)]}$$

For $E_P = E_N$, we can assume $S_p(E_c^* - E_P - B_N) = S_N(E_c^* - E_N - B_N)$, and we find that the ratio of the emission probabilities of a proton and a neutron is $\alpha^{al}\ \sigma_P/\sigma_N \cdot \exp\left[\frac{\Delta}{T}\right]$. If we choose a narrow range of elements we may neglect the small changes in σ_P/σ_N caused by the slightly different Coulomb correction, and we should then find that a plot of $\log_e\left\{F_P/F_N\right\}$ versus Δ is a straight line of slope $-\frac{1}{T}$.

In the "4π" spectra, we find that T measured from the evaporation spectra is approximately constant in the energy range where most of the proton and neutron emission takes place, so it will be a good approximation to replace $F_p(E_P)/F_n(E_N)$ by $\bar{\sigma}(n,p)/\bar{\sigma}(n,n)$ the ratio of the cross sections for the emission of a proton and a neutron from the compound nucleus. Values of $\bar{\sigma}(n,p)$ have been evaluated from our spectra and are presented in Table III.2. Assuming negligible contributions from reactions such as n,d and n,α, we may estimate $\bar{\sigma}(n,n')$ by subtracting the values of $\bar{\sigma}(n,p)$ from the reaction cross sections for neutrons of 14 MeV obtained by Flerov and Talyzin, 1957. It will be noted that this procedure accounts automatically for the reactions n,pp; n,pn; n,nn; n,np.

Figure V.1V shows the plot of $\log_{10}\left\{\bar{\sigma}(n,p)/\bar{\sigma}(n,n)\right\}$ against $\Delta = B_p - B_N$(MeV) for the odd-odd compound nuclei

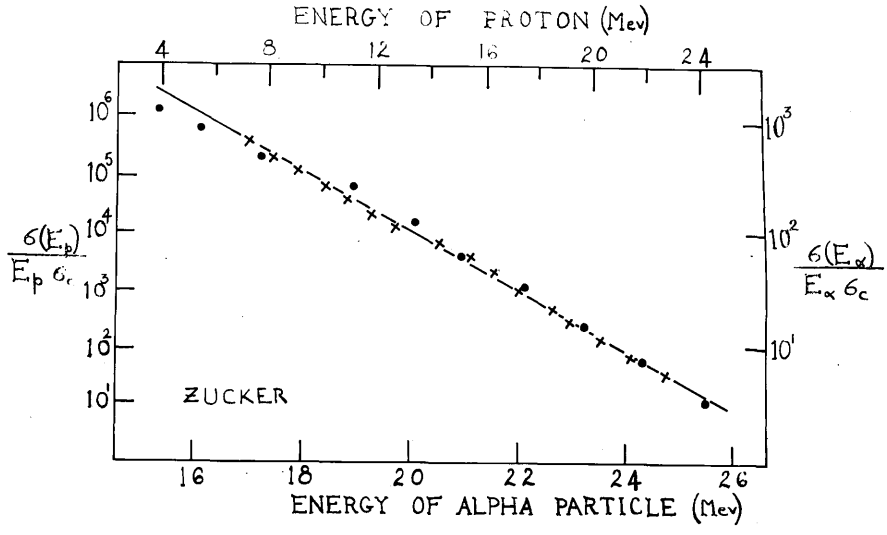

Figure V.iii. The energy spectra of protons (●) and alpha particles (x) emitted from the excited (39.3 MeV) nucleus ^{41}Ca formed in the heavy ion experiment $^{27}Al + ^{14}N$ of Zucker, 1958. The curves are displaced arbitrarily with respect to the ordinate scale.

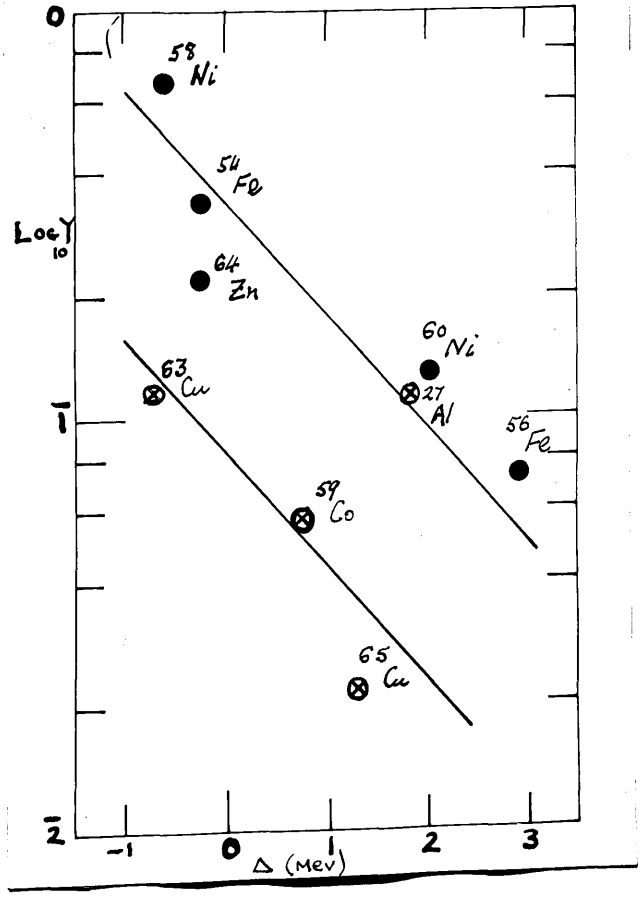

Figure V.1V.

$Y = \bar{\sigma}(n,p)/\bar{\sigma}(n,n)$ plotted as a function of $\Delta = B_p - B_N$ where B_p and B_N are the binding energies of a proton and a neutron respectively in the compound nucleus. ● - even-even target nucleus; ⊗ - odd-even target nucleus.

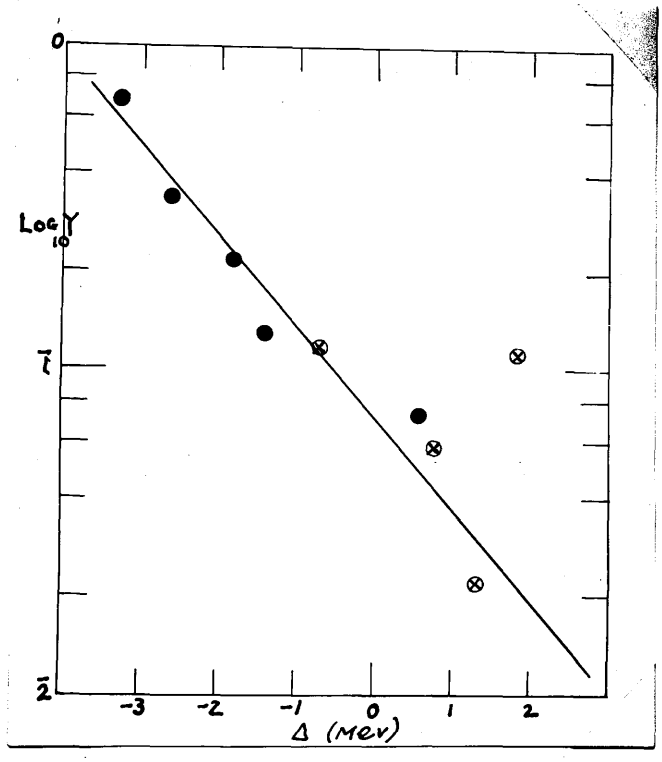

Figure V.V. $Y = \bar{\sigma}(n,p)/\bar{\sigma}(n,n)$ plotted as a function of $\Delta = B_p - B_N + P_p$ where B_p and B_N are the ~~limiting~~ binding energies of a proton and a neutron respectively, in the compound nucleus and P_p is related to the pairing energy. ● even-even target nucleus, ⊗ odd-even target nucleus.

(⊗ circles) and even-odd compound nuclei (full circles) formed in the present experiment at 14.1 MeV. The full lines have slopes representing the average "nuclear temperature" (T = 1.55 MeV) found from the evaporation spectra. It is seen that, with the exception of the light nucleus ^{27}Al, there is fair agreement with the simple theory above for each type of compound (or residual) nucleus. The difference observed for the two types of nuclei is caused by the fact that bombarding an even-even target with neutrons, proton emission leaves an odd-odd residual nucleus while neutron emission leaves an even-even residual nucleus. On the other hand, bombarding an odd-even target, proton and neutron emission lead to even-odd and odd-even residual nuclei respectively. But the simple theory above, did not take into account differences in level density depending on the type of nucleus involved. In an analysis of the available data, Brown and Muirhead, 1957, find ω(odd-odd): ω(even-odd): ω(odd-even): ω(even-even) $\simeq$ 12:5:5:1. This difference can be regarded as due to an energy gap in the level density at the ground state caused by pairing energy effects. We can effect a correction for this by replacing the binding energy of the proton in an even-odd compound nucleus by the average of the proton binding energies in the neighbouring odd-odd

compound nuclei i.e. for an even-even target nucleus we write $\Delta = B_p - B_N + P_p$ where $P_p = \frac{1}{2}B_p(A + p + n) + \frac{1}{2}B_p(A - p + n) - B_p(A + n)$; $B_p(A + p + n)$ etc. being the proton binding energies in the corresponding nuclei with A the atomic mass number of the target nucleus. The corrected results are shown in Figure V.V. P_p is of the order of 2 MeV.

The agreement of the relative cross sections with the average "nuclear temperature" of the evaporation spectra is quite good and, like the evaporation spectra, there is at least qualitative agreement with the predictions of the statistical theory.

V.4 Conclusions.

On the basis of the evidence presented so far, a fairly clear interpretation of the present results is possible. The situation is summarised below.

1) The simplest analysis of the spectra yields values of "a" for an excitation energy of the order of 14 MeV in good agreement with those deduced by Lang and Le Couteur, 1954, from evaporation spectra.

2) A more refined analysis gives lower values of "a" for an excitation energy of approximately 8 MeV. These values of "a" confirm to some extent the concept of an effective nucleon mass approximately half the real mass inside the nucleus. The lower values of "a" are in

closer agreement with the values of "a" obtained in excitation function experiments and with the approximate value of "a" derived by Blatt and Weisskopf, 1952, p.372, in a comparison of level densities at the neutron binding energy with those at low excitation energies ("a" $\sim$ 2 MeV^{-1} for A = 63).

3) There is some evidence for a pure exponential level density function at excitation energies less than 8 MeV. This conclusion depends upon the extent of the direct interaction contribution to the "4π" spectra.

4) The relative magnitudes of the $\sigma(n,p)_{\Lambda}^{\Psi}$ cross sections are in agreement with the predictions of the statistical theory.

Summing up, it appears that the "4π" spectra are in general agreement with the statistical theory with its implication of a compound nucleus mechanism. There is evidence that the level density distribution approaches that predicted by the simple Fermi gas model at high excitation energies. At lower excitation energies, the "nuclear temperature" varies more slowly with energy than the simple Fermi gas model predicts due to the effect of nucleon-nucleon interactions inside the nucleus. It is plausible that the Brueckner effective mass should approach unity at the higher excitation energies where nucleon-nucleon interactions may not be so important.

Comparing the magnitudes of the "nuclear temperatures" found here with those derived from other evaporation experiments, several discrepancies are apparent. The average "4π" temperature, T = 1.55 MeV, is in good agreement with those measured from the spectra of Gugelot, 1954 (Figure V.i., T = 1.64, 1.63 and 1.68 MeV for Fe, Ni and Cu); Thomson, 1956, (Figure V.ii. T = 1.7 MeV for $^{63}Cu(p,n)^{63}Zn$ at E_p = 18.3 MeV); and Zucker, 1958 (Figure V.iii. T = 1.7 MeV for A =40 implying T $\sim$1.4 MeV for A = 58). On the other hand, March and Morton, 1958a, and Allan, 1959, using the nuclear emulsion technique find a "nuclear temperature" of T = 1.2 MeV for the reaction $^{54}Fe(n,p)^{54}Mn$. Also, Cohen and Rubin, 1959, disagree with Gugelot, 1954, finding nuclear temperatures of approximately 1.1 MeV for the energy spectra of inelastically scattered protons of 14.5 MeV for targets of Fe, Ni and Cu, and Fulbright et al., 1959, find T = 1.15 $\pm$ 0.04 MeV for the 135° spectra of inelastically scattered alpha particles of 20 MeV from targets and Ni and Cu.

These discrepancies indicate that the conclusions noted above may be only qualitatively correct, the "4π" spectra containing an appreciable contribution from direct interactions, but at the moment the weight of evidence seems to be evenly distributed between the two magnitudes of nuclear temperature.

Chapter VI.

The Interpretation of the "0°" Spectra*.

VI.1 Anomalous and Single Particle Effects.

The first conclusion to be drawn from the spectra presented in Chapter IV is that the peaks in the spectra corresponding to an excitation energy of approximately 7 MeV are not due to an anomalous or single particle effect but are most probably caused by the detection of the n,d pick-up reaction. As might be expected, particularly high cross sections for the ground state n,d reaction are obtained when the target nucleus comprises a closed shell of protons with a single loosely bound proton outside the closed shell as in the case of ^{19}F, ^{63}Cu and ^{65}Cu. These fairly high n,d cross sections may be compared with the cross sections for the p,d reaction at proton energy 23 MeV measured by Cohen and Rubin, 1958. In this case too, the pick-up cross section is larger than that expected previously. (Colli et al., 1959b, have recently observed the n,d reaction bombarding the isotopes ^{31}P and ^{32}S with 14 MeV neutrons.)

Footnote * For convenience, we will call the spectra of protons emitted into a small solid angle in the forward direction the "0°" spectra.

The "0°" spectra show little evidence for systematic structure of the type found by Cohen et al., 1957, 1958, 1959, in the inelastic scattering of protons of energy 11 to 23 MeV. This is in agreement with the findings of Cohen and Rubin, 1958, who show that the anomalous behaviour - a proton group with fine structure corresponding to an excitation energy of approximately 2.5 MeV in the residual nucleus - first appears in the isotopes of Zn. In addition, they find that the cross section for the production of the anomalous group increases with bombarding energy, the dependence being most marked in the case of Zn. These authors also find a prominent proton group corresponding to an excitation of 1 to 1.5 MeV for the elements of atomic number Z = 26 to 30. Greenlees et al., 1958, studying the inelastic scattering of protons of 10 MeV find little evidence for the anomalous group at 2.5 MeV excitation energy, but the group at 1 to 1.5 MeV is confirmed. However, the latter group need not be regarded as due to an anomalous effect, since the level spacing is large in these elements at such low excitation energies. The present results for ^{54}Fe and ^{64}Zn seem to show this effect too, but the possibility of hydrogen contamination of the targets must be borne in mind.

The spectra for the reactions $^{56}Fe(n,p)^{56}Mn$ and

$^{60}Ni(n,p)^{60}Co$ shown in Figures 1V.XV11 and XX do show a similarity to those of Cohen et al., and it might be thought that there was some evidence for an anomalous effect, the structure in these reactions corresponding to excitations of 0.5 and 2.5 MeV in ^{56}Mn and 0.6 and 2.4 MeV in ^{60}Co. It is interesting to compare these spectra with the proton energy spectra from the reactions $^{55}Mn(d,p)^{56}Mn$ and $^{59}Co(d,p)^{60}Co$ studied by Green et al., 1958, and Foglesong and Foxwell, 1954, respectively. Plotting a histogram of the number of d,p protons observed per 0.4 MeV energy interval, we find broad peaks in both reactions at excitation energies of approximately 0.5 and 2.5 MeV, and it is tempting to assume the existence of a "modulation" or "giant resonance" effect of the type postulated by Blok and Jonker, 1957, and Colli et al., 1957. This effect is similar to the single particle effect discussed by Peck and Lowe, 1959, in the case of the d,p reaction where it is assumed that the neutron prefers to be captured into a single particle excited state of the residual nucleus, the rest of the nucleus remaining undisturbed. Considering that the n,p reaction to low lying states of the residual nucleus is likely to be a form of surface interaction like the d,p reaction, it would be reasonable to assume that this type of single

particle effect accounts for the peaks in the present spectra. However, this single particle interpretation would not be in accord with the conclusions of Cohen and Rubin, 1959, who are convinced that the anomalous peak at 2.5 MeV excitation energy in the inelastic proton spectra is due to the excitation of a band of levels of a collective model origin.

Upon closer examination, it appears that there is a simpler explanation of the "0^{o}" spectra. Plotting the number of levels per 0.4 MeV interval in the residual nuclei ^{56}Mn and ^{60}Co, Figure Vl.i, we find that the histograms do not show a monotonic increase of level density with excitation energy, but instead show a tendency to peak in the neighbourhood of 0.5 and 2.5 MeV. It follows that the "0^{o}" spectra are explained by any type of interaction which, neglecting selection rules concerning spin and parity of levels, attaches approximately equal weight to each level. We see, that if the present analysis is correct, the problem is no longer in deciding what kind of interaction is present, but in determining the cause of the irregularities in the level density function at low excitation energies. It is probably only a matter of time before these irregularities are explained by the shell and collective models.

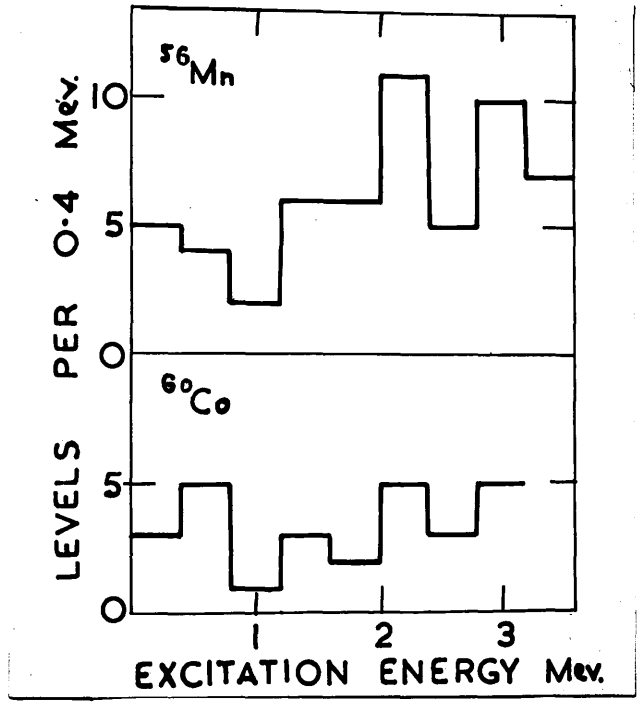

Figure VI.i. Histograms of the number of levels per 0.4 MeV in the residual nuclei ^{56}Mn and ^{60}Co.

VI.2 Direct Interaction and the Statistical Theory.

In Figure IV.XXIV and the preceding figures, it is seen that above 9 MeV proton energy there is a much larger contribution from higher energy protons in the "0^{o}" spectra than in the "4π" spectra. Their presence in the forward direction indicates that these additional protons are produced as a result of direct interactions. Considering that the lowest states of the residual nuclei seem to be preferentially excited, and in view of the theoretical arguments given in I.4, it is probable that the direct interactions involved occur in the surface of the nucleus. Below 9 MeV, the "0^{o}" spectra, with the exceptions ^{65}Cu and ^{59}Co, have the same exponential form as the "4π" spectra.

Having evaluated absolute cross sections in both the "0^{o}" and "4π" experiments, it should be possible to say something about the relative contributions of "direct"interactions and "compound nucleus" interactions and also comment on the angular distribution of the lower energy protons. Normally, a comparison of differential cross sections from two experiments with vastly different geometries would be doubtful. On this occasion, however, the same neutron monitor and separated isotope targets were used in both experiments, and in addition the ratios of differential cross sections at a specific energy can be compared with the angular

distributions obtained by other workers. Table VI.1. shows the ratio of differential cross sections at 0^{o} and 90^{o} at 6 MeV proton energy obtained by other workers for comparison with the ratio of the "0^{o}" and "4π" differential cross sections. Since the "4π" experiment measures the cross section for protons emitted into a large solid angle (3.5 steradian) centred at 90^{o}, the measured cross section will be slightly higher than the true 90^{o} differential cross section, so we expect the second ratio in Table VI.1 to be slightly smaller than the first. The small solid angle of acceptance of the telescope of Colli et al., 1958a, is similar to the geometry of the "0^{o}" experiment, and in the case of the high yield isotope ^{58}Ni, the agreement is good, the present ratio 1.46 being just less than 1.72 measured by Colli et al. (A recent experiment of Colli et al., 1959a, finds a smaller value for $\frac{\partial\sigma}{\partial\omega\partial E}(18^{o}) \div \frac{\partial\sigma}{\partial\omega\partial E}(90^{o})$ than would be expected on the basis of the 1958a experiment). The following quantities are listed in Table VI.2. a) the Q value of the n,p reaction involved. b) the "0^{o}" differential cross section integrated over the range of proton energy E_p = 5.6 MeV $\rightarrow \infty$ c) the ratio R_1 = "0^{o}" integrated differential cross section ÷ "4π" integrated

Table VI.1.

	Target Nucleus	^{54}Fe	^{56}Fe	^{58}Ni	^{60}Ni	^{63}Cu
a)	Other Experiments	1.56†; [1.0]	1.67†	1.72*; (1.58)	2.0†	[2.0]; (1.52)
b)	Present Experiment	1.73	2.10	1.46	1.78	1.74

a) The ratios of the 0° and 90° differential n,p cross sections at 6 MeV proton energy evaluated from the angular distributions of other experiments.

b) The ratio - differential n,p cross section at 6 MeV proton energy at approx. 0° (Telescope experiment) ÷ differential n,p cross section at 6 MeV proton energy at average angle of "4π" experiment.

Symbols:- [ ] - Allan, 1959; † March and Morton, 1958 a,b; ( ) Verbinski et al., 1958; * - Colli et al., 1958a.

Note:- In a recent experiment with improved apparatus, Colli et al., 1959a, find a smaller value of the anisotropy for ^{58}Ni (measuring $\frac{\partial\sigma}{\partial\omega\partial E}(180^{\circ}) \div \frac{\partial\sigma}{\partial\omega\partial E}(90^{\circ})$) than that quoted here.

Table VI.2.

	Target Nucleus	^{27}Al	^{54}Fe	^{56}Fe	^{58}Ni	^{60}Ni	^{59}Co	^{63}Cu	^{65}Cu	^{6}
a)	Q(n,p)MeV	-1.85	0.34	-2.93	0.62	-2.03	-0.72	0.78	-1.02	0.2
b)	$\int_{56}^{\infty} \frac{\partial\sigma}{\partial\omega\partial E} dE_p$ mb./ster.	8.9	39.2	11.1	48.8	17.5	9.2	12.3	2.4	37.2
c)	R_1	2.31	1.85	2.26	1.40	1.79	1.50	1.74	1.70	1.90
d)	R_2	2.76	3.36	5.31	1.88	4.34	4.88	-	-	5.90

a) Q value of the n,p reaction involved.

b) The differential n,p cross section at approx. 0° integrated over the proton energy range E_p = 5.6 MeV $\rightarrow \infty$

c) R_1, "0°" integrated differential cross section $\div$ "4π" integrated differential cross section, with limits of integration E_p = 5.6 - 9 MeV.

d) R_2, as c) with E_p = 9 MeV - ∞

differential cross section, with limits of integration E_p = 5.6 - 9 MeV.

d) R_2 as c) with E_p = 9 MeV - ∞

Comparing items b), c) and d) in Table VI.2, it is seen that, in general, as the yield decreases, the ratio R_2/R_1 increases. This implies that the cross section for the production of high energy protons from direct interactions does not depend on the Q value of the reaction to the same extent as the cross section for the protons originating in a compound nucleus mechanism. The exception to this rule is ^{64}Zn which has a high yield and a high value of R_2/R_1. The exceptionally large number of high energy protons present in this case is interesting, and it may be profitable to study their angular distribution at a later date. This high yield of protons may be connected with the fact that ^{64}Zn has two protons outside a closed shell of protons, and in a direct interaction ejecting one of the protons, the other proton is readily available to take up the balance of energy, being excited, perhaps, into a single particle state. In this connection, it will be remembered that the copper isotopes with a single proton outside a closed shell do not seem to be favourable for direct interaction although straight removal of the last proton

in the pick-up reaction leaving the residual nucleus unexcited is favoured.

Considering now the lower energy protons, we see from Table VI.1 and VI.2 (R_1) that there is considerable evidence to support the view that the protons of, say 6 MeV, have an anisotropic angular distribution. Even allowing for large errors in the differential cross sections measured here, normalising the R_1 value for ^{58}Ni to unity would still mean that many of the isotopes had appreciable anisotropies. These anisotropies are in conflict with the isotropic angular distribution expected by Hauser and Feshbach, 1952, for the statistical model, and they are an order of magnitude larger than the values of $\frac{\partial\sigma}{\partial\omega\partial E}(0^\circ) \div \frac{\partial\sigma}{\partial\omega\partial E}(90^\circ)$ predicted by the theory of Ericson and Strutinski, 1958. There is always the possibility, of course, that the anisotropy is caused by a non-random distribution of the phases of the levels excited in the compound nucleus. The little evidence on this, however, is not conclusive.

The assumption that the additional low energy protons in the "0°" spectra are the result of a direct interaction mechanism leads to a rather unsatisfactory conclusion. In Figure IV.XXIV we have seen that the "0°" log plots are a good fit to the "4π" nuclear temperatures in the range of proton energy 6 to 9 MeV. Now if we take

a spectrum of "nuclear temperature" 1.5 MeV and add to it another spectrum with only half the number of events in it but having a nuclear temperature of 2 MeV, the combined spectrum will have a nuclear temperature of 1.67 MeV. This order of change of "temperature" would be detectable in the present experiments, but does not seem to occur, so we are led to the conclusion that the energy distribution of the low energy direct interaction protons is approximately the same as that predicted by the statistical theory. (In passing, it may be noted that identical values of σ_c were used in the analysis of the "0°" and "4π" spectra. The influence of this term is not pronounced, since in the energy range 6 to 9 MeV, σ_c changes by 0.3 decade while the spectrum falls 0.87 decade.) This conclusion is rather unsatisfactory in view of the high "nuclear temperatures" of the energy distributions predicted by most direct interaction theories.

VI.3 Conclusions.

It is seen that n,d reactions contribute appreciably to the "σ" spectra and account for several low energy peaks which were previously attributed to anomalous and single particle effects. There is little evidence for systematic structure in the spectra at the higher proton energies, but there is some evidence for systematic

irregularities in the level density at low excitation energies. A direct interaction process is present at the higher proton energies, and probably occurs in the surface of the nucleus, since the preference for low lying states in the excited residual nucleus is evident. The lower energy protons may be a combination of "evaporation" protons and protons from a direct interaction process whose proton energy distribution is determined mainly by the level density in the residual nucleus. Alternatively, the anisotropy of the lower energy protons may result from a non-random distribution of the phases of the excited levels in the compound nucleus. There may also be the possibility that the anisotropic angular distributions and the other deviations from simple statistical theory observed in the 4π spectra are caused by a lack of thermal equilibrium in the excited compound nucleus when the proton is emitted. This is equivalent to saying that the protons originate from some form of cascade process in a compound system as opposed to a conventional compound nucleus.

Future Programme.

Having seen how the interpretation of the "4π" spectra is rendered uncertain because of the possibility that the spectra contain contributions from direct interactions, we hope to measure the "nuclear temperature" of the spectrum of protons emitted into a small solid angle in the backward hemisphere. The telescope used in this measurement will also be designed so that the angular distribution of the emitted protons can be determined. Improvements to this new telescope will include a thinner and more uniform thin CsI(Tl) crystal (prepared by an evaporation technique) which should give a better signal to background ratio. There will also be an improved light collection system on the dE/dx counter and it is hoped that a complete separation between protons and deuterons will be possible. It will then be possible to study the angular distributions of the groups of deuterons produced in pick-up reactions so that spin and parity assignments may be made to the excited states in the residual nuclei by application of the Butler theory. It must be remarked however that this aspect of the present programme will be limited by the fact that the ground state n,d pick-up reaction is the most common and the spins and parities of the ground

states of nuclei are fairly well known. Of more interest perhaps will be the angular distributions of the groups of high energy protons produced as a result of direct interactions. Application of the Butler theory to this data will again yield information on the spins and parities of excited states of nuclei. The anisotropies of the lower energy protons may be compared with the predictions of the statistical theory (Ericson and Strutinski, 1958).

Making use of the different decay times of the luminescence of CsI(Tl) for different particles, Mr Robertson of this group has devised electronics to record the pulses due to one type of particle only. We hope to use this technique to reduce the large electron background at the lower energies in CsI and by a similar arrangement to the "4π" experiment measure the n,p and n,np spectra at the lower proton energies and also the n,α spectra. Both the n,np proton spectra and the n,α spectra should be less susceptible to the influence of direct interactions and should be directly comparable with the statistical theory.

Appendix I.

a)

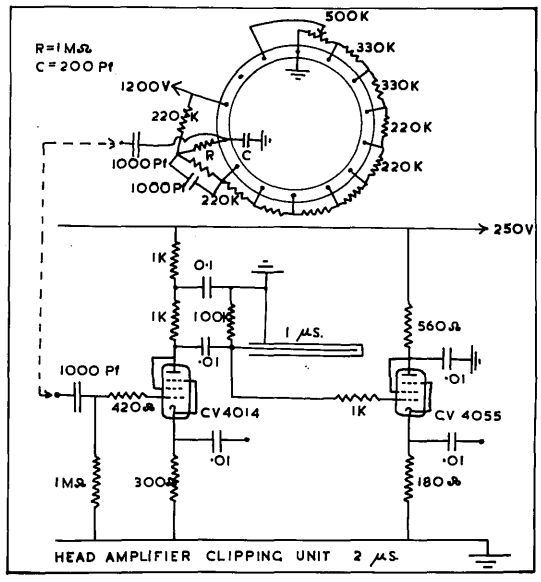

b)

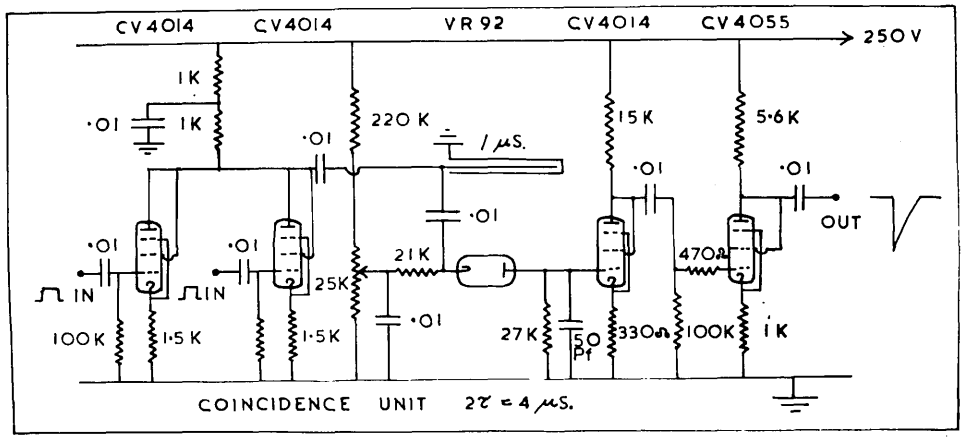

Circuit diagrams of a) Du Mont 6292 photomultiplier base assembly and head amplifier clipping unit. (A shorted 1 μ sec. delay line gives 2 μ sec. pulses). The output is fed to an I.D.L. 652 amplifier.

b) Coincidence unit used in the telescope experiment. The inputs are taken from the discriminator outputs of the I.D.L. 652 amplifiers. The negative output signal is fed to the gate circuit of the Hutchinson Scarrott pulse height analyser.

Appendix II.

The Preparation of Thin CsI(Tl) Crystals.

A grinding technique can be employed with CsI since it does not tend to cleave along crystal planes like NaI. The first thin crystals were prepared by rubbing down the crystal with finest grit paper on a glass plate. It was found that gentle scraping with a stainless steel razor blade imparts a smooth, uniform surface. To produce a fairly large crystal of minimum thickness (MK II) a technique employed in the geology department for the production of rock slides was used.

One face of a CsI crystal was ground plane on a glass plate using carborundum powder of different grades with liquid paraffin as lubricant. This plane face was attached to a glass slide using Canada Balsam, slide and crystal being heated to 120^{o}C on a hot plate until a good joint was obtained. The crystal was then ground down as before, the glass backing supporting the crystal. When the required thickness was reached, the crystal was removed from the slide by soaking in xylene for several days.

At the author's suggestion, Mr Lynch of this group has successfully prepared thin uniform layers of CsI(Tl)

by an evaporation technique. Layers as thin as $0.0005^{\mu t}$ have given 20% resolution with a polonium alpha source and will be used in the development of a telescope with better signal to background ratio.

REFERENCES.

Allan, D.L., 1957, Proc. Phys. Soc., A., 70, 195; 1958, Nuc. Phys. 6, 464; 1959, Ibid, 10, 348.

Ajzenberg, F., and Lauritsen, T., 1955, Rev. Mod. Phys., 27, 77.

Austern, N., Butler, S., and McManus, H., 1953, Phys. Rev., 92, 350.

Bame, S.J., Jr., Haddad, E., Perry, J.E., Jr., and Smith, R.K., 1957, Rev. Sci. Instr., 28, 997.

Barschall, H.H., 1952, Phys. Rev., 86, 431.

Beard, D.B., 1954, Phys. Rev., 94, 738.

Bethe, H.A., 1937, Rev. Mod. Phys., 9, 69.

Blaser, J.P., Boehm, F., Marmier, P., Scherrer, P., 1951, Helv. Phys. Acta., 24, 441.

Blatt, J.M., and Weisskopf, V.F., 1952, "Theoretical Nuclear Physics", (New York; Wiley).

Bleuler, E., Stebbins, A.K., and Tendam, D.J., 1953, Phys. Rev., 90, 460.

Bloch, C., 1954, Phys. Rev., 93, 1094.

Blok, J., and Jonker, C.C., 1957, Nuovo Cim., 6, 378.

Bohr, N., 1936, Nature, Lond., 137, 344.

Brolley, J.E., Jr., Fowler, J.L., and Schlacks, L.K., 1952, Phys. Rev., 88, 618.

Brown, G., and Muirhead, H., 1957, Phil. Mag., 2, 473.

Brueckner, K.A., 1955, Phys. Rev., 97, 1353.

Butler, S., 1957, Phys. Rev., 106, 272.

Butler, S.T., Austern, N., and Pearson, C., 1958, Phys. Rev., 112, 1227.

Cameron, A.G.W., 1958, Canad. J. Phys., 36, 1040.

Carlson, R.R., 1957, Phys. Rev., 107, 1094.

Chew, G., 1950, Phys. Rev., 80, 196.

Clementel, E., and Villi, C., 1958, Nuovo Cim., 9, 950.

Cohen, B.L., 1953, Phys. Rev., 92, 1245; 1957, Ibid, 105, 1549.

Cohen, B.L., and Mosko, S.W., 1957, Phys. Rev., 106, 995.

Cohen, B.L., and Rubin, A.G., 1958, Phys. Rev., 111, 1568; 1959, Ibid, 113, 579.

Colli, L., Facchini, U., and Micheletti, S, 1956, Nuovo Cim., 4, 671.

Colli, L., and Facchini, U., 1957a, Nuovo Cim., 5, 309.

Colli, L., Facchini, U., and Micheletti, S., 1957b, Nuovo Cim., 5, 502.

Colli, L., and Micheletti, S., 1957c, Nuovo Cim., 6, 1001.

Colli, L., Facchini, U., Iori, I., Marcazzan, M.G., and Sona, A., 1958a, Nuovo Cim., 7, 400.

Colli, L., Pignanelli, M., Rytz, A., and Zurmuhle, R., 1958b, Nuovo Cim., 9, 280.

Colli, L., Facchini, U., Iori, I., Marcazzan, M.G., and Sona, A.M., 1959a, Nuovo Cim., 13, 730.

Colli, L., Cvelbar, F., Micheletti, S., and Pignanelli, M., 1959b, Nuovo Cim., 13, 868.

Coleman, R.F., Hawker, B.E., O'Conner, L.P. and Perkin, J.L., 1959, Proc. Phys. Soc., 73, 215.

Culler, G., Fernbach, S., and Sherman, N., 1956, Phys. Rev., 101, 1047.

Eisberg, R.M., and Igo, G., 1954, Phys. Rev., 93, 1039.

Eisberg, R.M., Igo, G., and Wegner, H.E., 1955, Phys. Rev., 100, 1309.

Eisberg, R.M., and Hintz, N.M., 1956, Phys. Rev., 103, 645.

Elton, L.R.B., and Gomes, L.C., 1957, Phys. Rev., 105, 1027.

Endt, P.M., Haffner, J.M., and Van Patter, D.M., 1952, Phys. Rev., 86, 518.

Endt, P.M., and Kluyver, J.C., 1954, Rev. Mod. Phys., 26, 95.

Ericson, T., 1958, Nuc. Phys., 8, 265.

Ericson, T., and Strutinski, V., 1958, Nuc. Phys., 8, 284.

Eubank, H.P., Peck, R.A., and Hassler, F.L., 1958/59, Nuc. Phys., 9, 273.

Eubank, H.P., Peck, R.A., Jr., and Zatzick, M.R., 1959, Nuc. Phys., 10, 418.

Evans, J.A., 1959, Proc. Phys. Soc., 73, 33.

Evans, R.D., 1955, "The Atomic Nucleus" pp. 716/7. McGraw-Hill.

Fernbach, S., Serber, R., and Taylor, T.B., 1949, Phys. Rev., 75, 1352.

Feshbach, H., Porter, C.E., and Weisskopf, V.F., 1954, Phys. Rev., 96, 448.

Fireman, E.L., 1953, Phys. Rev., 91, 922.

Flerov, N.N., and Talyzin, V.M., 1957, Jour. Nuc. Energy, 4, 529.

Foglesong, G.M., and Foxwell, D.G., 1954, Phys. Rev., 96, 1001.

Frenkel, I, 1936, Sov. Phys., 9, 533.

Fulmer, C.B., and Cohen, B.L., 1958, Phys. Rev., 112, 1672.

Fulbright, H.W., Lassen, N.O., and Roy Poulsen, N.O., 1959, K. Danske Vidensk. Selsk. Mat-fys. Medd, 31, No.10.

Green, L.W., Smith, A.J., Buechner, W.W., and Mazari, M., 1957, Phys. Rev., 108, 841.

Greenlees, G.W., Lowe, J., Robbins, A.B., and Rolph, P.M., 1958, Proc. Phys. Soc., 71, 904.

Glendenning, N.K., 1959, Phys. Rev., 114, 1297.

Gugelot, P.C., 1954, Phys. Rev., 93, 425.

Haling, R.K., Peck, R.A., and Eubank, H.P., 1957, Phys. Rev., 106, 971.

Hauser, W., and Feshbach, H., 1952, Phys. Rev., 87, 366.

Haxel, O., Jensen, J.H.D., and Suess, H.E., 1949, Phys. Rev., 75, 1766.

Hayakawa, S., Kawai, M., and Kikuchi, K., 1955, Progr. Theor. Phys., (Japan), 13, 415.

Hinds, S., Middleton, R., and Parry, G., 1958, Proc. Phys. Soc., 71, 49.

Hofstadter, R., Fechter, H.R., and McIntyre, J.A., 1953, Phys. Rev., 92, 978.

Holt, J.R., and Marsham, T.N., 1953, Proc. Phys. Soc., A., 66, 258.

Hutchinson, G.W., and Scarrott, G.G., 1951, Phil. Mag., 42, 792.

Igo, G., and Wegner, H.E., 1956, Phys. Rev., 102, 1364.

Kondaiah, E., and Iyengar, K.V.K., 1958, Nuc. Phys., 5, 346.

Kondaiah, E., Badrinathan, C., and Iyengar, K.V.K., 1959, Nuc. Phys., 9, 561.

Konijn, J., Van Nooijen, B., Mostert, P., and Endt, P.M., 1956, Physica 22, 887.

Lane, A.M., and Wandel, C.F., 1955, Phys. Rev., 98, 1524.

Lane, A.M., Thomas, R.G., and Wigner, E.P., 1955, Phys. Rev., 99, 693.

Lang, J.M.B., and Le Couteur, K.J., 1954, Proc. Phys. Soc., A., 63, 259.

Levinson, C.A., and Bannerjee, M.K., 1957/58, Ann. Phys., 2, 471; Ibid, 2, 499; Ibid, 3, 67.

Livesey, D.L., 1955, Canad. J. Phys., 33, 391.

March, P.V., and Morton, W.T., 1958a, Phil. Mag., 3, 143; 1958b, Ibid, 3, 577; 1958c, Ibid, 3, 1256.

Mayer, M.G., 1949, Phys. Rev., 75, 1969; 1950, 78, 16.

Melkanoff, M.A., Moszkowski, S.A., Nodvik, J., and Saxon, D.S., 1956, Phys. Rev., 101, 507.

McManus, H., and Sharpe, W.T., 1952, Phys. Rev., 87, 188.

Newton, T.D., 1956, Canad. J. Phys., 34, 807.

Nemirovski, 1956, "Peaceful Uses of Atomic Energy" (New York) 2, 86.

Paul, E.B., and Clarke, R.L., 1953, Canad. J. Phys. 31, 267.

Peck, R.A., Jr., 1957, Phys. Rev., 106, 965.

Peck, R.A., Jr., and Lowe, J., 1959, Phys. Rev., 114, 847.

Porges, K.G., 1956, Phys. Rev., 101, 225.

Purser, K., and Titterton, E.W., 1959, Aust. J. Phys., 12, 103.

Ribe, F.L., 1957, Phys. Rev., 106, 767.

Rosen, L., and Stewart, L., 1955, Phys. Rev., 99, 1052.

Ross, A.A., 1957, Phys. Rev., 108, 720.

Sargent, C.P., and Bertozzi, W., 1957, "Proceedings of the International Conference on the Neutron Interactions with the Nucleus", Columbia University.

Saxon, D.S., 1954, Phys. Rev., 95, 577.

Scott, J.M.C., 1954, Phil. Mag., 45, 441.

Shapira, M.M., 1953, Phys. Rev., 90, 171.

Storey, R.S., Jack, W., and Ward, A., 1958, Proc. Phys. Soc., 72, 1.

Tamura, T., and Choudhury, D.C., 1959, Phys. Rev., 113, 552.

Thomson, D.M., 1956, Proc. Phys. Soc., A., 69, 447.

Tomasini, A., 1957, Nuovo Cim., 6, 927.

Trainor, L.E.H., and Dixon, W.R., 1956, Canad. J. Phys., 34, 229.

Weisskopf, V.F., 1937, Phys. Rev., 52, 295.

Weisskopf, V.F., and Ewing, D.H., 1940, Phys. Rev., 57, 472.

Woods, R.D., and Saxon, D.S., 1954, Phys. Rev., 95, 577.

Zucker, A., 1958, Nuc. Phys., 6, 420.